

AD-A068 892

HARRIS CORP MELBOURNE FLA ELECTRONIC SYSTEMS DIV  
HUMAN READ - MACHINE READ MICROFILM MASS MEMORY SYSTEM.(U)  
MAR 79 T H OTTEN, R H NELSON

F/G 14/5

F30602-74-C-0152

UNCLASSIFIED

RADC-TR-79-30

NL

1 OF 2  
AD  
AO 68892



AD A 068892

DDC FILE COPY

**LEVEL**

12 NW

RADC-TR-79-30  
Final Technical Report  
March 1979



**HUMAN READ-MACHINE READ  
MICROFILM MASS MEMORY SYSTEM**

Harris Corporation

T. H. Otten  
R. H. Nelson

DDC  
RECEIVED  
MAY 24 1979  
C

APPROVED FOR PUBLIC RELEASE; DISTRIBUTION UNLIMITED

**ROME AIR DEVELOPMENT CENTER  
Air Force Systems Command  
Griffiss Air Force Base, New York 13441**

79 05 21 016

This report has been reviewed by the RADC Information Office (OI) and is releasable to the National Technical Information Service (NTIS). At NTIS it will be releasable to the general public, including foreign nations.

RADC-TR-79-30 has been reviewed and is approved for publication.

APPROVED:

*Fred Haritatos*

FRED HARITATOS  
Project Engineer

APPROVED:

*Howard Davis*

HOWARD DAVIS  
Technical Director  
Intelligence and Reconnaissance Division

FOR THE COMMANDER:

*John P. Huss*

JOHN P. HUSS  
Acting Chief, Plans Office

If your address has changed or if you wish to be removed from the RADC mailing list, or if the addressee is no longer employed by your organization, please notify RADC (IRDE) Griffiss AFB NY 13441. This will assist us in maintaining a current mailing list.

Do not return this copy. Retain or destroy.

UNCLASSIFIED

SECURITY CLASSIFICATION OF THIS PAGE (When Data Entered)

REPORT DOCUMENTATION PAGE		READ INSTRUCTIONS BEFORE COMPLETING FORM
1. REPORT NUMBER <b>18</b> RADC-TR-79-30	2. GOVT ACCESSION NO. <b>19</b> TR-79-30	3. RECIPIENT'S CATALOG NUMBER
4. TITLE (and Subtitle) <b>6</b> HUMAN READ - MACHINE READ MICROFILM MASS MEMORY SYSTEM	5. TYPE OF REPORT & PERIOD COVERED <b>9</b> Final Technical Report, April 1974 - July 1978	6. PERFORMING ORG. REPORT NUMBER
7. AUTHOR(s) <b>10</b> T. H. Otten R. H. Nelson	8. CONTRACT OR GRANT NUMBER(s) <b>15</b> F30602-74-C-0152	
9. PERFORMING ORGANIZATION NAME AND ADDRESS Harris Corporation Electronic Systems Division Melbourne FL 32901	10. PROGRAM ELEMENT, PROJECT, TASK AREA & WORK UNIT NUMBERS <b>16</b> 64750F 27160106 <b>17</b> 84	
11. CONTROLLING OFFICE NAME AND ADDRESS Rome Air Development Center (IRDE) Griffiss AFB NY 13441	12. REPORT DATE <b>11</b> March 1979	
14. MONITORING AGENCY NAME & ADDRESS (if different from Controlling Office) Rome Air Development Center (IRDE) Griffiss AFB NY 13441	13. NUMBER OF PAGES 180	15. SECURITY CLASS. (of this report) UNCLASSIFIED
16. DISTRIBUTION STATEMENT (of this Report) Approved for public release; distribution unlimited. <b>12</b> 789 p.		15a. DECLASSIFICATION/DOWNGRADING SCHEDULE N/A
17. DISTRIBUTION STATEMENT (of the abstract entered in Block 20, if different from Report) Same		
18. SUPPLEMENTARY NOTES RADC Project Engineer: Fred Haritatos (IRDE)		
19. KEY WORDS (Continue on reverse side if necessary and identify by block number) Computer Data Storage      Storage and Retrieval Microfilm                      Mass Memory Holography                     Film Handling Optical Data Processing		
20. ABSTRACT (Continue on reverse side if necessary and identify by block number) → The Human Readable/Machine Readable (HRMR) Microfilm Mass Memory System is an information storage and retrieval system for machine readable digital data and human readable microimages. Development of the HRMR system was undertaken as a step toward solving some of today's information processing challenges. The storage, retrieval and dissemination of information by Government organizations has continued to be expensive and time consuming. Information is collected and maintained at such a rate that the effectiveness and efficiency of some organizations is limited by the available data handling equipment.		

DD FORM 1 JAN 73 1473

cont'd over

UNCLASSIFIED

SECURITY CLASSIFICATION OF THIS PAGE (When Data Entered)

408 972

slh

cont'd from over

UNCLASSIFIED

SECURITY CLASSIFICATION OF THIS PAGE(When Data Entered)

The Human Readable/Machine Readable Microfilm Mass Memory System (HRMR) was developed as an engineering development model under Contract F30602-74-C-0152 for the Rome Air Development Center, Griffiss AFB NY. The system is designed to record, via laser, both human readable microimages and machine readable binary data on nominal 105mm by 148mm film chips. Each film chip provides the storage capacity for up to 98 human readable microimages or ~~30 x 10<sup>6</sup>~~ binary bits. The system provides on-line automated storage and retrieval of film chips. This is achieved by the storage and retrieval unit which provides the capacity to store 6,750 film chips (containing a total of ~~2 x 10<sup>11</sup>~~ bits of binary data). Under computer control, it is designed to provide rapid, random access to these film chips and on-line readout of the machine readable data recorded on any chip.

thirty million

2 times 10 to the 11th power

ACCESSION for	
NTIS	Write Section <input checked="" type="checkbox"/>
DDC	Buff Section <input type="checkbox"/>
UNANNOUNCED JUSTIFICATION <input type="checkbox"/>	
BY	
DISTRIBUTION/AVAILABILITY CODES	
	SPECIAL
A	

UNCLASSIFIED

SECURITY CLASSIFICATION OF THIS PAGE(When Data Entered)

## TABLE OF CONTENTS

<u>Section</u>	<u>Title</u>	<u>Page</u>
I.	INTRODUCTION.	1-1
1.1	Background	1-1
1.2	Technical Report Synopsis	1-4
II.	SYSTEM DESCRIPTION	2-1
2.1	System Description Overview	2-1
2.2	System Component Description	2-7
2.2.1	Controller Group	2-7
2.2.2	Recorder (1A1) Functional Description	2-8
2.2.2.1	Film Handling	2-8
2.2.2.2	Data Recording	2-11
2.2.3	Verifier (1A3) Functional Description	2-14
2.2.3.1	Microfiche Transport Assembly Film Handling	2-14
2.2.3.2	Film Handling in the Verifier (1A3)	2-16
2.2.3.3	Data Readout and Verification	2-18
2.2.3.4	Readout Optics	2-19
2.2.4	Storage and Retrieval Functional Description (Unit 7)	2-20
2.2.4.1	Microfiche Handling	2-20
2.2.4.2	Data Readout	2-24
2.3	Operational Capabilities	2-24
2.3.1	Film Chip Cassette Loading	2-24
2.3.2	Queue Transports Maximize Throughput	2-25
2.3.3	Verifier Data Readout of Clipped Fiche	2-25
2.3.4	S/R Unit Purge/ Load	2-25
2.3.5	Fault Monitoring and Display	2-26
2.3.6	Optics Monitors	2-27
2.3.7	HRMR Software	2-27
2.3.8	Controller Tasks	2-28
2.3.9	Offline Capabilities	2-28
2.4	Technology Developments	2-30
2.4.1	AOBD Linearizer	2-30
2.4.2	AOM Linearizer	2-31
2.4.3	Photodiode Detector Array	2-32
2.4.4	Air Bearing Platen	2-32
2.4.5	Transform Generator	2-33
2.4.6	Spinner Development	2-34

## TABLE OF CONTENTS (Continued)

<u>Section</u>	<u>Title</u>	<u>Page</u>
2.4.7	Carousel/Elevator Assembly	2-35
2.4.8	Clipless Fiche Handling	2-36
2.4.9	Automatic Film Handling and Processing	2-37
2.5	Problem Areas and Potential Improvements	2-38
2.5.1	AOBD Drive Linearization	2-38
2.5.2	AOBD Cell	2-39
2.5.3	HR Spinner	2-40
2.5.4	Threshold Averaging Technique	2-40
2.5.5	S & R Counterbalance Technique	2-41
2.5.6	System Thermal Stabilization	2-42
2.5.7	Vibration Effects	2-43
2.5.8	Data Interleaving	2-43
2.5.9	Film Processing	2-43
III.	REQUIREMENTS AND ACHIEVEMENTS	3-1
3.1	Technical Requirements	3-1
3.2	Technical Approach	3-5
3.2.1	System Concept Overview	3-5
3.2.1.1	Data Format	3-5
3.2.1.2	Synthetic Holography	3-6
3.2.1.3	Recorder System	3-6
3.2.1.4	Reader System	3-8
3.2.2	Selection of Key Technologies	3-9
3.2.2.1	Synthetic Holography	3-10
3.2.2.2	Recording Format	3-12
3.2.2.2.1	Data Capacity Constraint	3-12
3.2.2.2.2	Data Readout Time Constraint	3-13
3.2.2.2.3	Scratch Immunity/Heading Legibility Constraint	3-14
3.2.2.3	Laser Wavelength and Vendor Selection	3-15
3.2.2.4	Scanning Techniques	3-17
3.2.2.4.1	MR Recorder Scanning Tradeoff	3-17
3.2.2.4.2	HR Recorder Scanning Tradeoff	3-18
3.2.2.5	Film Emulsion Selection	3-19
3.2.2.5.1	Candidate Emulsions	3-20
3.2.2.5.2	Other Considerations	3-21
3.2.2.6	Film Processor Selection	3-21
3.2.2.7	Film Positioning Platen Design	3-23
3.2.2.8	Photodetector Array	3-25

TABLE OF CONTENTS (Continued)

<u>Section</u>	<u>Title</u>	<u>Page</u>
3.2.2.8.1	Performance of the HRMR-I Array	3-26
3.2.2.8.2	Evaluation of Candidate HRMR-II Arrays	3-28
3.2.2.8.3	Testing of the HRMR-II Reticon Array	3-30
3.2.2.9	Optical Design and Packaging	3-33
3.2.2.9.1	Design/Packaging Tradeoffs	3-34
3.2.2.9.2	Recorder Optical Design Approach	3-35
3.2.2.9.3	Verifier Optical Design Approach	3-37
3.3	Assessment of Selected Approaches and Problems Encountered	3-40
3.3.1	Synthetic Holography	3-40
3.3.2	Microfiche Unit Records	3-41
3.3.3	Carousel Storage and Retrieval	3-42
3.3.4	Computer Controller and I/O Interface	3-44
3.3.5	Film Handling	3-46
3.3.6	X-Y Microfiche Positioning Servo	3-47
3.3.7	Bit Error Rates	3-48
IV.	TEST AND RESULTS	4-1
4.1	System Optimization and Integration	4-1
4.1.1	TGA Studies	4-2
4.1.1.1	Test Procedure	4-2
4.1.1.2	Digital Filter Test Result	4-3
4.1.1.3	Digital Filter Test Interpretations	4-6
4.1.1.4	TGA Gain Test Results	4-6
4.1.1.5	TGA Gain Test Interpretation	4-8
4.1.2	AOM Equalization Studies	4-8
4.1.2.1	Test Procedure and Result	4-11
4.1.3	TGA and AOM Equalizer Combined Effects	4-13
4.1.3.1	Test Procedure and Results	4-13
4.1.3.2	Test Interpretation	4-17
4.1.4	Digital Filter Effect at Readout	4-17
4.1.4.1	Test Procedure and Result	4-18
4.1.4.2	Test Interpretation	4-18
4.2	System Performance Characterization	4-21
4.2.1	Recorder Performance	4-21
4.2.1.1	AOBD Frequency/Linearization Interaction	4-22
4.2.1.2	Diffraction Efficiency Studies	4-22
4.2.2	Reader Performance	4-28

TABLE OF CONTENTS (Continued)

<u>Section</u>	<u>Title</u>	<u>Page</u>
4.2.2.1	Detected Data Signals	4-28
4.2.2.2	Bit-Error Rate Measurements	4-30
4.3	Diagnostic Studies	4-33
4.3.1	Along-Track Recorder Signatures	4-34
4.3.2	Reader Vibration Effects	4-36
4.3.3	AOBD Linearity Stability	4-39
4.3.4	TGA Gain Vs Bit Height Fluctuation	4-43
4.3.5	Effect of Film Processing on BER	4-44
4.3.6	Fixed Pattern Noise Investigation	4-48
V.	BIT ERROR RATE ANALYSIS	5-1
5.1	Achievable Bit Error Rate Improvements	5-1
5.1.1	Initial System BER Predictions	5-2
5.1.2	Error Statistics Evaluation Experiments	5-4
5.1.2.1	Track Analysis	5-5
5.1.2.2	Burst Block Analyses	5-6
5.1.2.2.1	Single-Error Correcting Code	5-7
5.1.2.2.2	Interleave Depth Studies	5-7
5.1.3	Achievable Improvements and Recommendations	5-12
VI.	PERFORMANCE DEMONSTRATIONS AND CONCLUSIONS	6-1
6.1	Results of Acceptance Testing	6-1
6.2	Recommendations of System Upgrade	6-3

APPENDIX A

## LIST OF FIGURES

<u>Figure</u>	<u>Caption</u>	<u>Page</u>
2.1-1	HRMR Microfilm Mass Memory System	2-2
2.1-2	Simplified Functional Block Diagram of the Microfilm Mass Memory System	2-3
2.1-3	HRMR Microfiche Format	2-6
2.1-4	Fiche Carousel Module	2-6a
2.2.2	Functional Block Diagram of the Recorder (1A1)	2-9
2.2.3	Functional Block Diagram of the Microfiche Transport (1A4) and Verifier (1A3)	2-15
2.2.4	Functional Block Diagram of the S & R (Unit 7)	2-21
3.2.2.9.2-1	Recording System Block Diagram	3-36
3.2.2.9.3-1	Verifier System Electro-Optical Block Diagram	3-38
4.1.1.2-1	Spectral Analysis of TGA Output for Digital Filter Setting of 1/4	4-4
4.1.1.2-2	Spectral Analysis of TGA Output for Digital Filter Setting of 1/2	4-4
4.1.1.2-3	Spectral Analysis of TGA Output for Digital Filter Setting of 3/4	4-5
4.1.1.2-4	Spectral Analysis of TGA Output for Digital Filter Setting of 1	4-5
4.1.1.4-1	Output of TGA for Gain of 5, DF of 1/4, Showing 512 DFT Coefficients	4-7
4.1.1.4-2	Output of TGA for Gain of 10, DF of 1/4	4-7
4.1.1.4-3	Spectral Analysis of TGA Output with Gain of 5	4-9
4.1.1.4-4	Spectral Analysis of TGA Output with Gain of 10	4-9
4.1.1.4-5	Spectral Analysis as in Previous Figure but at 2dB/div.	4-10
4.1.2.1-1	AOM Linearization, Showing Equalizer Memory Contents (Thin Line), and Linearized AOM Output (Fuzzy Line)	4-12
4.1.3.1-1	Spectral Analysis of AOM Output. TGA Gain=5 Without AOM Linearization	4-14
4.1.3.1-2	Spectral Analysis of AOM Output. TGA Gain=5 With AOM Linearization	4-14
4.1.3.1-3	Spectral Analysis of AOM Output. TGA Gain=8 Without AOM Linearization	4-15
4.1.3.1-4	Spectral Analysis of AOM Output. TGA Gain=8 With AOM Linearization	4-15

LIST OF FIGURES (Continued)

<u>Figure</u>	<u>Caption</u>	<u>Page</u>
4.1.3.1-5	Spectral Analysis of AOM Output. TGA Gain = 11 Without AOM Linearization	4-16
4.1.3.1-6	Spectral Analysis of AOM Output. TGA Gain = 11 With AOM Linearization	4-16
4.1.4.1-1	Detected Data in Digital Filter Study. TGA Gain 11, DF Setting 1/4	4-19
4.1.4.1-2	Detected Data in Digital Filter Study. TGA Gain 11, DF Setting 1/2	4-19
4.1.4.1-3	Detected Data in Digital Filter Study. TGA Gain 11, DF Setting 3/4	4-20
4.1.4.1-4	Detected Data in Digital Filter Study. TGA Gain 11, DF Setting 11	4-20
4.2.1.1-1	Detected Intensity of Film Plane During One Hologram Scan Time - AOBD Using Nominal Frequency Band	4-24
4.2.1.1-2	Same as Previous Photo, But With AOBD Frequency Band Displaced Downward by 6 MHz	4-24
4.2.1.1-3	Same as Previous Photo, But With AOBD Frequency Band Displaced Downward by an Additional 6 MHz	4-24
4.2.1.1-4	Same as Previous Photo, But With AOBD Frequency Band Displaced Downward by an Additional 6 MHz	4-24
4.2.1.2-1	Diffacted Light Intensity Received Versus Number of "One" Bits Set in Holograms	4-27
4.2.2.1-1	Output Signals During Readout: Analog Data With Superimposed Threshold, and Resulting Digital Data	4-29
4.2.2.1-2	Even and Odd Analog Data Readout Channels	4-31
4.3.1-1	Early Recorded Fiche, Showing Inter-Track Spacing Variation	4-35
4.3.1-2	Recently Recorded Fiche, Showing Reduced Inter-Track Spacing Variation	4-35
4.3.2-1	Upper Trace: Detected Sync Bit Amplitude with Vibration Sources Off. Lower Trace: Same with Processor and Fan On. 10 ms/cm, 0.5 V/cm, Both Curves Riding on 1.5 V Bias	4-38

LIST OF FIGURES (Continued)

<u>Figure</u>	<u>Caption</u>	<u>Page</u>
4.3.2-2	Same as Previous Figure, Showing Vibration Due to MR Recording Process	4-38
4.3.3-1	Sum of AOBD Reference Frequency and Chirp Differential Frequency Showing Poor Linearization	4-41
4.3.3-2	VCO Signal (Upper Trace) and PMT Detected Focus Signal Corresponding to Figure 4.3.3-1	4-41
4.3.3-3	Sum of AOBD Reference Frequency and Chirp Differential Frequency Showing Good Linearization	4-42
4.3.3-4	VCO Signal and Focus Signal Corresponding to Figure 4.3.3-3	4-42
4.3.4-1	Even and Odd Video Data Channels. TGA Gain 5	4-45
4.3.4-2	Even and Odd Video Data Channels. TGA Gain 7	4-45
4.3.4-3	Even and Odd Video Data Channels. TGA Gain 9	4-46
4.3.4-4	Even and Odd Video Data Channels. TGA Gain 10	4-46
4.3.5-1	Z-Mod Error Display - Hand Processed Fiche	4-49
4.3.5-2	Z-Mod Error Display - Machine Processed Fiche	4-49
4.3.6-1	Even and Odd Video Data, Every Other Bit Set. TGA Gain 5, DF Setting 1/4	4-51
4.3.6-2	Spectrum Analysis of Data Input to Recording System. TGA Gain 5, DF 1/4	4-51
5.1.2.2.2-2	Result of Interleave Simulation Experiment	5-10

## LIST OF TABLES

<u>Table</u>	<u>Title</u>	<u>Page</u>
3.1	Key Requirements Summary	3-2
3.2.2.3-1	Comparison of Candidate Record Lasers - 1975	3-16
3.2.2.4.1-1	Calculated MR Spinner Solutions	3-18
3.2.2.4.2-1	AOBD/Spinner Tradeoff Parameters	3-19
3.2.2.6-1	Film Processor Performance Requirements	3-22
3.2.2.7-1	Comparison of Air Bearing and Flat Head Vacuum Platens	3-24
3.2.2.8.2-1	Desired Readout Array Characteristics	3-30
5.1.1-1	Bit Error Sources	5-3
5.1.2.2.2-1	Data Set for Interleave Depth Studies	5-8
5.1.2.2.2-2	No. of Words In Error Versus Interleave Depth	5-9

## EVALUATION

The purpose of this effort is to design, fabricate and evaluate an engineering development (6.4) model utilizing computer-generated (synthetic) holography for mass data storage on microfiche.

The Human Read - Machine Read (HRMR) Microfilm Mass Memory System is an on-line information storage and retrieval system for machine readable digital data files and human readable microimages. System operation has demonstrated the benefits of holography to information storage applications.

The most significant achievement of this program was the development of near real-time optical recording and playback techniques for storage of 30 million bits of user data on standard microfiche. In addition, advanced high-speed laser scanning and fast Fourier transform electronics were developed to circumvent the traditional constraints associated with interferometric holography.

Through the selection of commercial ADP equipment (PDP 11/45 minicomputer), the HRMR system can be easily interfaced with the AN/GYQ-21(V) Intelligence Analyst Station for either stand-alone operation or via digital communication networks (i.e. ARPA, Autodin and WICS).

This technology will have an important impact on improving the production and utility of intelligence reports disseminated throughout the DOD intelligence community. This effort was conducted under RADC Technical Planning Objective R1E - Integrated Intelligence Systems.

*Fred Haritatos*  
FRED HARITATOS  
Project Engineer

## I. INTRODUCTION

### 1.1 Background

The Human Readable/Machine Readable Microfilm Mass Memory System (HRMR) was developed as an engineering development model under contract F30602-74-C-0152 for the Rome Air Development Center, Griffiss Air Force Base, N. Y. The system is designed to record, via laser, both human readable microimages and machine readable binary data on nominal 105mm by 148mm film chips. Each film chip provides the storage capacity for up to 98 human readable microimages or  $30 \times 10^6$  binary bits. The HRMR System provides fully automated film handling including: extraction of film chips from the supply magazine, X-Y transport past the record station, transport to, through and from the on-line film processor, and X-Y transport past the read station of the data verifier or reader. In addition, the system provides on-line automated storage and retrieval of film chips. This is achieved by the storage and retrieval unit which provides the capacity to store 6750 film chips (containing a total of  $2 \times 10^{11}$  bits of binary data). Under computer control, it is designed to provide rapid, random access to these film chips and on-line readout of the machine readable data recorded on any chip. <sup>(1)</sup>

Development of the HRMR system was undertaken as a step toward solving some of today's information processing challenges. The storage, retrieval and dissemination of information by Government organizations has continued to be expensive and time consuming. Information is collected and maintained at such a rate that the effectiveness

---

(1) Program funding limitations precluded completion of integration of readout electro-optics into the storage and retrieval units.

and efficiency of some organizations is limited by the available data handling equipment. An on-going goal of the information handling community has been the establishment of a document storage and retrieval system which will (a) achieve a significant reduction in the amount of space required to store the document collections, (b) result in increased productivity through better use of manpower resources, and (c) allow for the creation of efficient, effective, and economical procedures for accomplishment of the data handling functions. While some of these advantages could have been achieved by utilizing magnetic drum, disk or tape storage, the unusually large data banks needed to store and retrieve textual, cartographic, and photographic information has made the cost and physical space requirements of such devices very unattractive, if not prohibitive. In addition, the necessary expensive periodic maintenance of certain storage media made them less than desirable.

Optical recording technologies combined with automatic film handling techniques promise a solution to the above operational information processing and handling challenges. Thus a significant and fruitful step toward the realization of much needed information handling equipment was undertaken -- the HRMR Engineering Development Model program.

Under this program a demonstrable system was realized and tested. The HRMR System demonstrated many important advances in mass storage and handling of information. It proved that 30 million bits of digital data can be recorded in the holographic form on a 105 by 148mm film chip and be subsequently machine read -- all under computer control. It demonstrated several advances in rapid and precise automatic film handling. Furthermore, the design of an on-line high-capacity microfilm storage retrieval unit was developed and demonstrated.

Although the above and much more was achieved as part of the HRMR program, a limitation in Government funds precluded the full realization of all system performance parameters. As subsequently presented in this report, certain technical challenges were more difficult to address than originally envisioned. None-the-less, although a fully operational HRMR System was not realized, significant technical advances in information processing and handling were achieved. Thus the HRMR program significantly contributed to the technology base upon which the information handling community is depending for solutions to enhance their operational capabilities.

This report describes the HRMR System and documents some of the technical problems encountered, major achievements realized, and recommendations for improvements resulting from the HRMR program effort.

## 1.2 Technical Report Synopsis

This chapter has presented an overview of the goals and achievements of the HRMR program, from a general description of the need for and applications of an archival mass storage system to a brief synopsis of the attainments of HRMR-II. In the remaining chapters of this report, the full technical achievements of the system will be detailed, from conceptual description and block diagrams through system experiments, problem areas and potential improvements.

Chapter II will begin the system description task with functional block diagrams and conceptual descriptions of each key system and subsystem. These top level views will include the Recorder, Processor, Verifier, Controller, Storage and Retrieval, and Auxiliary units, and will detail the operational layouts and fiche flow diagrams for each. Operational capabilities of the system as currently configured and implemented will be detailed, and a summary of the technical developments of the program in the key components and subsystems will be given. Finally, a description of system limitations, problem areas, and suggestions for improved performance will be presented.

The complete requirements and achievements of the program will be described in Chapter III. After a discussion of the technical requirements of the program, including such issues as I/O rates, packing density, bit error rates, etc., a detailed description of the technical approach will be presented. Details of the operation of each key component and subsystem, as well as many of the tradeoff considerations which entered into their selection, will be presented. An assessment of the performance levels achieved and an overview of what was learned about relevant system and device level topics will be included.

The results of system testing and experimentation will be the subject of Chapter IV. The first subsection, system initialization, will

present the experiments which were performed during system integration and which helped to establish the operating conditions and parameters for the system. Then a section on system performance will characterize the operating values and capabilities achieved by the system after its basic parameters had been firmly established. Finally, a section on diagnostic studies will document the experimental work done in response to the identified problem areas of the system, including problem identification and isolation activities, as well as the development and testing of potential and actual solutions.

Chapter V is devoted to the discussion of system bit error rate, and specifically to an investigation of a technique for achieving a lower corrected BER. In this interleaving technique, the effects of locally high BER areas can be distributed among a number of different error-correcting codewords, overcoming the tendency of such "burst" errors to overwhelm the correcting power of the code. The description in Chapter V will include the results of a multi-part experiment in which: 1) error data from actual HRMR fiche were collected and analyzed; 2) a computer was used to simulate the effect of various depths of interleaving on the corrected BER of the collected data; and 3) a projection was made on the basis of these results which allowed recommendations for future code implementations to be made, including performance predictions of the BER levels thus achievable.

The report concludes with Chapter VI, an overview and evaluation of achieved system performance. To begin this process, the results of the system's Acceptance Test are synopsized, including procedures and data. A discussion of the variances of the system performance from the initial objectives follows, including where possible the reasons for the observed variances. Finally, an assessment of the extent to which the techniques and components developed during the

**HRMR program can be extended to support improved performance levels in future systems is presented, with concluding remarks on the needs filled by the HRMR MSS and the most profitable directions for future development.**

## II. SYSTEM DESCRIPTION

The HRMR Microfilm Mass Memory System is an information recording, storage, and retrieval system utilizing 4" x 6" microfiche as the storage media. Both human readable (HR) and machine readable (MR) recordings (or a combination of each) can be generated. The human readable fiche containing 98 reduced text images conforms to the NMA, ANSI, and military DIAR 5903 microfiche format standards for on-line recording of alpha numeric text or graphic arts scanned and digitized text. The machine readable format consists of 30 million bits of binary data storage recorded on seventy tracks with random access to any track during readout.

### 2.1 System Description Overview

The system components include a Controller unit (DEC PDP 11/45 computer) with I/O peripherals; a Recorder unit to record microfiche, with automatic film processing and fiche verification (MR data validation); and a Storage and Retrieval (S & R) unit to access to any of 6750 microfiche providing a  $2 \times 10^{11}$  bit data base capacity. Figure 2.1-1 depicts a typical 625 sq. ft. HRMR Microfilm Mass Memory System installation. Additional components include a Graphic Arts Digitizer; CRT and TTY keyboard terminal; output Hard Copy unit; Microfiche Viewer for validation of HR microimages; a Code Clipper to affix a metal code clip to the top edge of MR microfiche slated for the S & R unit; and an Ancillary unit (AUX RACK) which provides pneumatics for mechanical actuation in the Recorder and S & R units.

Figure 2.1-2 presents an abbreviated and much simplified functional block diagram of the system which shows data, command and status flow from/to the Controller, and a graphical presentation of the itinerary of a MR microfiche.

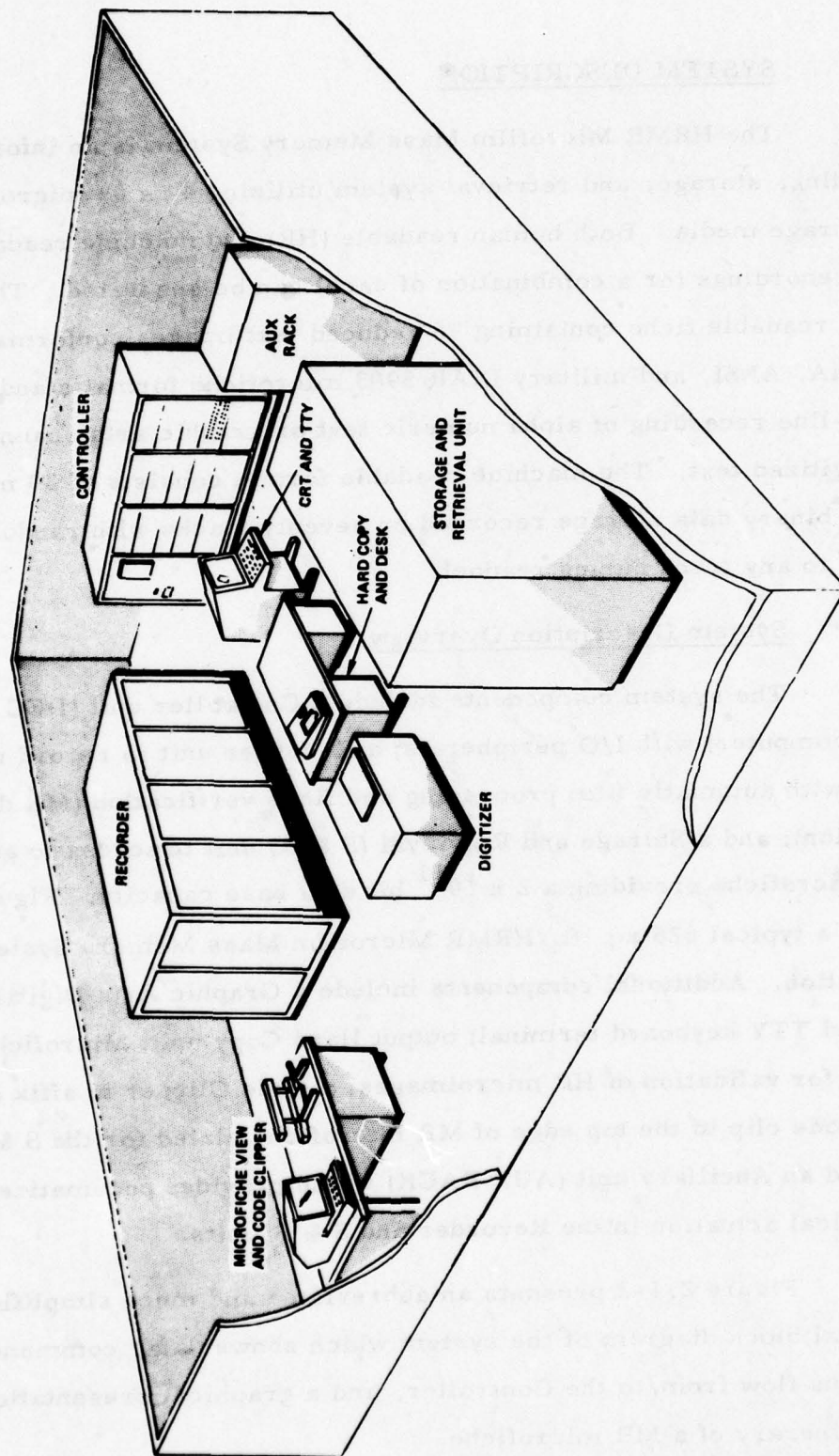


Figure 2.1-1. HRMR Microfilm Mass Memory System



An operator initiates a microfiche recording at the Controller unit via the CRT keyboard by listing the files of data to be recorded and enters a record command. Upon receiving this command, the Recorder removes a film chip from the film cassette, transports and loads it onto an X-Y axis assembly which positions and moves the fiche during recording. Microfiche recording consists of film chip exposure by an amplitude modulated and deflected light beam to produce a MR track of individually spaced, raster scanned holograms inclined  $30^{\circ}$  to vertical or a HR microimage produced by contiguous, horizontal, left-to-right raster scans.

The machine read (MR) data is recorded as a series of synthetically generated holograms (8950 per track along the 6 inch dimension) with each 0.012 by 1.4mm hologram containing the Fourier transformation of 48 user bits. The Fourier transformation coefficients amplitude modulate the raster scanned spot to record each two-Rayleigh synthetic hologram. Human read (HR) data is recorded as 24 X reduced microimages utilizing 1650, 1280 pixel left-to-right scans to support bilevel graphic arts at 150 lines/inch, or 60 lines of alpha numerics at 80 characters per line, generated by a 9 x 7 character generator.

Once the data is recorded, the film chip exits the Recorder and enters the film Processor for immersion in developer and fix fluids, washing, and drying. It exits the film Processor and travels through a Queue transport to be loaded onto the Verifier X-Y axis assembly which positions and moves the fiche during readout (hologram illumination diffraction onto a linear photodiode array).

Data is reconstructed from bit decisions made when the static readout beam is in registration with each recorded hologram. The data is verified and the controller informed of the data quality via the raw Bit Error Rate (BER) count, as well as the encounter of any

uncorrectable bit errors. Human read microfiche are verified at a Microfiche Viewer after exit from the Verifier.

Machine read microfiche to be filed in the Storage and Retrieval Unit exit the Verifier and are manually carried to the Code Clipper to affix a three decade Binary Coded Decimal (BCD) metal clip to the top edge of the microfiche. Each unique code clip number can be recorded in the fiche title area immediately above the MR or HR recording area. Figure 2.1-3 presents the microfiche recording format for reference.

In order to insert a microfiche into the Storage and Retrieval Unit, the Controller operator specifies the carousel level and a dummy fiche is purged, to be replaced by the recently clipped microfiche via the carousel access door. Once in the Storage and Retrieval Unit, the microfiche can be accessed by the operator from the Controller Unit for readout at any track. This is physically accomplished by a selector mechanism which partially extracts the clipped microfiche, a spreader mechanism to separate microfiche from each side of selected microfiche, and a T-bar which retracts to place this microfiche onto the X-Y axis assembly for positioning and motion during readout. The readout process is identical to that of the Verifier with verification of the data quality, as well as reconstructed data transfer to the Controller Unit. Once the desired data readout is complete, the microfiche is reinserted into the carousel and the readout station may be moved to any other carousel level for a subsequent microfiche selection and readout.

The carousel with code clipped microfiche is the key feature of the Storage and Retrieval Unit. Figure 2.1-4 presents an Image Systems, Inc., Remcard carousel module which led to the development

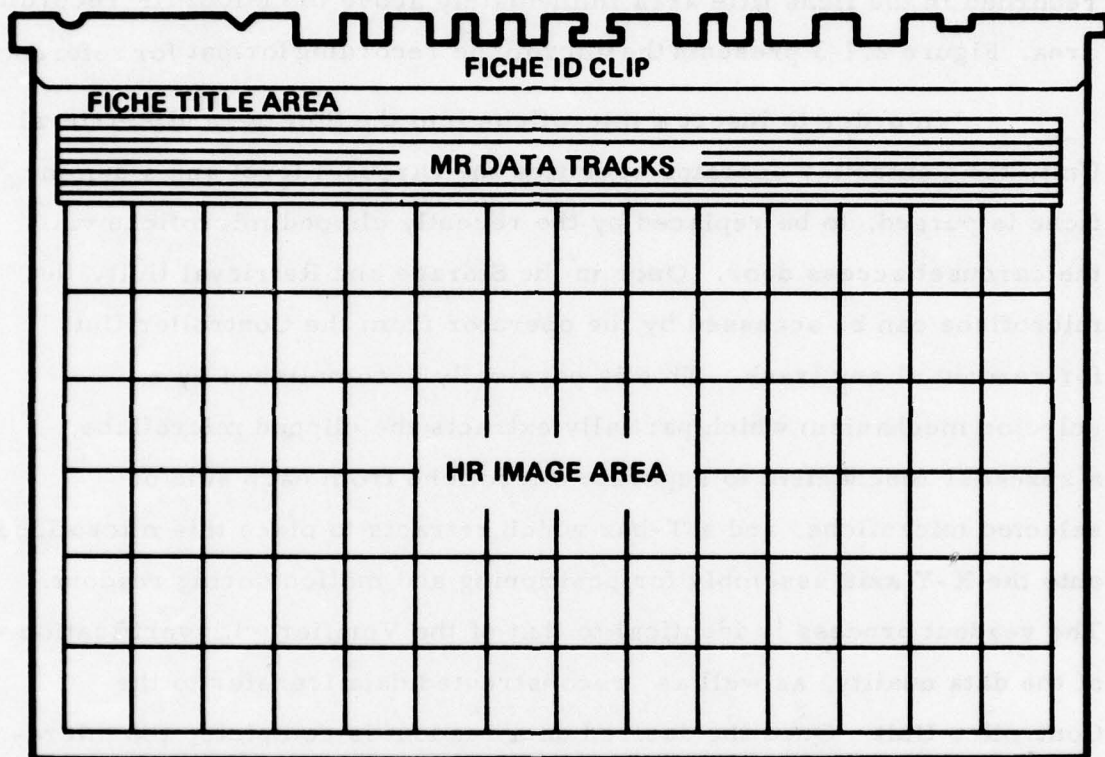
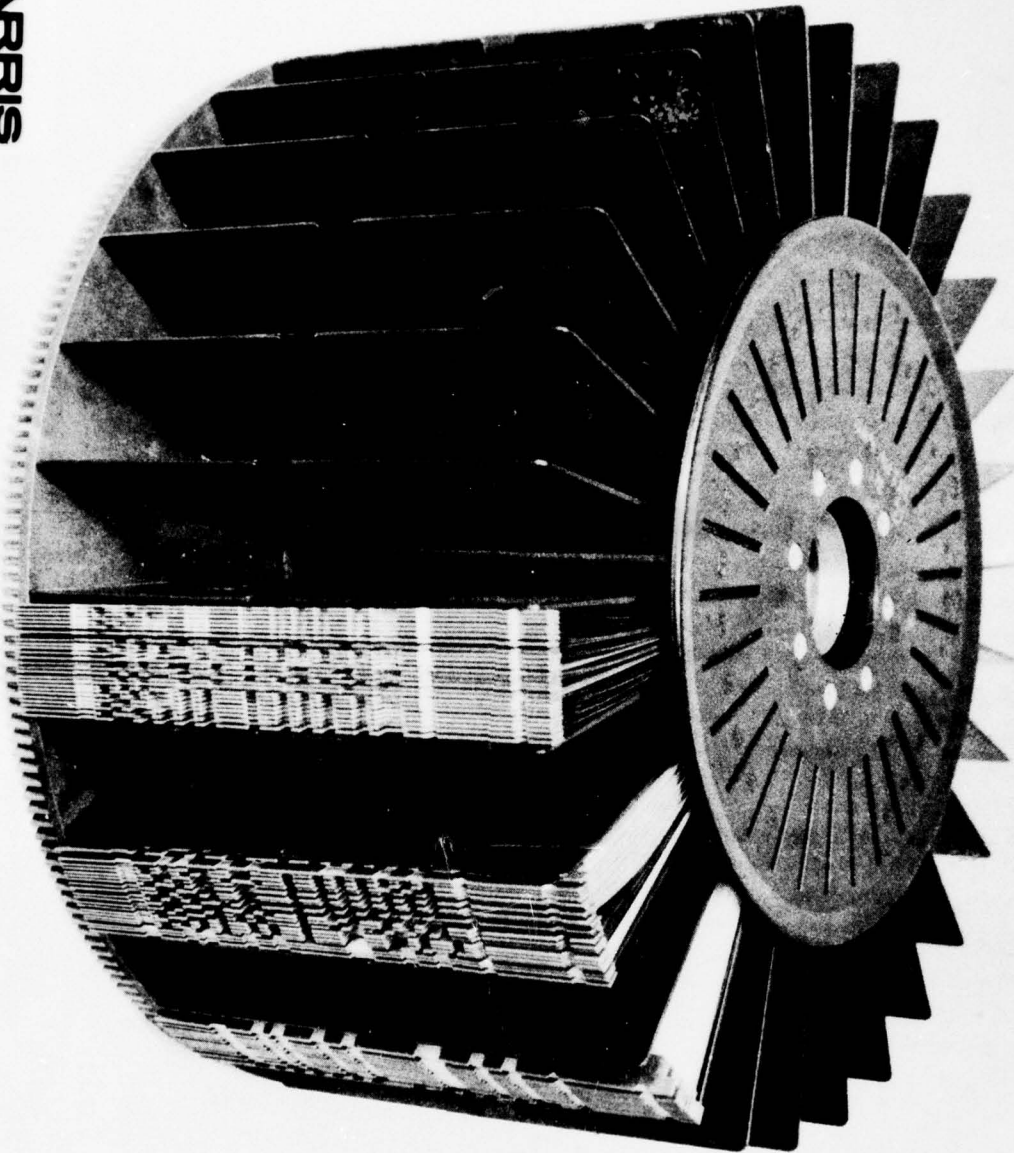


Figure 2.1-3. HRMR Microfiche Format



**HARRIS**  
COMMUNICATIONS AND  
INFORMATION HANDLING



88757-14

Figure 2.1-4. Fiche Carousel Module

2-6a

of the (nine) stacked carousel assembly. The S & R unit also utilizes a purchased selector and spreader mechanism from this vendor.

As an additional capability, the Verifier in the Recorder Unit serves as a back-up reader to the Storage and Retrieval Unit for code clipped microfiche.

## 2.2 System Component Description

The HRMR Microfilm Mass Memory System consists of various units associated with the Controller Group, the Recorder Unit, Storage and Retrieval Unit, Ancillary Unit, Microfiche Viewer, and Microfiche Coder. This section presents features of Controller Group units, and functional descriptions of the Storage and Retrieval Unit and Recorder Unit.

### 2.2.1 Controller Group

The Controller Group consists of the DEC PDP 11/45 computer mainframe designated the Controller (Unit 4); the Tektronix 4014 CRT Display and Keyboard (Unit 5) with vectoring line graphics and alpha- numerics capability; the standard DEC writer teletype (Unit 6); Dest Data 150 Graphic Art Digitizer (Unit 7) with 150 samples/inch scanning resolution for 8-1/2 by 11 inch source material; and the Tektronix 4631 dry silver Hardcopy Generator for output copy of the CRT display.

The Controller (Unit 4) is configured with 16K core memory (expandable to 64K); TU10 Mag Tape, two RK05 Disc drives, PC 11 paper tape reader and punch, an expander with I/O panel to provide four DR-11B (Direct Memory Access device for I/O data transfer) and three DR11-C (device controller for command and status transfer) with capability to add a communication interface to an existing Unibus port. One DR11-B supports data transfer from the Dest Data 150 via a Harris

designed run length converter configured on a W941 DEC wire wrappable card while the remaining three DR11-B and DR11-C, in pairs, are utilized to communicate with the Recorder (1A1), Verifier (1A3), and S & R (Unit 7).

The RT-11 operating system is utilized to maximize the transfer of data during recording or readout with minimum core utilization. Operational software developed for the system is file oriented and a maximum use of standard DEC software and device handlers has been incorporated to minimize orientation and maintain a high degree of programming flexibility.

#### 2.2.2 Recorder (1A1) Functional Description

Discussions in this section provide descriptive narrative with reference to Figure 2.2.2 for film handling and data recording.

##### 2.2.2.1 Film Handling

Prior to recording, the sheet film cassettes must be loaded or contain film (105 x 148mm Kodak 7 mil Estar base S0-343). Once the film cassette is in place, attached to the Fiche Loader (1A1A10), then recording may be initiated.

Recording commands from the Controller (Unit 4) interface with the Record Logic Assembly (RLA, 1A1A1) via a standard DEC DR11-C device controller. The RLA then interfaces with the Mech-Optics Controller (1A1A5) which accepts the commands by transitioning from Park to Load and then to Mech Load sequence states. The Load state moves the X-Y assembly mechanisms via the X-Y Controller (1A1A7) and both axis motors, to the microfiche Load position at the exit of the Fiche Loader (1A1A10) and then initiates the Mech Load sequencer to remove a film chip from the cassette. This is accomplished by extending a vacuum head into the cassette, applying vacuum via the



Vacuum Control Assembly (1A1A12), and retracting and inserting the film chip into the edge guided, center drive, motorized film transport as vacuum is released. A film transport exit switch notifies the Mech-Optics Controller to initiate accurate positioning of the fiche onto the X-Y Assembly and it proceeds to do so via the Pneumatic Interface Panel (1A1A15). First it assures fiche contact with a guide pin, then it moves the fiche from the bottom against two pins located on the X-Y Assembly vacuum head, and finally it pushes the top area of the fiche against the vacuum head where vacuum is applied to hold the fiche securely during the recording process.

Once the fiche is secured to the X-Y Assembly vacuum head the Mech-Optic Controller transitions to the Record state, moves the fiche to the correct X and Y axis start-of-record positions and then it either accelerates along the -Y axis to achieve constant velocity for MR raster scan of 83, 6 point alpha numeric characters for the title block or a MR raster scan of 8960 data holograms per track, or it accelerates along the +X axis to achieve constant velocity for left-to-right HR raster scan of 24X microimages for alpha numerics or graphic arts recording.

Servomechanisms motion is achieved by lead-screw displacement along the X and Y axis with the Load position defined as absolute zero. DC motor drive control is provided by the CSR System 550 X-Y Controller (1A1A7) which receives 5 decade BCD X and Y axis Go To positions and Go commands calculated by the Mech-Optics Controller. The X-Y Controller responds primarily with X and Y axis In Position status and 5 decade present position derived from the encoders located on the X and Y axis motors.

After a track or microimage recording the Y or X axis retraces and the Mech-Optics Controller monitors the RLA interface for the continuation of recording and the desired record format.

This recording process continues until the RLA to Mech-Optics Controller interface indicates end-of-fiche. This terminates fiche recording and places the Mech-Optics Controller in the Exit state to move the fiche mounted on the X-Y Assembly to the exit entrance of the Fiche Loader and Exit Transport (1A1A10). Once it achieves this position the Mech-Optics Controller transitions to the Mech Exit sequence state which automatically releases the fiche vacuum hold-down and turns on the exit transport motors. The fiche drops into the transport and is propelled into the Film Processor (1A2) tripping the exit transport switch, and completing the Mech Exit sequence. The Mech-Optics Controller then transitions to the Park sequence to move the X-Y Assembly vacuum head to the park position to await further recording commands.

Two sequence states of the Mech-Optics Controller not discussed are the Hard Fault and Absolute Zero sequence states which precede the Park state. Briefly, the Hard Fault state indicates that a potentially damaging fault condition (i. e. , servo travel into limit switches, arithmetic computation error, etc.) or a condition requiring operator intervention (i. e. , no film in the Film Cassette causing vacuum fault) has been detected by the Mech-Optics Controller and all mechanisms are brought to a halt. The Controller via the RLA can clear this fault. On the receipt of Fault Clear, the Mech-Optics Controller then transitions to the Absolute Zero Sequence to establish the absolute zero reference for all subsequent motion of the X-Y Assembly and in the process, check all redundant limit switches.

#### 2.2.2.2 Data Recording

Before the recording process is initiated, the Controller (Unit 4) establishes the Direct Memory Access data transfer via a standard DEC DR11-B to the RLA (1A1A1) and stages data in both 1024 word Input/Output Buffer (IOB) intermediate memories. The

IOB memories operate in a ping-pong fashion to allow data processing for recording out of one buffer while the other is being filled, thereby assuring uninterrupted data during recording.

MR data proceeds from the IOB memories through Error Correction Encoding (ECC) to add parity and provide correction during readout of single and double errors, thereby decreasing the Bit Error Rate (BER) of recorded data to the Controller. After parity has been added to each group of 48 bits, it is sent to the Transform Generator Assembly (1A1A6) where the discrete Fourier transform is generated, resulting in 512 transform coefficients. These coefficients are routed back to the RLA and placed in a cycle buffer which releases the set coefficients twice in succession with end guard bands to ultimately form a two-Rayleigh, one dimensional hologram during a single raster scan of a MR track recording. However, prior to light modulation, the coefficients are altered by a prestored, amplitude dependent transfer function stored in the RLA Equalizer to compensate for predictable, nonlinear effects to be encountered during recording. These altered coefficients then produce light modulation during the raster scan via amplitude modulation of a 95MHz oscillator residing in the Transform Generator Assembly. The modulated RF signal is amplified by the AOM Amplifier (1A1A13) and light modulation results at the Acousto-Optic Modulator (AOM; 1A1A9A2).

HR data proceeds from the IOB memories through alpha numerics or graphic arts controllers which reformat ASCII characters or Huffman encoded run lengths into left-to-right pixel bit streams to on-off modulate the record light beam. This data bypasses coefficient generation, cycle buffering, and equalization to produce bi-level light modulation during raster scan via the amplitude modulation of the 95MHz oscillator in the Transform Generator as for MR recording.

After acousto-optic modulation, the light is routed to the Acousto-Optic Beam Deflector (AOBD, 1A1A9A5) for MR recording or to the Optical Line Scanner (OLS, 1A1A9A2M3) for HR recording. This mode Selection is performed by a mirror attached to an air piston (1A1A9MP7) which intercepts the light to the AOBD and sends it to the OLS in response to the HR data type command received by the Mech-Optics Controller.

For MR data recording, the modulated light proceeds through beam forming optics to the AOBD where it is linearly deflected at a 10.4 KHz repetition rate to produce each hologram raster scan. Linear deflection is achieved by applying an RF signal whose frequency is increased at a fixed rate (1.25MHz per microsecond) for 94 microseconds, followed by a 2 microsecond retrace. This RF modulation is produced by the AOBD drive circuitry residing within the Mech-Optics Controller, the AOBD Amplifier (1A1A14) with directional coupler, RF Mixer Amplifier Assembly (1A1A15A3), and Delay Line (1A1A16DL1). Linearity calibration of AOBD deflection is established each time a microfiche is to be produced (i. e., the Mech-Optics Controller will not leave the Park sequence and transition to Load until acousto-optic beam deflection is linearized).

After acousto-optic deflection, the modulated laser beam passes through 3X reduction optics and beam shaping to strike the moving film chip affixed to the X-Y Assembly vacuum head.

For HR recording, the left-to-right raster scan is produced by a twenty-faceted, pyramidal mirror controlled by a phase-locked OLS Drive Assembly (1A1A5) referenced to a 12.5MHz stable clock. Not shown in Figure 2.2.2, is the start of scan detector utilized to rejustify the pixel data to each facet for the start of each line raster.

The amplitude modulated, deflected laser beam then passes through beam imaging optics to the HR record station at the air bearing platen and onto the moving film chip affixed to the X-Y Assembly vacuum head.

### 2.2.3 Verifier (1A3) Functional Description

Discussions in this section provide descriptive narrative with reference to Figure 2.2.3 for film handling, data readout, and readout optics in the Verifier, as well as film handling through the Microfiche Transport Assembly.

#### 2.2.3.1 Microfiche Transport Assembly Film Handling

The Microfiche Transport Assembly (1A4) receives dry, developed microfiche from the Film Processor via a stacking mechanism in the Film Receiver. A microfiche is detected dropping out of the Film Processor by the interruption of air flow to a switch. The Mech-Optics Controller (1A3A2) then activates air pistons to move the fiche sideways over the transport entry and releases an air piston to drop the fiche into the edge-guided, center drive, motorized film transports. A switch indicates the fiche is entering the Q Transport sections and allows the Mech-Optic Controller to reset the Film Receiver air pistons. The Q Transports operate to smooth the fiche throughput by staging up to four fiche for the Verifier before queue overflow occurs. Each section has a switch which indicates to the preceding section that it already contains a fiche. If a section is holding a fiche, the section supplying it with the next fiche will halt its fiche and hold it by means of removing the drive to the AC motor until a fiche has been loaded at the Verifier allowing all queued fiche to automatically advance one section. Although not shown in Figure 2.2.3, solid state relays featuring zero voltage turn-on and zero current turn-off are utilized to switch each AC motor thereby minimizing EMI effects. In the event the Verifier does not

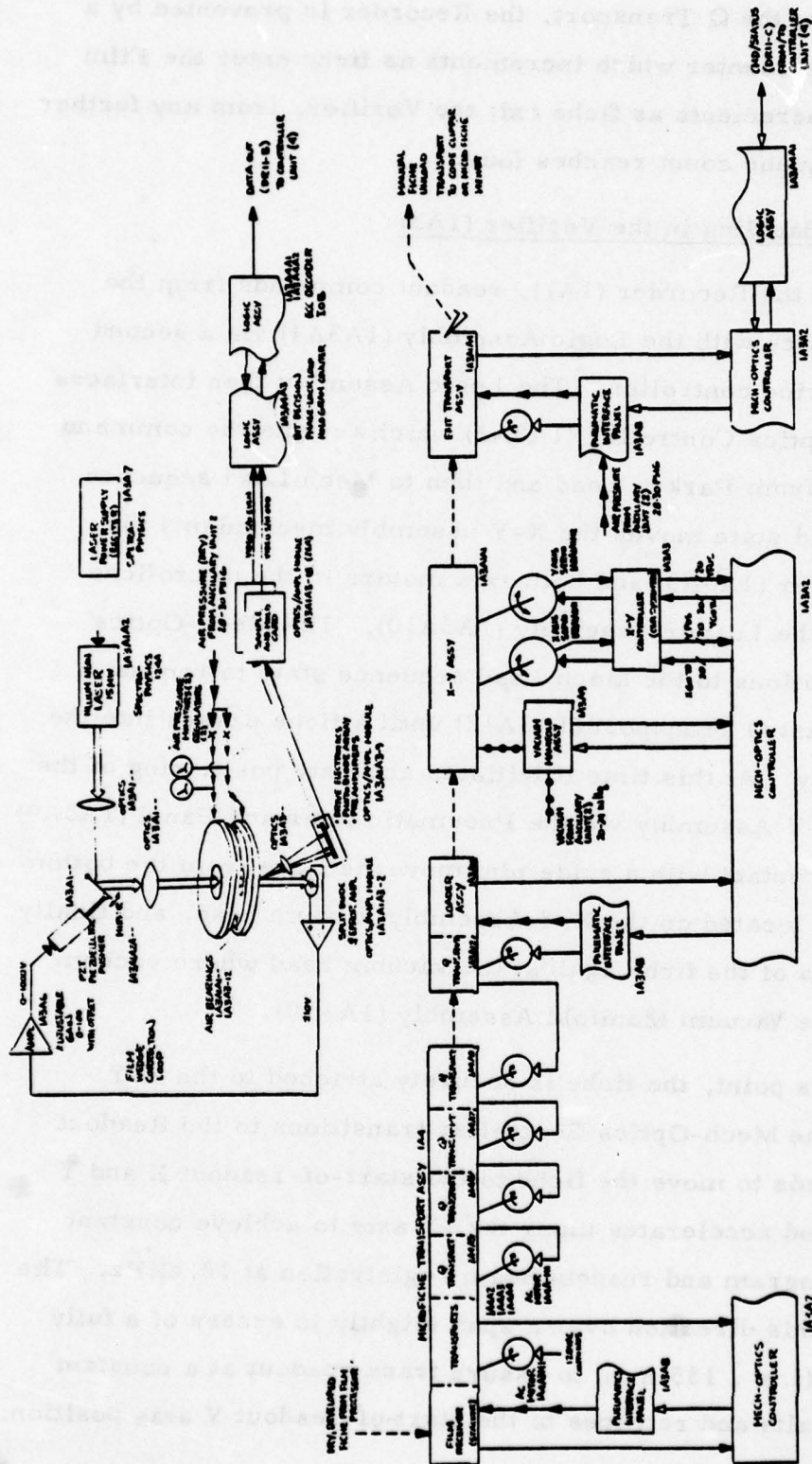


FIGURE 2.2.3  
FUNCTIONAL BLOCK DIAGRAM  
OF THE MICROFICHE TRANS-  
PORT (IA4) AND VERIFIER (IA3)  
T-100-478

remove fiche from the Q Transport, the Recorder is prevented by a mechanical Queue counter which increments as fiche enter the Film Processor and decrements as fiche exit the Verifier, from any further recording if the queue count reaches four.

#### 2.2.3.2 Film Handling in the Verifier (1A3)

As for the Recorder (1A1), readout commands from the Controller interface with the Logic Assembly (1A3A4) via a second DEC DR11-C device controller. The Logic Assembly then interfaces with the Mech-Optics Controller (1A3A2) which accepts the command by transitioning from Park to Load and then to Mech Load sequence states. The Load state moves the X-Y assembly mechanisms via the X-Y Controller (1A3A3) and both axis motors to the microfiche load position at the Loader Assembly (1A3A10). The Mech-Optics Controller transitions to the Mech Load sequence state to request a fiche from the last Q Transport (1A3A12) until a fiche passes into the Loader Assembly. At this time it initiates accurate positioning of the fiche onto the X-Y Assembly via the Pneumatic Interface Panel (1A3A9) to assure fiche contact with a guide pin, move the fiche from the bottom against two pins located on the X-Y Assembly vacuum head, and finally push the top area of the fiche against the vacuum head where vacuum is applied via the Vacuum Manifold Assembly (1A3A9).

At this point, the fiche is securely attached to the X-Y Assembly and the Mech-Optics Controller transitions to the Readout State. It proceeds to move the fiche to the start-of-readout X and Y axis positions and accelerates along the -Y axis to achieve constant velocity for hologram and readout beam registration at 10.4KHz. The fiche moves in this direction over a span slightly in excess of a fully recorded track (i. e. , 135 mm) to assure track readout at a constant rate, and then halts and retraces to the start-of-readout Y axis position.

The Mech-Optics Controller waits at this position until it receives a second track readout command or an end-of-fiche to exit the fiche. Naturally, only those recorded areas with MR holograms are attempted as the Verifier does not process HR or title block information. On receipt of the second track readout command the Mech-Optics Controller computes the new X axis position, commands the X-Y Controller to move the fiche along the X axis to the next track and then accelerates along the -Y axis for readout.

If the Mech-Optics Controller receives an end-of-fiche command, it transitions to the Exit sequence state and moves the fiche to the entrance of the Exit Transport Assembly (1A3A1A4). It then transitions to the Mech Exit sequence releasing the X-Y Assembly vacuum. This drops the fiche into the Exit Transport where the Exit Transport center drive motors have been started, to propel the fiche to one of two output chutes. The bottom chute is designated for acceptable fiche and the other for rejected fiche as selected by the Controller upon bit error rate status evaluation. As the fiche enters the selected chute, an exit switch indicates that the Mech Exit Sequence is complete. The Mech-Optics Controller then transitions to the Park sequence and proceeds to move to the Park position.

The two sequence states (Hard Fault and Absolute Zero Sequence) preceding the Park state are incorporated in a manner identical to that of the Recorder.

An additional capability of the Verifier is to readout code clipped microfiche to serve as a readout backup for the S & R Unit. This is accomplished from the Mech-Optics Controller front panel with the Mech Load and Mech Exit sequence states bypassed as the fiche must be placed and removed manually from the X-Y Assembly vacuum head while in the Park position. Naturally, vacuum hold-down

of the fiche during readout is not provided as the fiche is affixed against two alternate positioning pins and held down with a spring clip.

The optics functions of the Verifier Mech-Optics Controller are limited to photodiode monitors and front panel meter displays for alignment purposes.

#### 2.2.3.3 Data Readout and Verification

The Verifier normally reads the MR data on a hologram and verifies the readout quality (BER) transferring only status to the Controller. Alternately, the Logic Assembly can be commanded to transfer data and it sets up the two Input/Output Buffer (IOB) memories controller to accept data, and transfer it via a second DEC DR-11B DMA interface to the Controller. In either case, the photodetector array, hologram synchronization, bit decision, and Error Correction Encoding (ECC) decoding processes are identical.

As the X-Y Assembly reaches constant velocity for readout along the -Y axis, the Mech-Optics Controller (1A3A2) signals the Logic Assembly (1A3A4A3) hologram counter that the readout beam should be encountering the first holograms of a recorded MR track. The readout phase-locked loop acquires synchronization well within the first 64 sync and threshold holograms which are followed by a unique hologram signaling the beginning of 8960 data holograms of the track. A running average threshold is generated during the sync and threshold holograms and the bit decision process is well established to correlate the special data pattern with readout of the unique start-of-track hologram.

Once the unique hologram is recognized, the Hologram Counter is loaded with 8960 and is thereafter decremented each time reconstructed hologram data is sent to the ECC Decoder.

The Logic Assembly ECC Decoder receives 64 codeword bits, passes the codeword through a syndrome generator, and then on the second pass, the syndrome generator alters the bit polarity of detected and correctable error sites. Since the parity bits are of no interest, only the 48 data bits associated with each hologram are sent to the IOB memories for possible output transfer to the Controller.

The ECC Decoder also counts the number of corrected errors which provides measure of the raw bit error rate and transmits this status to the Controller. As the ECC Decoder can detect and correct single and double errors, as well as detect all triple but uncorrectable errors, it also transmits the occurrence of uncorrectable errors as status to the Controller.

#### 2.2.3.4 . Readout Optics

The output beam of a 15MW HeNe Laser (1A3A1A2) is modified by beam forming optics into a 0.007mm by 1.4mm readout beam at the Air Bearing platen. The incident angle along the 1.4mm dimension is controlled to minimize readout displacement on the photodiode array due to film wedge effects. Film wedge effects caused by film emulsion or film base thickness gradients is detected in displacement of the undiffracted portion of the readout beam at a split photodiode detector. This error signal is generated by a difference amplifier monitoring the split detector. Further amplification by a Burleigh PZ-70M high voltage amplifier (1A3A6) followed by mirror displacement (via a piezoelectric pusher) of the readout beam incident to the microfiche removes error in readout displacement caused by film wedge.

The diffracted readout beam modified by readout optics preceding the array serves to focus the hologram's inverse Fourier transform onto the photodiode array. This results in a series of light intensity spots corresponding to data bits incident upon a linear photodetector array.

The Reticon 256EBH photodiode array consists of 0.5 mil x 24 mil detectors on 2 mil centers, alternately connected to two video lines. The photodiode sites connected to each video line are sequentially interrogated each scan cycle and integrate charge proportional to incident light intensity between interrogations. The output of each video line is preamplified and routed to Sample and Hold cards located nearby. The Sample and Hold circuitry operates to minimize synchronous sampling noise and provide drive from the optics bench to the Logic Assembly readout electronics (1A3A4A3).

#### 2.2.4 Storage and Retrieval Functional Description (Unit 7)

Discussions in this section provide descriptive narrative with reference to Figure 2.2.4 for microfiche handling and data readout.

##### 2.2.4.1 Microfiche Handling

As for the Verifier (1A3), readout commands from the Controller interface with the Logic Assembly (A10) via the third DEC DR11-B device controller.

The Logic Assembly interfaces with Mech-Optics Controller (A9) which accepts a read command, microfiche code clip identification, and carousel level to transition from the Park state to Load sequence. In the Load sequence state, the Mech-Controller retracts the magnetic Selector Assembly (A14A7) from close proximity to the carousel, repacks any clipped fiche into the carousel which followed the selector, and requests the desired carousel level from the Carousel and Elevator Servo Controller (A8).

The Carousel and Elevator Servo Controller unlocks the elevator via the Pneumatic Interface Panel (A6) and drives the X-Y Assembly to the desired carousel level via the elevator motor pinion gear mounted on the X-Y Assembly. As the X-Y Assembly approaches

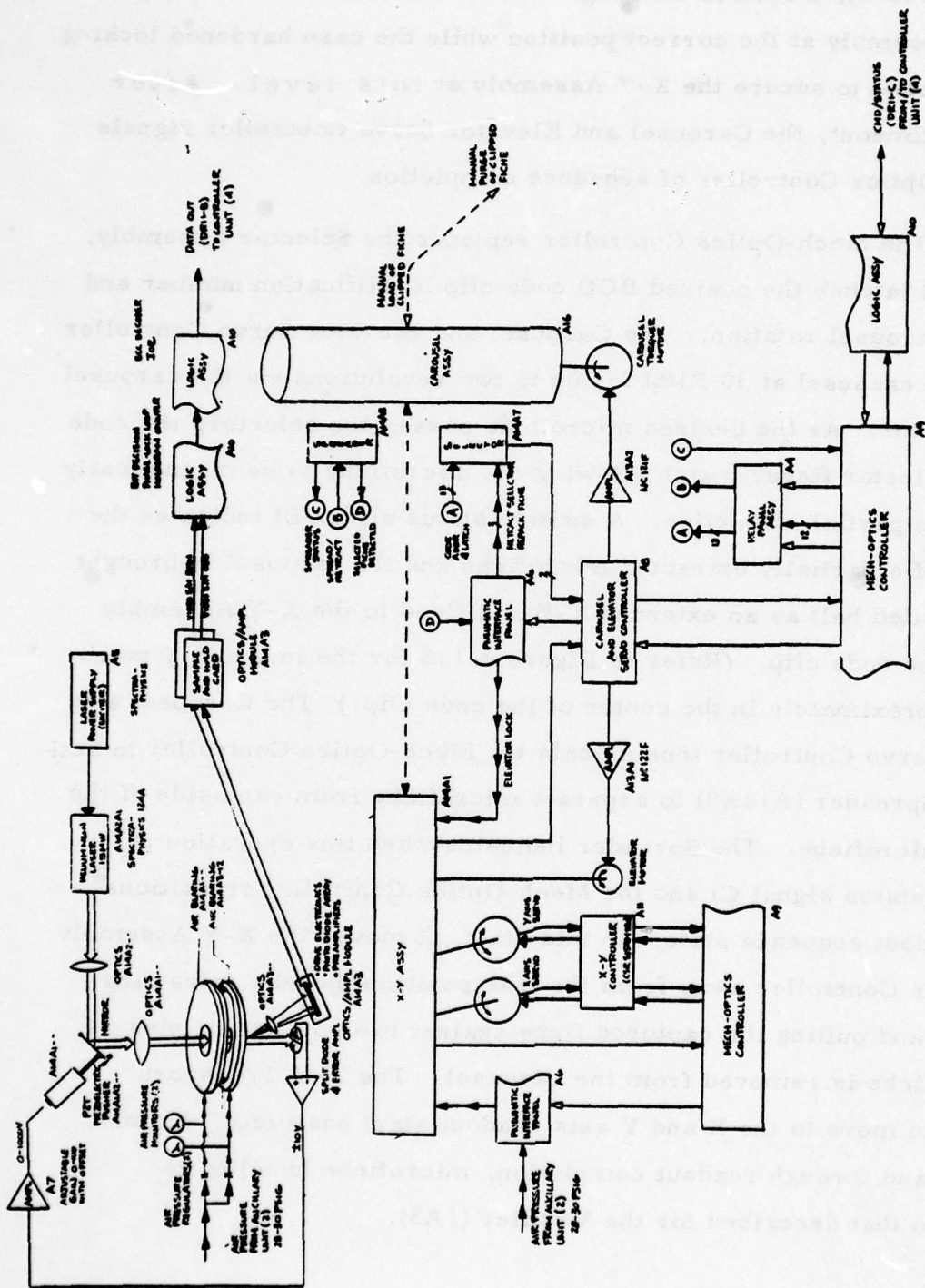


FIGURE 2.2.A  
FUNCTIONAL BLOCK DIAGRAM  
OF THE SRR (UNIT 7)

Toll-68

the correct level, a split IR sensing diode is utilized to accurately place the X-Y Assembly at the correct position while the case hardened locking pin is extended to secure the X-Y Assembly at this level. After a suitable timeout, the Carousel and Elevator Servo Controller signals the Mech-Optics Controller of sequence completion.

The Mech-Optics Controller replaces the Selector Assembly, sets up and latches the desired BCD code clip identification number and requests carousel rotation. The Carousel and Elevator Servo Controller rotates the carousel at 30 RPM for up to two revolutions via the carousel torquer motor. As the desired microfiche passes the selector, the code clip and selector finger match allowing the microfiche to be magnetically attracted to partial extraction. A switch (status signal D) indicates the presence of a partially extracted microfiche and the carousel is brought to a controlled halt as an extended T-Bar affixed to the X-Y Assembly captures the code clip. (Refer to Figure 2.1.3 for the inverted T notch located approximately in the center of the code clip.) The Carousel and Elevator Servo Controller then signals the Mech-Optics Controller to activate the Spreader (A14A8) to separate microfiche from each side of the selected microfiche. The Spreader indicates when this operation is complete (status signal C) and the Mech-Optics Controller transitions to the Readout sequence state. In this state, it moves the X-Y Assembly via the X-Y Controller away from the load position thereby retracting the T-bar and pulling the captured fiche against two positioning pins as the microfiche is removed from the carousel. The X-Y Transport proceeds to move to the X and Y axis readout start positions. From this point and through readout completion, microfiche handling is identical to that described for the Verifier (1A3).

Upon completion of MR data readout at desired tracks, the Logic Assembly issues an end-of-fiche command to the Mech-Optics Controller which transitions to the Exit sequence to move the microfiche back to the load position and reinsert it into the carousel. The Mech-Optics Controller then transitions to the Mech Exit sequence state to retract the spreader mechanism and request a carousel bump (rotation) of the Carousel and Elevator Servo Controller. The bump serves to disengage the selected microfiche from the extended X-Y Assembly T-Bar. Once the bump is completed, the Mech-Optic Controller returns to the Park sequence state, commands the X-Y Controller to move the X-Y Assembly servos to the Park position, retracting the T-Bar.

In order to purge a dummy microfiche and replace it with microfiche containing data or replacing/updating an existing data microfiche, some modifications to readout sequencing have been incorporated. Fiche selection occurs just as for readout by selecting any dummy microfiche (up to 25 dummy microfiche reside at any unfilled carousel level) or the unique data microfiche to be replaced. However, instead of halting the carousel with the partially extracted microfiche at the Spreader\*, the carousel is rotated to the access door in the environmental enclosure allowing manual access to any carousel level. Here, the Mech-Optics Controller transitions to the Exit State, bypassing the Readout and Mech Exit States to signal the operator via the PRG indicator that a fiche is ready to be purged. After the partially extracted microfiche is replaced, the front panel PRG switch on the Mech-Optics Controller is reset allowing the Mech-Optics Controller to request a bump from the Carousel and Elevator Servo Controller.

\*During a purge process, the Spreader is not activated and it remains in the retracted position.

With the bump complete the Mech-Optics Controller returns to the Park sequence state, ending the purge and microfiche replacement process.

#### 2.2.4.2 Data Readout

For the Storage and Retrieval Unit, the X-Y Assembly readout optics and electronics are identical to that for the Verifier and need no further description. Similarly, the Logic Assemblies of the S & R Unit and Verifier are identical and interchangeable. This precludes further description of bit decision, hologram synchronization, ECC decoding, and output data transfer to the Controller except to note that the Logic Assembly is primarily operated as a data readout rather than verifying device.

#### 2.3 Operational Capabilities

The operational capabilities of the HRMR system provided in response to SOW requirements and/or necessary to system operation are summarized in this section. These include capabilities provided by the approach taken in the hardware design for nominal operation, the capabilities or features provided by the software development, and off-line capabilities. Various technology development items which provide the HRMR system unique capabilities (i. e., AOBD linearization, air bearing platen, automatic film handling, etc.) are treated extensively elsewhere and will not be included in the summaries to follow.

##### 2.3.1 Film Chip Cassette Loading

Two film cassettes, each capable of holding fifty film chips, are provided so that uninterrupted recording can be sustained. A single cassette is affixed to the Fiche Loader Assembly located at the interior environmental enclosure panel of the Recorder (1A1). Film chips are then extracted, one at a time from the cassette, by the Fiche Loader

vacuum head and inserted in the film transport where it is routed to the X-Y Transport for accurate positioning during recording. Empty cassette replacement is possible during recording of the last film chip.

#### 2.3.2 Queue Transports Maximize Throughput

Five queue (Q) transport sections automatically queue fiche between the Film Processor and the Verifier in a first-in-first-out jobbing sequence. The Q transport sections operate to pass a fiche through the section to the next section unless the next section is empty. If the next section is full, the fiche is captured and the preceding section is notified to keep fiche from entering the next section. When a fiche is removed to the Verifier, each section advances one fiche.

#### 2.3.3 Verifier Data Readout Of Clipped Fiche

Although the Verifier is normally used to verify data integrity of unclipped fiche, it can be placed in a mode to read clipped fiche as a backup to the S & R Unit. The Verifier is interlocked at the front panel to bypass fiche loading at the Load Transport as the clipped fiche is affixed to the X-Y transport in the Park position, it does not apply vacuum for fiche hold-down as a spring bar performs this function, and it does not drop the fiche into the Exit Transport as the fiche is to be manually removed after the X-Y Transport returns to the Park position. Interlocking intercepts computer commands to prohibit any motion from the Park position unless the front panel LD/EX switch is activated.

#### 2.3.4 S/R Unit Purge/Load

As the purge, load, or exchange of fiche at the S & R Unit involves automatic sequencing and manual replacement of fiche to the carousel, this process is interlocked by the purge (PRG) switch and computer command (OP CODE 02) such that a front panel light indicates

when fiche selection and proper carousel rotation to the purge/load door is complete, and inhibits all carousel motion until the purge switch is reset.

### 2.3.5 Fault Monitoring And Display

Extensive fault monitoring is employed throughout the HRMR System to insure immediate notification and/or equipment shutdown to prevent potential damage to electro-mechanical components. Faults are categorized and displayed on front panels and the CONTROLLER's CRT display. These include:

- A. Faults associated with the X-Y Transport (3) and CSR Servo Controller (6) are monitored by the appropriate Mech-Optics Controller and each fault results in equipment shutdown.
- B. Self test faults associated with improper calculation of X-Y axis Go-To positions (3) by the Mech-Optics Controller also result in equipment shutdown.
- C. Laser output power out-of-tolerance, AOBD linearization degradation, and human read spinner loss-of-facet synchronization at the Recorder result in front panel and CRT reported faults by the Mech-Optics Controller.
- D. Data recording or readout rate which exceeds data transfer rate from or to the Controller Unit results in a fault reported by each Logic Assembly.
- E. Film Stacker faults (2) in the Recorder Unit and Carousel Elevator faults (3) in the S & R Unit are reported to the appropriate Mech-Optics Controller and appear on the CRT display.

F. Q Transport fiche overflow is prevented by a non-volatile up/down counter that prevent further recordings if the count reaches four. The RCDCTL programs also monitors a software queue count to prevent overflow.

G. Film Processor overflow tripping a water level indicator in the processor drain pan deactivates a solenoid to shut off inlet water and initiates an audio alarm. The overflow circuit must be manually reset.

H. Servo beam positioning is provided for readout to maintain bit reconstruction and diode position alignment.

#### 2.3.6 Optics Monitors

Laser power monitors provide out-of-tolerance faults, as well as front panel meter display of record and readout power. Additionally, readout beam position (3) monitors are provided by panel meters to indicate any necessary optics alignment at the Verifier and S/R Logic Assemblies.

#### 2.3.7 HRMR Software

All HRMR software has been written in assembly language and runs on the DEC PDP-11/45 (Controller; 1A4) under the RT-11 foreground/background monitor. No special software apart from the RT-11 system is needed for HRMR system operation. The software includes programs to control the recording processes (Record Control: RCDCTL), the verification process (Verifier Control: VERCTL), which operates under the RCDCTL, and storage and retrieval readout (S & R Control: SARCTL).

As recording and verification take place in a time shared mode with several fiche "in between", the VERCTL communicates with the foreground Record Monitor (RCDMON) program to obtain control

data as to which microfiche is to be verified. A timer is set to alarm should verification take too long and error count is monitored to control fiche ejection into an acceptable or reject stack (chute) at the Verifier exit.

#### 2.3.8 Controller Tasks

Typical tasks within the HRMR system initiated by execution of programs in the Controller are:

- A. Scan a document on the Digitizer and store the resultant data on disc.
- B. Provide statistical (Huffman) encoding on digitized data and transfer encoded data to mag tape.
- C. Retrieve digitized data for CRT display or recording.
- D. Transfer an input file from mag tape to disc.
- E. Transfer a file from disc to the Recorder for HR or MR recording.
- F. Monitor recording and verification of fiche to validate all recorded MR files.
- G. Transfer any file from Verifier or S/R to Controller.

#### 2.3.9 Offline Capabilities

The offline capabilities include those functions which may be easily initiated at the front panels to interrupt normal operation and maintenance aides incorporated in the circuitry to allow rapid isolation of malfunctions. A few examples of each provides insight to off-line functions.

Those initiated at front panels include:

A. Jog controls to allow motion of the X-Y Transports with "end-this-sequence" interlock to allow jog control from known positions. Additionally, jog controls are normally "lock-out" by a switch in the environmental enclosure (recorder) or logic switch behind the Mech-Optics Controller front panel to prevent accidental activation.

B. Load/Exit activation from the Park position to load and exit a fiche bypassing record or readout to allow monitoring of fiche transports and accurate fiche positioning of the X-Y Transport vacuum load.

C. Queue counter reset provided by queue advance to zero at Recorder after queue overflow and queue decrement switch at the Verifier to set the counter to any initial value as dictated by the quantity of fiche in the Film Processor and Q Transports.

D. Displays provide status of 16 bit Controller command words, single and double readout error count, X-Y Transport position to 110 ppm, and opcodes of faults.

E. Front panel switches allow S/R Elevator/Carousel off-line exercising.

Examples of maintenance aids includes:

A. Chassis isolation from system with input command exercising for chassis response.

B. Load response simulation to allow repetitive cycling of functions.

C. Macrofunction isolation and sequencing.

D. Built in exercising of memories and accumulation functions with incrementing and decrementing ramps.

## 2.4 Technology Developments

The purpose of the HRMR program was to address a set of challenging requirements in a number of technical areas related to data storage and retrieval; these included data capacity, data rate, archival storage, system throughput time, on-line recording, processing, and verification, data integrity, etc. To address these requirements successfully, the program required the successful use of a powerful combination of modern electro-optical technologies, some of which were not yet fully developed at the program's inception. As a result, many of these technologies were specifically developed and improved during the HRMR phases, to the point that they could be responsive to the system's needs. In subsequent sections of this report, we will provide detailed discussions of each key technology area, addressing several contexts including experimental testing and tradeoff analysis, system performance, and problem areas. To prepare the groundwork for those later sections, and to give added depth to the previously presented system overviews, this section will present brief synopses of each of the key devices or technologies used in the HRMR-II system.

### 2.4.1 AOBD Linearizer

To scan the laser beam along the length of the hologram during recording, the HRMR-II system employs an acousto-optic beam deflector (AOBD). This device (explained more fully below in Section 3.2) functions by causing the light beam to be deflected from a sound wave within a crystal. The sound wave is generated by an external voltage-controlled oscillator (VCO) which feeds a piezoelectric transducer attached to the crystal. The angle of beam deflection is proportional to the frequency of the sound wave; thus a time-linear scan requires a time-linear VCO frequency ramp output. The scan linearity is an important system parameter, since nonlinearity can be a

mechanism for crosstalk between stored data bits, degrading the system SNR and hence the achieved bit-error rate.

The degree of frequency ramp linearity required for proper system performance exceeds that achievable with a simple ramp-driven VCO, due to thermal drifts, etc. Accordingly, a technique has been developed for use in the HRMR-II system which senses linearity deviations and provides feedback to correct the VCO output (usually prior to every recording). Essentially, this technique involves the use of a RAM memory, in which appropriate VCO drive level information is stored. This stored information can be changed to reflect currently appropriate values, based on received feedback signals describing the light beam's time of flight past fixed reference points and the linearity of the VCO's frequency sweep. Once the updating of the RAM memory is complete, its values are used to drive a digital to analog converter, which in turn feeds the VCO. The development of this linearization process was a key element in the system's history, since it permitted the practical implementation of the AOBD scanning system.

#### 2.4.2 AOM Linearizer

A very similar process to that described above was involved in linearizing the acousto-optic modulator (AOM). This device, which precedes the AOBD in the optical path, is used to control the laser beam intensity as it travels along the length of the hologram. It does this by interacting the light beam with a variable-intensity, fixed-frequency sound wave within a crystal. Thus the beam angle is not changed, but its intensity becomes a copy of the amplitude of the AOM's input signal.

In this device, the quantity that needs linearizing is the relationship between the input signal amplitude and the output beam intensity. Since this somewhat nonlinear relationship is a device characteristic and not subject to thermal or other drift sources, it

need not be re-linearized for every recording as was the case with the AOBD. Accordingly, the technique developed to accomplish this task in the HRMR-II system involves the use of PROM memory. This memory serves as a look-up table to translate the commanded input amplitude into an input which will produce the desired output. A further discussion of this procedure and the experimental results achieved with it is given in Section 4.1.2.

#### 2.4.3 Photodiode Detector Array

When the holographically stored data is reproduced in the verifier unit, its format is that of a linear array or line of optical spots. To detect these spots for thresholding and electronic processing, a detector array is required. After appropriate tradeoff analyses and experimental evaluations were completed (full details of these studies appear below in Section 3.2.2.8), the decision was made to use a self-scanned integrated photodiode array based on a modification of a standard Reticon, Inc., device. The technical requirements for this device were high sensitivity, wide dynamic range, good element-to-element uniformity, and good interelement isolation. The subcontracted device development program performed by Reticon to a Harris spec resulted in a 256 element array with 0.5 mil by 24 mil photoreceptor sites on 2.0 mil centers. Performance of this device in the HRMR system far exceeded anything attained by the previously available integrated arrays, and contributed significantly to the successful recovery of data at the required rates.

#### 2.4.4 Air Bearing Platen

High packing density recording, a desirable feature of mass data storage systems, requires that each recorded hologram be as small as possible consistent with later successful playback of the recorded data. Optical recording of small holograms requires the use

of tightly focused light beams, which produces a restricted depth of focus within which successful recording can take place. Traditionally (and in the HRMR-I system) the approach taken to positioning the film within the depth of focus region has been to hold it rigidly in contact with a vacuum platen located just behind the focal plane. This, however, produces film surface degradations (scratches, digs, etc.) which seriously degrade the system bit-error rate performance. For the HRMR-II system, an alternative scheme, based on the use of a dual-surface, positive pressure air bearing platen, was developed. This technique proved capable of restricting film motion to within a  $6 \mu\text{m}$  range (well within the depth of focus) without touching or degrading the film surface, and thus contributed to the successful recording experiments achieved by the system. Some additional details of this tradeoff are given in Section 3.2.2.7.

#### 2.4.5 Transform Generator

To record a synthetic Fourier Transform hologram, the recording system must have serial access to the Fourier coefficients representing the data pattern to be stored. These coefficients, which are generated automatically in an interferometric holographic recording system, must be rapidly calculated electronically in the HRMR-II system. To accomplish this, a transform generator assembly (TGA) is used. First, digitized cosines of various frequencies are stored in a PROM; when a bit in a hologram is set to "one", the corresponding cosine is added into the hologram coefficient representation; finally, the summed cosines can be scaled as appropriate to match the various frequency response characteristics of the system, and the resulting coefficients sent serially to the recording modulator. The TGA implementation in the HRMR-II system has performed well and has fully supported the

required data rates and resolutions. Some details of the experiments involving the TGA can be found in Section 4.1 and 4.3.

#### 2.4.6 Spinner Development

The HRMR recording system is configured to use a single light source and modulation technique, while the scanning mechanisms for the HR and MR systems are separate. For the MR system, an AOBD is employed, as discussed in Section 2.4.1 and elsewhere. For the HR system, the tradeoff process described in Section 3.2.2.4 resulted in the selection of a different scanning technique, a multi-faceted spinning mirror. This optical line scanner (OLS) provides the capability to record microimages (24X reduction) at a speed of 1.7 seconds per page. The pages are recorded in a raster scanned format using 1700 horizontal lines.

During the design effort a table of spinner/lens solutions was generated around the baseline parameters of a 9.0 mm scan field and a 50-75% duty cycle; also considered were the number of facets and spinner configuration (pyramidal or polygonal). These four parameters are sufficient to completely specify the spinner/lens configuration. An attractive solution was found at 20 facets in the pyramidal configuration, which took advantage of an existing flat field scan lens design. The resulting spinner turns at 2930 RPM in order to meet the 1.024 msec line record time and 1.7 second page record time.

The OLS generates a start-of-line pulse when each facet is in the proper orientation to begin a scan line. This start of scan feature reduces the effect of velocity errors as well as facet-to-facet angular errors resulting from spinner head manufacture. Velocity errors within a line can still contribute to image degradation even though reset is accomplished at the beginning of each scan line. For this reason Harris imposed a 0.01% short term velocity specification

on the spinner controller. Another major contributor to potential image degradation is spinner facet-to-axis errors from facet to facet. In this case, Harris specified that this error be less than  $\pm 1$  arc second between adjacent facets and  $\pm 2$  arc seconds between any two. In future systems, because of the cost and complexity of these two specifications, electronic correction may be called for. The tight velocity control requirement can be eliminated by generating a position clock which corresponds to the position of the beam along the page, and using it to properly sequence the data. Tight facet-to-axis tolerances can be eliminated by deflecting the record beam in a programmed manner to compensate for these errors.

#### 2.4.7 Carousel/Elevator Assembly

The carousel and elevator mechanisms of the Storage and Retrieval unit provide the means to select and extract or replace a microfiche at a unique location on any of nine levels. A Harris developed carousel with Harris perfected (Image Systems Remcard compatible) code clips bonded to each microfiche is used along with the Image Systems Remcard selector and fiche spreader mechanisms.

Each code clip includes the following features: pin seating notches to assure precise location of each microfiche relative the the readout beam; a unique (0 through 999) notched code which the selector can use to separate each microfiche from its neighbors and partially extract it from the carousel perimeter; a "T" bar to capture the extended microfiche as the carousel rotates to a stop; and a spreading mechanism to minimize interfiche contact during removal and replacement operations.

A carousel consists of two circular plates separated by 31 partitions, resulting in 30 wedge-shaped fiche storage cubicles. Up to 25 fiche can be placed in each cubicle, with the code clips facing

outward to be accessed by the stationary selector. The carousel is rotated about its axis in two seconds, passing each code clip once through the selector station. The selector consists of a magnet to attract the clips and a series of solenoid-actuated fingers to handle the decoding. As the clips are rotated, the fingers hold unmatched clips in the carousel, while the clip that matches the finger positions is allowed to be drawn out by the magnetic field. The selected fiche is then captured by the T-bar as the carousel comes to a controlled stop.

The elevator system is a unique HRMR development. It moves the entire read station to one of the nine carousel levels which are vertically stacked along a common axis.

The elevator/carousel approach has been successfully demonstrated to be a reliable technique of random access to multi-level fiche storage, and to provide convenient purge/update capability for a microfiche oriented mass data store. A potential disadvantage is the hand operation necessary to affix the code clip to the fiche. Reasonable care must be exercised in positioning the clip and fiche in the vacuum holding fixture during bonding. A potentially acceptable alternative to clipped microfiche would be to assign a specific location in the carousel to each fiche and index the carousel to this location to remove or replace the fiche.

#### 2.4.8 Clipless Fiche Handling

Another important achievement was the internally funded development by Harris of a proprietary clipless carousel, which is dimensionally similar to the Remcard carousel. It provides 500 dedicated, indexed microfiche storage slots along the circumference of the carousel (as opposed to the 750 provided by the standard Remcard device). It achieves microfiche extraction by a unique vacuum platen assembly,

rather than a T-bar capture of a notched code clip; also, a spreading mechanism is not necessary, as no contact between microfiche is possible.

The overriding design feature of this device is that it allows a slight decrease in storage capacity per carousel to be traded for a completely clipless fiche handling system. This development promises to be of significance in all future fiche-oriented data storage and retrieval systems.

#### 2.4.9 Automatic Film Handling and Processing

The HRMR system provides completely automatic film handling from recording to processing and finally to the Verifier unit. This is accomplished using fiche transport mechanisms to move the fiche and pneumatic pistons to position the fiche on the recording and verification XY assemblies. Film processing, including development, fixation, rinsing, and drying, is provided by a built in Kodak Versamat 5N processor, which is interfaced to the system by automatic entrance and exit transports. A special queue transport at the processor exit provides greater microfiche throughput flexibility.

The key to the automatic film handling concept employed in HRMR-II is the fiche transport using edge-guide slots and pinch roller drive. The fiche are moved through the slots (along their long dimension) by the motorized pinch rollers, which are spaced so that they can pass the fiche along from one to the next. Each pinch roller assembly consists of a large diameter polyurethane bonded roller with a high frictional coefficient, surrounding a small diameter self-equalizing anodized aluminum rollers. This inner roller maintains a constant pressure point of contact on the polyurethane surface, providing some accommodation of any eccentricities or flat spots on the roller without affecting film velocity or permitting slippage.

The performance of these transport systems has been good for more than one year since installation. However, recent experience indicates that a desirable additional feature for these mechanisms is the use of sealed bearings; the unsealed bearings originally used have been found to be a source of minute amounts of oil which can eventually migrate to the film surface. Although no system performance degradation attributable to this oil has yet been noted, it could be a source of film surface damage and hence impact the system's achievable bit-error rate levels.

## 2.5 Problem Areas and Potential Improvements

As we will see in the later sections of this report, the HRMR-II system was successful in meeting most of its original goals in the key technical areas of data rate, data capacity, data integrity, and fiche handling and processing. However, during the course of the system's development and integration, a number of problem areas were identified which imposed limitations on the system's performance in several important areas. In Section 3.3 below we will provide a detailed description of many of these problem areas, while Section 4.3 describes the experimental and diagnostic procedures undertaken to seek solutions to the problems and to suggest future implementation improvements. In this section, by way of summary of these results, we will now present a set of descriptions of those areas in which desirable and cost-effective gains can clearly be made in terms of future system performance.

### 2.5.1 AOBD Drive Linearization

As discussed above in Section 2.4.1, the AOBD linearizer was an important development in the life of the HRMR program; by permitting a linear input/output relationship to be maintained, it made the use of the simple, solid state acousto-optic scanner possible. However, the linearization process currently must be repeated prior

to each recording. A possible cure for this instability is an increase in signal-to-noise ratio in the detector which provides feedback to the linearizer. This could be accomplished by simply replacing the mask that provides scan position reference marks with a negative of itself. This would make the signal of interest a positive-going signal out of an essentially zero reference level, rather than the current negative-going signal from a high, noisy light level. Thus about a 6dB increase in SNR could be achieved, greatly increasing the system's reliability, maintainability, and stability with respect to optical power level variations. Since the scale of the recorded data also depends on proper linearization, this change would also provide greater independence of scale from laser power level variations. A second potentially cost-effective improvement to the linearizer system would be the upgrading of the D/A unit. A unit (not currently available but projected for the near future) with improved transient characteristics would provide a surer, smoother adaptation of the feedback system to the correct values, with reduced overshoot and therefore faster and more accurate linearization.

#### 2.5.2 AOBD Cell

Reduction of potential sources of bit-to-bit crosstalk is always a worthwhile activity in a system like HRMR-II. Such a potential source is provided by unwanted light reflections within the AOBD cell. In the system as currently configured, these reflections are filtered downstream in the optical system, so that they do not degrade system performance; however, the small aperture through which the beam must pass to perform this filtering is a critical point in the system's alignment. Thus removal of the unwanted reflections at their source could make the use of the aperture unnecessary, increasing the optical alignment stability of the system. To remove the reflections requires simply a

modification of the angles at which the faces of the AOBD cell are polished. Thus replacement of the AOBD cell with an improved design would be the simplest way to solve this problem.

### 2.5.3 HR Spinner

Another component which could provide a performance improvement with only minor alteration is the HR spinner. This unit, a multifaceted spinning mirror which deflects the recording beam across the 9 mm width of the HR image plane, could be improved both mechanically and optically. Mechanically the required change is increased rate accuracy. Currently the amount of "jitter" experienced, after the re-synchronization that occurs on each line, is great enough to cause recorded letters near the end of scan to begin to break into separate pieces, decreasing legibility. Solutions to this problem include repair (cleaning, etc.) or remanufacture of the bearing structure, and adding inertia to the spinner head to integrate out the jitter and vibration.

Optically the change required is protection for the mirrored surfaces of the device, as well as replacement of the current head. The lack of such protection during the previous system integration has resulted in noticeable deterioration of the optical quality of the facets. The specification and performance of the spinner unit are judged to have been correct; the required changes are in the areas of protection and maintenance.

### 2.5.4 Threshold Averaging Technique

To make decisions on the recovered analog data, the readout electronics employs a thresholding scheme which averages the detected values from the previous seven holograms. This provides a measure of immunity to rapid fluctuations in signal intensity level, allowing the threshold level to track the fluctuations and maintain the proper

value. Two potential improvements to this technique have been suggested. First and most simply, an increase in the averaging time from 7 holograms to 15 or more would provide additional threshold immunity to the rapid bit height fluctuations which have been observed. This technique could provide a modest decrease in the system's raw BER, since the threshold would more accurately track the proper decision level.

The second suggested change involves a major alteration in the recording and thresholding processes. This "differential encoding" scheme would record two bits for each bit to be stored. In readout, the difference of the two bits would be the signal to be thresholded. Thus the proper decision level would be permanently and identically zero, and no threshold tracking would be required. To achieve this advantage, either a packing density reduction (recording two bits for one) or a change to the TGA unit (recording the two bits at reduced resolution) would be required. Therefore, differential encoding cannot be fully recommended until appropriate tradeoff analyses and system use studies are completed. Nevertheless, it does represent a potentially significant improvement in system BER performance and design simplicity, and should therefore be given serious consideration.

#### 2.5.5 S & R Counterbalance Technique

Rapid access time from level to level within the S & R elevator mechanism is an important system goal. To achieve a decreased access time, a true counterbalance system could be employed. Currently, a spring-tension device is used. Initially, the spring device was set for null force near the center of the elevator's travel, with increasing restoring forces near either end; however, that technique made excessive demands on the servo compensation loop and stability was difficult to achieve. A stable design was achieved by moving the

null force point to or beyond the end of the elevator's travel. The only remaining problem was the necessity for the servo to work against the spring force; this design resulted in a system which was stable but slow. The most reasonable solution to improved elevator access time is to implement an improved counterbalance scheme designed around a true counterweight; although this would require new mechanical and servo designs to be implemented, the improvements offered may be of sufficient importance to some system scenarios to merit the effort.

#### 2.5.6 System Thermal Stabilization

Forced air ventilation of the system enclosures of the HRMR-II system provides a level of cooling and temperature stability which is adequate to support the performance levels described in this report. However, in certain areas, unexpected levels of thermal sensitivity were observed which made frequent system optimization a necessity. This problem was especially acute with the vendor-supplied CSR Systems 550 XY controllers, and especially in the recorder, which has a larger heat load and higher component density than the other system modules. The effect observed is that, due to thermal overload, offsets build up in the servo controllers and power amplifiers which prevent proper servo nulling. The solution to this problem is straightforward: provide additional ventilation. The efficiency of the forced air system can be increased by operating in a positive pressure mode to increase the heat capacity of the flowing air; additionally, accurate baffling for flow direction of the moving air to the areas most in need of cooling would enhance the system's efficiency. Implementation of these few simple changes to the system could greatly increase its short and long-term alignment stability.

### 2.5.7 Vibration Effects

The effect of mechanical vibrations on the recorded holograms, and the attempts to isolate and eliminate the vibration sources undertaken during the HRMR-II program, are discussed in the experimental section of Chapter IV. Basically, such vibrations cause variations in the spacing of the recorded holograms, which results in a frequency change as a function of track position during readout. Thus the phase-locked-loop (PLL), which generates the hologram-synchronous readout clock, must accommodate these changes, or else the data decisions will be made at times not correctly corresponding to the hologram positions, and the BER will be degraded. During the experiments reported in Chapter IV, several potential vibration sources (including the air blowers, film processor, and reader-recorder interaction) were investigated and determined not to be major contributors to the problem. Another potential source is the smoothness of the lead screw in the fiche transport mechanism; also, mechanical resonance effects are known to be present and to be capable of increasing or decreasing the vibrations, depending on the configuration. This area is one which is worthy of further investigation and design correction, with the benefit to be gained being a reduction in raw bit error rate and more repeatable system performance.

### 2.5.8 Data Interleaving

Because of the presence of highly correlated (burst) errors in the raw data recovered from a recorded fiche, the full power of the error-correcting code employed by the system is not currently being achieved. For truly random errors, the implemented code should be able to correct the observed raw BER (of around  $2 \times 10^{-4}$ ) to a level between  $10^{-7}$  and  $10^{-8}$ . The fact that this is not achieved (in fact, corrected BER's are observed to be usually worse than  $10^{-6}$ ) is clear

evidence that such burst error activity is taking place. There is a straightforward solution to this problem: interleave the stored data to such an extent that any error burst can affect at most one bit in any codeword. This would result in a dramatic decrease in the system's corrected BER. The only price paid for this gain (other than hardware costs) is that a large buffer is required to allow deep interleaving during record and readout. Interleaving to the deepest extent practical is highly recommended. The tradeoffs involved in the interleave process, as well as an attempt to determine experimentally the proper interleave depth, are discussed in detail below in Section 5.1.

#### 2.5.9 Film Processing

To make high-density archival data storage on microfiche practical, a method of rapid, high quality film processing is required. The tradeoff process (described elsewhere in this report) which led to the selection of the Kodak Versamat 5N processor for use in the HRMR-II system included consideration of cost, size, and processing performance. The resulting processor, as integrated into the system, provided a dependable source of on-line film processing capability fully contained within the system cabinet. Experiments performed during system evaluation phase, however, indicated that the machine processing added a noticeable contribution to the bit-error-rate of the system (as detailed in Section 4.3). Thus, although the Versamat 5N appears to be the best choice under the current constraints, it is clear that relaxation of one or more of these constraints could lead to the selection of a processor which would support substantially lower system error rates. Therefore, it is recommended that, for any future system where BER is an important consideration, the film processor tradeoff be critically reviewed to determine the best way of achieving the required BER levels.

### III. REQUIREMENTS AND ACHIEVEMENTS

Section II provided a functional description of the HRMR System. In addition, the major technical challenges at a system level were reviewed and the performance levels achieved were presented. Thus Section II provided the background necessary to appreciate the technical detail to follow.

This section begins with a synopsis of the original requirements established for the HRMR System. Following that, the technical approaches chosen to implement subsystems to meet the requirements are described. Tradeoffs of various technologies with final approach selections are reviewed. Merits and encountered limitations of selected technical approaches are discussed. Finally, this section concludes with an assessment of the approaches taken with consideration for further improvements.

#### 3.1 Technical Requirements

The HRMR Microfilm Mass Memory System design was guided by requirements specified in the RADC PR#I-4-4422 (Revised) Statement of Work (SOW). Key requirements have been extracted and itemized in Table 3.1 with each item referenced to the applicable SOW paragraph, as well as the acceptance test procedure (ATP) sequence number for future reference in the Performance Demonstrations and Conclusions Section.

TABLE 3.1 KEY REQUIREMENTS SUMMARY

Requirement	Test Method		Reference	
	Inspect	Demo Measure	SOW	ATP Sequence
Physical Characteristics				
HRMR Microfilm Mass Memory System				
HRMR Subsystem	*		4.1.1.1	0001-0008
MS & R Subsystem	*		4.1.1.2.1	0145-0148
Recorder Unit of HRMR Subsystem				
Utilizes 105 mm x 148 mm sheet film		*	4.1.1.1.1	0010
Title Block Recording (6 point type size)		*	4.1.1.1.1	0039
MR Binary Data Recording		*	4.1.1.1.1	0009
30 x 10-6 Bits/Microfiche		*	4.1.1.1.1	0012
500K Bits/Sec Record Rate		*	4.1.1.1.1	0015
HR Alpha Numerics Recording				
(8.5 x 11 Inch)		*	4.1.1.1.1	0017
24X Microimage Reduction			4.1.1.1.1	0024
98 Microimage/Microfiche		*	4.1.1.1.1	0026
80 Characters/Line		*	4.1.1.1.1	0035
60 Lines/Page		*	4.1.1.1.1	0036
STD NMA Format		*	4.1.1.1.1	0038

Table 3.1 Key Requirements Summary (Continued)

Requirement	Test Method		Reference	
	Inspect	Demo Measure	SOW	ATP Sequence
HR Graphic Arts Recording	*		4.1.1.1	0018
Curves		*	4.1.1.1	0020
Charts		*	4.1.1.1	0021
Maps		*	4.1.1.1	0022
Line Drawings		*	4.1.1.1	0023
Automated MR Recording		*	4.1.1.2	0064
Automated HR Recording		*	4.1.1.2	0063
Automatic Film Processing		*	4.1.2.5.4	0161
Verifier/Reader of HRMR Subsystem		*	4.1.1.2	0084
Read Binary Data		*	4.1.1.2.1	0099
Random Access of Readout		*	4.1.1.2	0095
Transfer Data to Controller CPU		*	4.1.1.1.2	0065
Readout Bit Error Rate $1 \times 10^{-7}$		*	4.1.1.2	0096
500K Bit/Sec Readout Rate		*	4.1.1.2.3	0103
Automated Readout		*	4.1.1.2.3	0104
Manual Load Readout		*	4.1.1.2	0092
Accept MS & R Code Clipped Fiche		*	4.1.1.2	0093
Readout MS & R Code Clipped Fiche		*	4.1.1.2	0093

Table 3.1 Key Requirements Summary (Continued)

Requirement	Test Method		Reference	
	Inspect	Demo Measure	SOW	ATP Sequence
<b>HRMR Subsystem Software</b>				
Operate Software	*		4.1.1.3	0120
Info Retrieve Software	*		4.1.1.3	0123
Multi-task Operation	*		4.1.1.3	0124
Graphic Arts Digitization	*		4.1.1.3.1.1	0129
Graphic Arts Data Compression	*	*	4.1.1.3.1.1	0134, 0135
<b>MS &amp; R Subsystem</b>				
6750 Fiche Storage Capacity	*		4.1.2.1	0145
15 Second Random Fiche Access		*	4.1.2.4	0150
Purge and Refile Microfiche	*		4.1.2.4	0151
Read Binary Data	*		4.1.2.5.1	0155
Readout Bit Error Rate $1 \times 10^{-7}$		*	4.1.2.5.1	0158
500K Bit/Sec Readout Rate		*	4.1.2.5.1	0156
<b>Laser Safety Interlocks</b>		*	4.1.3	0168

### 3.2 Technical Approach

To achieve the requirements set forth in the previous section, the HRMR system employs a unique combination of optical, mechanical, and electronic technologies. The selection, optimization and integration of these technologies into a system capable of meeting the stated goals was the key activity on the HRMR program. In most cases, a number of technical approaches were considered as candidates for each system function, and were evaluated in terms of performance and compatibility with the rest of the system. The central criteria used in evaluating each technical approach involved its ability to support the global system parameters (I/O rate, I/O format, storage accuracy, and storage capacity) in a cost-effective way and with minimum risk.

In this section we will describe the technical tradeoff and parameter selection process as it was applied to many of the important techniques employed in the HRMR system. We will begin with an overview of the HRMR system concept and its approach to the problem; then we will describe in some detail the design choices and tradeoffs made in several important component and subsystem areas.

#### 3.2.1 System Concept Overview

The approach to mass archival data storage taken by the HRMR-II system is based on the key concepts of fiche format storage and synthetic holography. The following paragraphs provide a basic description of the functioning of the MR recording and readout systems.

##### 3.2.1.1 Data Format

Data is stored in the HRMR system in blocks of 48 user bits. To each incoming 48 user bits are added 13 parity bits for error detection and correction purposes, as well as 7 additional overhead bits used for sync, threshold, and maintaining optimum hologram bit populations. These 68 bits are then stored in synthetic one-dimensional Fourier holograms. One-dimensional here implies that the hologram shape is long and narrow, with holographic fringes (and hence information) being recorded only along

the length of the hologram. Because they are Fourier holograms, each "one" bit stored is represented by a sinusoidal fringe pattern extending through the entire length of the hologram. Thus the fringe pattern written in a given hologram is a superposition of sinusoids of different frequencies representing those bits that should be "ones" in that hologram.

#### 3. 2. 1. 2 Synthetic Holography

In an interferometric holography approach, the fringe patterns representing the bits to be stored are generated by interfering a reference beam with a group of binary-weighted signal beams. The resulting interference pattern is a combination of different frequencies representing "one" bits, the frequency of each bit being determined by its angle of incidence on the film with respect to the reference beam. To generate a synthetic Fourier transform hologram, a different approach is required. In that technique, a single beam sweeps the length of each hologram, writing appropriate amplitude fringes as it goes. This implies that instead of being generated by an interference process, the fringe amplitudes must be electronically calculated in advance, so that they can be serially written along the hologram's length. Thus a discrete Fourier transform process is employed to calculate the required number of coefficients for adequate bit-to-bit resolution. In the HRMR system, 512 coefficients are calculated and written twice along the hologram to provide double Rayleigh resolution of the 68 data bits. The writing process is accomplished via a laser beam which is intensity modulated and scanned as described in the following paragraph.

#### 3. 2. 1. 3 Recorder System

The light source employed by the HRMR system is a 15 mW Argon - Ion laser. The beam intensity is temporal modulated to represent the calculated fringe amplitude as described in the previous paragraph. This modulation is accomplished by means of an acousto-optic modulator (AOM). The AOM is an optical crystal in which light and acoustic waves

interact. The desired modulation amplitude is placed on a fixed frequency RF carrier and input to a piezoelectric transducer, producing travelling acoustic waves within the crystal. The variations in index of refraction produced by the travelling pressure waves then deflect at a fixed angle an amount of the laser beam which is proportional to the RF input amplitude, and hence to the desired modulation.

After amplitude modulation of the laser beam is accomplished by the AOM, it is conducted (via suitable lenses and mirrors) to the acousto-optic beam deflector, which performs the actual deflection of the beam along the hologram length. The AOBD is similar to the AOM, except that the input amplitude of the RF signal is held constant while its frequency is varied. Since the beam deflection angle is proportional to the drive frequency, this causes the beam to sweep in angle, and this motion is changed by appropriate scanning optics into a sweep in position along the hologram.

The fiche on which the holograms are written is held in place by a vacuum platen mounted on an X-Y transport mechanism. This transport moves the fiche parallel to its long dimension until approximately 9000 holograms have been written in a track with a length of 135 mm. Then the transport indexes one track width, retraces to the track start location, and is ready to record the next track. This process is repeated up to a total of 70 tracks per fiche (containing  $3 \times 10^7$  user bits).

When a fiche is completely recorded, the X-Y transport deposits it in the input of a linear transport assembly through which it is conducted to the built-in automatic film processor. After the develop, fix, rinse, and dry steps are complete (a matter of approximately 5 minutes), the fiche exits the processor and enters the queue at the entrance to the reader unit.

Several additional features of the recorder are worthy of note here. Photodiode monitors are placed at a number of strategic locations along the optical path; they provide information about beam intensity, as well as spatial and temporal modulation characteristics. One important function of these monitors is to provide feedback to the linearization

systems, primarily the AOBD linearization. The AOBD, because of the nonlinear and environmentally sensitive relationship between its input (the voltage to the VCO) and output (the beam deflection angle), must be linearized in a closed-loop way for each recording. This is done by using two of the monitor photodiodes to detect the arrival times of the beam at two fixed reference marks; the linearity of the chirp input frequency is also detected by a photodiode monitor. These data are then used to program a nonlinear input capable of producing the desired linear AOBD output. The AOM that performs the intensity modulation is the subject of a similar linearization process. Its linearization of input power versus output power, however, need only be done once, and hence is programmed into PROM.

#### 3.2.1.4 Reader System

When a recorded fiche is called for from the queue, it is conducted via the reader linear transport to the read station, where the vacuum platen mounted on the reader's X-Y transport accepts it. The holograms are then translated in order past the read station by the X-Y transport. At the read station, they are illuminated by a light beam whose source is a 15 mW He-Ne laser. The laser beam passes first through appropriate shaping optics, where it is formed in such a way that it can illuminate a single  $13 \mu\text{m} \times 1.4 \text{ mm}$  hologram; it is then conducted to the film. At this point, the hologram being illuminated causes part of the light to be diffracted into a number of directions, one direction for each "one" bit present in the hologram (because each bit is represented by a different frequency in the recorded holographic fringe pattern). These data carrying beams are then sent through a series of mirrors and lenses which shape them into individual spots for input to a photodiode array. Additionally the beam passes through several filters (slits or apertures) which serve to remove as much spatial noise or scattered light as possible. Finally the bits, now represented by spots of light, are incident on a linear array of photodetectors (a Reticon self-scanned array). This device converts the presence (or absence) of a bright spot at each detector to the detection

of a one (or zero) bit, using a threshold circuit capable of adapting to any slow changes in the average bit height. The detected bits can then be sent to the error-correction decoder for processing and transmission of the recovered user data back to the controlling computer.

When the data light is diffracted from the hologram, a portion of the input light is not diffracted; this light is used for a different purpose. By detecting the position of this undiffracted beam (with another photodiode monitor), any deviation of the beam due to film thickness variations can be observed. Since such deviations would also affect the diffracted data beams and cause them to be misaligned with respect to the data detectors, this "film wedge" effect is corrected by a closed loop feedback system. An electrically adjustable mirror in the film illumination path is changed slightly in position such as to ensure that the undiffracted beam stays centered on a split detector; this in turn guarantees that the diffracted data beams will also remain stationary on their detectors.

Both the Recording and Reader Systems receive timing and control signals from the control electronics subsystem; in addition, the control electronics system handles the tasks of interface with and data transfer to and from the main system computer.

### 3.2.2 Selection of Key Technologies

To meet the requirements for the HRMR-II system, a system design activity was required which would take full advantage of any and all advances made since the completion of HRMR-I in a number of key technical areas. In many cases, techniques used and tentative decisions made during the earlier program were no longer appropriate, due to the existence of new techniques or to more favorable experiences with previously non-competitive ones. Thus most of the decisions and techniques finally implemented in HRMR-II were the result of tradeoff studies which balanced the cost or performance advantages of the newly available techniques (or devices) against the proven performance and availability of the older methods. Sources of information used in these tradeoff studies included:

analysis and design calculations, experience obtained on HRMR-I, experience obtained on other related programs, experimental work, vendor survey data, and reports of the current state of the art from key component developers.

In this section we will detail the tradeoff studies and analyses made in a number of these key areas, and show why the system that resulted was configured as described in section 3.2.1.

### 3.2.2.1 Synthetic Holography

The advantages of recording digital data through the use of Fourier transform holograms are well known. Since the data is distributed over a relatively large area, significant reduction in the sensitivity of the recording to dust and other amplitude imperfections is achieved. In addition, the reconstructed data is spatially invariant under translation of the hologram which eases mechanical tolerances during the readout process. Fourier transform holograms may be generated synthetically or interferometrically. If implemented properly, both approaches result in essentially the same intensity distribution on the film. Thus, the reader unit is the same for both recording approaches.

In interferometric holography a spatially modulated beam of coherent light, called the signal beam, is mixed at the film surface with an unmodulated beam of light, called the reference beam. The interference pattern thus generated on the film surface is a hologram. Synthetic holography is different in that only a single beam of intensity modulated light is scanned across the film to create the hologram. The modulation is controlled electronically so that the proper pattern is exposed on the film surface.

Synthetic holography has an inherently simple optical system, and is quite versatile since scanning and modulating are electronically controllable. It requires the use of an electronic Fourier transform generator having enough bandwidth to expose the hologram sequentially, i. e., the synthetic recorder is a serial bit stream system. Interferometric

holography reduces electronic and mechanical complexity at the expense of increased optical complexity. Since the interferometric approach is essentially a parallel bit stream system, it has a higher speed potential. Required control electronics are simple and there are no moving parts except for the film. It requires an interferometrically stable mechanical platform during the hologram exposure time and high peak laser power to keep the fringes stationary during the exposure interval. In addition, a critical element in an interferometric recorder is the page composer (signal beam modulator). During the design effort for HRMR, several page composer candidates were functioning in laboratories, but they were not yet fully proven, operational components.

The decision to use synthetic holography in the HRMR system was prompted by the success with this technique achieved by the earlier phases of the program. By putting much of the burden of stability on the electronics subsystem, a higher probability of producing an operational deliverable system was assumed. Furthermore, the system simplicity mentioned above promotes a much more maintainable, repairable system which can be enhanced with a modular design approach.

Another important consideration for the choice of synthetic holography was the availability of high-performance acousto-optic beam deflectors (AOBD's). The use of an AOBD, provided that an adequate number of resolved spots can be produced, permits the MR recorder to maintain the desirable feature of no moving parts (except for the film). Available AOBD's could easily provide the number of spots required to write fringes corresponding to double Rayleigh resolution of 64 bits.

Additionally, for a given data rate, the serial production of fringes requires less optical power than the interferometric method; thus, a lower power recording laser can be used. This point is important because stable and reliable operation of any optical data storage system can be obtained only with a stable and reliable laser light source, and currently only the lower power units readily provide these characteristics.

### 3. 2. 2. 2 Recording Format

In determining the data recording format to be used on the fiche (for the MR data), both practical implementation considerations and system compatibility questions had to be resolved. The following subsections detail some of the design constraints and the resulting system parameter choices.

#### 3. 2. 2. 2. 1 Data Capacity Constraint

The availability of a fixed area in which to store the required 30 Mb of user data, combined with several practical implementation considerations, forces the adoption of specific recording format parameters in a number of areas. Specifically:

- a) The total number of hologram tracks per fiche should be divisible by 7 to fit within the NMA HR frame format. After consideration of all the factors herein, 70 tracks were selected as being optimum; there are then 10 MR tracks per HR row.
- b) The available track height must be accessible in  $12.7 \mu\text{m}$  (0.5 mil) Y position steps for economical lead screw implementation and 10 tracks should nest in each HR row. The closest solution is  $98 \times 12.7 \mu\text{m} = 1.2446 \text{ mm}$  per track, plus  $4 \times 12.7 \mu\text{m} = 50.8 \mu\text{m}$  steps every 10 tracks, plus two additional  $12.7 \mu\text{m}$  steps between the first MR track and the heading track.
- c) There must be at least 8929, 48 bit user holograms per track to obtain 30 Mb storage, plus 65 sync/error correction holograms per track for a total of 8994 holograms per track.
- d) The total inclined recorded length of each hologram track must allow for acceleration/deceleration at the end of each track so that the record window in the air-bearing platen comes to rest no closer than 1 mm inside the edge of the fiche. Ideally, at least 4 mm of unrecorded edge should

exist at each end of the track. The minimum fiche width based upon present Kodak cutting tolerances is 146.43 mm with up to 0.01% aging shrinkage allowed. Aging shrinkage was included in the 1 mm start/stop band allocation. The selected recorded track length is 136.4 mm peak-to-peak.

- e) Hologram tracks must be recorded far enough apart to allow for mechanical and optical positioning tolerances. The selected value of track separation is  $95\mu\text{m}$  as a result of experimental evaluation of these tolerances.
- f) Hologram width should be as wide as practical within other constraints herein for optical design purposes. Tradeoff studies considered 12.5 to 13.5  $\mu\text{m}$  hologram center-to-center spacing as being practical. A spacing of 13.0  $\mu\text{m}$  was selected as a compromise value because it yielded a workable track-to-track separation distance, a desirable scratch immunity, and an esthetically acceptable heading track character inclination.

#### 3.2.2.2.2 Data Readout Time Constraint

The requirement to read an entire fiche within two minutes is a constraint which pushes some of the mechanisms in the system to the limits of their capabilities. Some of the tradeoff considerations and the resulting compromise are:

- a) The following maximum platen movement rates have been established for reliable servo implementation:

X record velocity -	160 mm/sec
X retrace velocity -	200 mm/sec
Acceleration -	$\pm 3400 \text{ mm/sec}^2$

MR record direction is restricted to one platen travel direction (i. e. , left to right) to preserve record optica simplicity.

- b) The selected platen record velocity must coincide with recording holograms at a  $96 \mu\text{sec}$  rate to be consistent with system timing.
- c) Tradeoff studies which calculated the achievable readout time using the constraints herein showed that readout in two minutes or less requires a slight violation of the above velocity/acceleration limits. The selected solution provides a 2.02 minute readout time.
- d) Record time for a 71 track MR fiche (includes one heading track) is then also calculated to be 2.05 minutes

#### 3.2.2.2.3 Scratch Immunity/Heading Legibility Constraint

To provide some immunity to noise generated by scratches or other mechanically induced marks running parallel to the edges of the fiche, it is desirable to tilt the holograms at an angle to the fiche edges, thus taking better advantage of the "distributed coding" property of holographic systems. However, since the MR recording system must use the hologram format to write the heading track, the legibility of the track also constrains the hologram tilt angle. Some of the key considerations which led to the final tilt angle selection of  $31^\circ$  are:

- a) For optimum immunity to noise generated by fiche-edge-parallel structures, a hologram tilt of close to  $45^\circ$  is desirable.
- b) A design review of potential  $29^\circ$  and  $45^\circ$  heading character writing inclinations (inclined to the right) revealed  $29^\circ$  to be acceptable, but  $45^\circ$  was unacceptable. The selected  $31^\circ$  tilt to the right is thus considered acceptable without character tilt correction.
- c) The characters must be large enough to be easily read without magnification. Using Paragraph 7a of DIAR 59-3 as a guide, the characters should be 4.5 point type or larger.

The 31° tilted characters are 1.245 mm high or about the size of 6 point type.

### 3.2.2.3 Laser Wavelength and Vendor Selection

On the basis of the tradeoff analysis which is summarized in Table 3.2.2.3-1 the Spectra-Physics Model 163-02 Argon-Ion laser was selected for the recorder. The principal reasons for this choice were superior reliability, lifetime, noise characteristics, stability and warm-up time and the favorable performance of this laser on HRMR-I. Both of the He-Cd lasers were in the pre-OEM stage at the time of this study which presented a potential unnecessary risk for HRMR-II. The high power dissipation of the argon unit was not a problem on HRMR-II since adequate cooling was provided in the recorder cabinet housing the laser.

The noise characteristics of the argon laser were considerably better than those of the He-Cd. For all candidate lasers, an AOM would have been required to attenuate the light to the record level (less than or equal to the 10 mW end of life level). A complete comparison of candidate laser parameters is provided in Table 3.2.2.3-1.

The use of a He-Ne laser was precluded by a twofold disadvantage. The long He-Ne wavelength increases the required lens aperture ratios, thereby decreasing the depth of focus tolerances throughout the record optical path. This increases the optical design and hardware costs. In addition, the low cost option backup film (SO-343) is not sensitized to red light. This film offers the best alternative to 649F with the added advantage of red safe-light darkroom manipulation capability.

Note that the data presented in Table 3.2.2.3-1 is that which was current when the tradeoff study was done. Thus, although no clear invalidation of the selection described above has occurred in the interim, the laser manufacturers may have modified the price or performance specifications somewhat.

TABLE 3. 2. 2. 3-1

COMPARISON OF CANDIDATE RECORD LASERS - 1975

Type	Argon	He-Cd	He-Cd
Manufacturer	Spectra-Physics	RCA	Liconix
Model	162-02	LD 2186	402
Wavelength	488.0 nm	441.6 nm	441.6 nm
Power Output			
Typical	14 mW	15-20 mW	20 mW
End of Life	10 mW	10 mW	18 mW
Mode	TEM <sub>00</sub>	TEM <sub>00</sub>	TEM <sub>00</sub>
RMS Noise	<1%	2%	2%
Beam Diameter	0.65 mm	0.80 mm	0.83 mm
Beam Divergence			
(full angle)	1.0 mrad	0.8 mrad	0.68 mrad
Long Term			
Stability	± 0.5%	± 3%	± 5%
Warm-up to 90% Power	<1 min.	30 min.	5 min.
	(stabilizes in 30 min.)		
Polarization	100:1 vertical	500:1 vertical	1000:1 vertical
Laser Size	12.7"x5.0"x5.75"	26.0"x7.0"x7.0"	24.75"x4.25"x6.0"
(L x W x H)			
Laser Weight	10.5 lbs.	12 lbs.	8 lbs.
Power Supply			
Size	16.75x5.2x11.5	Not available	Not available
Weight	29 lbs.	28 lbs.	10 lbs.
Power			
Dissipation	1100 watts	250 watts	250 watts
Lifetime	2500-4000 hours	800-1000 hours	≈1000 hours
Warranty	1 year	1 year/1000 hrs.	1 year/1000 hours
Unit Cost	\$4400.00	\$3600.00	\$3750.00
Reliability	OEM, very good (HRMR-I record laser)	Developmental quality	Principally lab use
Noise	Good, raw laser beam can be used	Poor, must filter out noise (+\$1000- \$2000)	Poor, must filter out noise (+\$1000- \$2000)
Relative MTF Loss	100 /mm: 1.37 dB 200 /mm: 5.49 dB	100 /mm: 1.30 dB 200 /mm: 5.20 dB	

#### 3.2.2.4 Scanning Techniques

The selection of the techniques of scanning the laser beam to record on the film is an important facet in the production of a cost-effective and operable data recording system. The central choice to be made is between AOBD (acousto-optic beam deflector) scanning and spinner (multi-faceted spinning mirror) scanning. AOBD's offer the advantage of no moving parts and short retrace times, while spinners can produce a much greater number of resolvable spots across the scan field. Thus AOBD's are usually preferable in any application where very high resolution is not needed. The two paragraphs below summarize some of the tradeoff analyses performed in selecting the current HRMR recorder scanning approaches.

##### 3.2.2.4.1 MR Recorder Scanning Tradeoff

The use of a spinner approach in the MR scanning system is apparently precluded by the system rate requirements. A comparison of HRMR-I and HRMR-II scan rate requirements illustrates the increased difficulty of the problem. The scan rate increases 15-fold from the 1.5 msec per facet of HRMR-I to 96  $\mu$ sec per scan required by: (1) the 25% reduction in the hologram data content to allow for error correction coding, (2) the elimination of the dual hologram readout technique and (3) a 5-fold increase in record data rate. Another problem is the complexity of the scan lenses which would be required to support a spinner scanning approach. Through a calculation of the key parameters in a scanning system, the possible spinner solutions given in Table 3.2.2.4.1-1 were derived, and are presented with the corresponding values from HRMR-I as a reference. The major derived variables in the calculation were: scanner lens focal length, reflected beamwidth, facet width, spinner angular velocity, spinner diameter, and hologram length.

TABLE 3. 2. 2. 4. 1-1  
CALCULATED MR SPINNER SOLUTIONS

	HRMR-II			
	<u>HRMR-I</u>	<u>A</u>	<u>B</u>	<u>C</u>
Number of facets	15	30	40	60
Focal length (mm)	19.5	3.8	5.1	7.6
Angular velocity (rpm)	2750	20,830	15,620	10,420
Diameter (inches)	3	2.0	3.5	7.9
Duty cycle (%)	13	80	80	80
Facet cycle time ( $\mu$ sec)	1455	96	96	96

The three spinner solutions shown in the table all require a very complex two stage scanner lens to reach effective focal lengths under 8 mm. The fabricational complexities of solutions A, B, and C are approximately the same, trading increased size for reduced speeds.

The current sophistication in AOBD technology, however, makes AOBD scanning an attractive alternative. Acousto-optic deflectors are available with up to 1000 resolution-element outputs and can deflect the 680 spots required for HRMR-II in 40  $\mu$ sec with 80% duty cycle. Through the use of acousto-optic beam deflector scanning, future systems can reach 1 Mb/s record rates and above, while the spinner reaches its limits at about 500 KB/s.

As a result of the above considerations, AOBD scanning was selected for use in the HRMR-II system. The major spinner drawbacks were; high angular velocity and/or large diameter of the spinner, and the extremely short focal lengths of the required scanner lens. The key AOBD advantages were: no moving parts, reliability, and adequate speed and resolution.

#### 3. 2. 2. 4. 2 HR Recorder Scanning Tradeoff

The HR system requires a larger number of resolved spots across the scanned field than does the MR system; thus, a separate trade-off consideration was necessary to select the HR scanning technique.

TABLE 3. 2. 2. 4. 2-1

AOBD/SPINNER TRADEOFF PARAMETERS

<u>Parameter</u>	<u>AOBD</u>	<u>Spinner</u>
Speed	Very high. <20 $\mu$ sec/scan	High, 200 $\mu$ sec/scan
Retrace time	$\approx 8\mu$ sec.	50-100 $\mu$ sec.
Optical efficiency	40 - 60%	80%
Resolvable elements per scan	<1000 pixels	>6000 pixels
Pixel rate	50 x 10 <sup>6</sup> pixel/sec	30-10 <sup>6</sup> pixel/sec
Technical risk	New technology	Engineering effort
Operability	Critical alignment Temperature effects	Mechanically stable
Reliability	Transducer failure	Bearing & motor failure
Lifetime	Unlimited	4000-10,000 hours
Special requirements	Anamorphic optics Long optical path	f- $\theta$ scanner lens
HRMR-II, HR Cost		
Development	3	Reference (=1)
Recurring	0.75	Reference (=1)

The AOBD is currently limited to approximately 1000 resolvable elements per scan while 1700 are needed for human read recording. As many as 1800 resolvable elements per scan have been generated with AOBD's in state-of-the-art technology development efforts within Harris, but the technology is not yet adequately developed. See Table 3. 2. 2. 4. 2-1.

This tradeoff indicates that at the present time the spinner is the better approach for the HRMR human read recording. Since the technology and resulting capabilities of the AOBD are rapidly improving, this tradeoff should be rereviewed for any future generation HRMR machines.

### 3. 2. 2. 5 Film Emulsion Selection

The primary criteria used in evaluating the various available emulsions for use in the HRMR system were: vendor, holographic performance, sensitivity, availability on thick polyester base material,

and archival storage capability. The choice of vendor was immediately narrowed down to Eastman Kodak Company because of their reputation and past performance in the areas of quality control and film availability; accordingly, emulsions produced by Agfa Gaevert and other film vendors were not extensively considered for use in the HRMR-II system.

#### 3. 2. 2. 5. 1 Candidate Emulsions

The initial screening of available emulsions considered the key parameters of holographic diffraction efficiency and signal to noise ratio, and produced the following list of emulsions judged to be of holographic quality:

649F	SO173
SO343 (649GH)	FE-3807-1
SO141 (SO424)	PSR

All of these emulsions have been previously tested at Harris, and a compilation of their relevant characteristics produced. Some of the key features in the descriptions of each of these emulsions are as follows:

- 649F is the emulsion used by the HRMR-I System.
- SO343 (649GH) is the same basic emulsion as 649F without the red sensitization. Its cost is lower than 649F by 25 to 40%.
- SO141 is an Argon laser recording film on 4 mil ester base which has been used successfully in other holographic recorder programs. Its speed is over an order of magnitude faster than that of 649F. The same emulsion is used in SO424, the Kodak Minicard II Film (triacetate base).
- SO173 is a low noise He-Ne holographic film. At 633 nm it is about 3 times faster than 649F. At 488 nm, however, it becomes much slower than 649F.

- FE-3807-1 is a very fast He-Ne sensitive holographic emulsion (5 ergs/cm<sup>2</sup>). Its signal to noise ratio is comparable to that of SO141, but about 3 dB worse than 649F. A disadvantage of this emulsion is the need for a 50% methanol wash stage for the removal of a residual royal blue sensitizer.
- PSR films (Prestabilized Reversal) have good sensitivity and due to the positive nature of the film, black guard bands would be automatically formed between hologram tracks thus aiding noise suppression. Shelf life of this film is a serious problem.

#### 3.2.2.5.2 Other Considerations

In addition to their holographic properties, an important consideration is the base material on which the candidate emulsions are regularly coated. Use of the thick (7 mil) estar base is mandatory for proper S & R operation. Of the emulsions considered, only 649F and SO343 are readily available on this base.

The final emulsion choice for the system was made on the basis of sensitivity: at the projected operating system wavelength of 488 nm, the 649F emulsion was faster; thus it became the baseline choice for use in the system. It was recommended, however, that SO343 be considered as an attractive low-cost option for the system, provided that adequate light levels to properly expose it could be obtained.

#### 3.2.2.6 Film Processor Selection

The film processor for the HRMR system had to meet a number of criteria in the areas of size, cost, performance, reliability, etc. It must fit conveniently into a space compatible with standard electronic rack packaging of the whole system; it must be inexpensive to

operate and maintain, as well as to minimize its impact on the overall system cost; and it must provide quality processing compatible with the high-integrity storage and retrieval of data in an office environment.

Some of the key technical performance requirements established at the outset of the processor selection activity are given in Table 3.2.2.6-1.

TABLE 3.2.2.6-1

FILM PROCESSOR PERFORMANCE REQUIREMENTS

- Capability to transport a single 105 x 148 mm x 178  $\mu$ m thick microfiche without jamming.
- Full developer temperature control to  $\pm 1/2^{\circ}$ F.
- Accurate microfiche transport rate control to  $\pm 1\%$ .
- Automatic chemical replenishment cycle(s) with adequate, non-critical, automatic chemical replenishment capacity.
- Adequate developer path length for fast development combined with proven reliability and performance.
- Dry to dry processing time of 5 minutes or less.
- Variable dryer temperature control.
- Absence of scratches or marring during processing.

The least expensive processor which meets or exceeds all of the above criteria is the Kodak Versamat Model 5N. This unit is capable of continuous tone sensitometric performance and will hold the density variations to  $\pm 0.05D$  maximum or less over days of operation. The Model

5-AN has a 5 inch wide transport, dual pass through the developer tank, and water spray rinse. This unit is about five feet long and can readily be mounted in a standard electronics cabinet with connecting transports. The Model 5-AN has a transport rate control of  $\pm 1\%$  and a temperature control stability of  $\pm 1/4^{\circ}\text{F}$ .

The Kodak Versamat Model 11C also meets the performance criteria but it is somewhat more expensive because of its 11 inch wide transport (which would be needlessly oversized for microfiche processing). The Model 11C unit length of approximately 11 feet would be very awkward to package in standard electronics cabinets.

Other processors which will develop a single fiche and which were considered include: (1) Pako, (2) Cordell, and (3) custom designed units. Compared to the above requirements, the Pako processor does not have sufficiently accurate rate control, has insufficient developer path length and its small chemical reservoir capacity promotes critical replenishment-mix problems. The Cordell units unacceptably mar and/or scratch the film surfaces, have very small chemical tank capacity, and have inadequate temperature controls. Custom units can be designed by several vendors to meet the requirements but at three or more times the Versamat Model 5N price.

The result of all of the above considerations was the selection of the Kodak Versamat Model 5N film processor for incorporation into the HRMR-II system.

#### 3.2.2.7 Film Positioning Platen Design

The technique used to hold the film in place during recording and playback has an impact on two critical system performance parameters: film surface quality preservation and system depth of focus tolerance. In the earlier system design, a flat-head vacuum platen was

used to hold the fiche during recording and readout. Performance was adequate, but a number of problems were identified which made an improved technique a desirable goal for the HRMR-II system.

To provide an improved performance alternative fiche positioning system, experiments were conducted with an air-bearing based unit. It was shown that in a dynamic test mode of the air bearing platen, film position could be held stably constant within 6.0  $\mu\text{m}$  peak-to-peak at air gaps of .008 to .009 inches with input air pressure of 8.0 psi. Thus the depth of focus tolerance, one of the key parameters, could be improved using the air bearing technique. Comparison findings in other critical areas are delineated in Table 3.2.2.7-1.

TABLE 3.2.2.7-1

COMPARISON OF AIR BEARING AND FLAT HEAD VACUUM PLATENS

<u>Configuration/Operating Consideration</u>	<u>Air Bearing</u>	<u>Flat Head</u>
Worst case film positioning stability	$\pm 3 \mu\text{m}$	$\pm 12 \mu\text{m}$
Fiche area available for recording	Maximum	Constrained
Mechanical mass required for support	Minimal	Significant
Sensitivity to dust and dirt particles on film positioning surface	Minimal	Significant
Integral optics and platen design	Easy	Very difficult
Film scratch susceptibility	Minimal	Significant
Film readout capability with code clips attached	Easy	Difficult

The clear conclusion drawn from these tradeoff considerations was that the air bearing technique should be adopted for use in the HRMR-II system. This decision has been fully supported by the results obtained in operation of the system: the air bearing platen has met or exceeded all of its design requirements, and has been one of the most trouble-free components in the system.

### 3.2.2.8 Photodetector Array

A recorded one-dimensional Fourier transform hologram of binary data can be recovered by an anamorphic optical system which performs the inverse Fourier transform as the hologram is illuminated by a readout laser beam. The result is a linear array of optical spots, each spot representing a data bit. A linear photodetector array located at the data reconstruction image plane converts the optical data to electrical signal amplitudes for subsequent thresholding. Two common means of recovering binary data are: linear self-scanned arrays, and discrete photodiodes linked to a fiber optics array. In either approach, each detector is assigned to a single data bit reconstruction position.

The discrete photodiode approach provides greater than 60 dB dynamic range and unsurpassed cross-talk isolation between detector elements but requires extensive ancillary circuitry. Self-scanned integrated circuit arrays provide total data recovery in a single package, which minimizes the number of interconnections while providing high component reliability and ease of maintenance. However, serious performance limitations in self-scanned arrays must be overcome so that their use does not appreciably degrade the recovered data bit error rate. The impact of these performance limitations when not properly overcome was seen in the HRMR-I research prototype equipment to lower packing density and increased bit error rate.

The HRMR-II research prototype employs a conventional bit detection approach characterized by the presence of a photodiode output (data bit reconstruction) for one of the binary states ("1") and the absence of photodiode output for the remaining binary state ("0"). In order to achieve the desired bit error rate (BER), an accurate decision threshold which separates the binary states must be provided. This is accomplished by monitoring the peak amplitude of special bits which are allocated to

perform decision threshold estimation. It is important that each photo-detector output provide a minimum dynamic range of 20 dB to accommodate the following effects:

- 1) the output switch between decision threshold and peak signal;
- 2) the peak signal variation due to noise;
- 3) residual spatial frequency dependent intensity loss (MTF roll off);
- 4) intensity variations due to nonuniform film processing; and
- 5) recording/readout laser power output variation

Since each bit decision is independent, there exists an additional requirement for high diode-to-diode isolation (20 dB minimum) otherwise a corresponding reduction in dynamic range is exhibited.

#### 3.2.2.8.1 Performance of the HRMR-I Array

A single Fairchild FPA-602, 128-element linear self-scanned array was used in the HRMR-I system. Various compromises were required to accommodate major performance limitations of this array. The first limitation was that the dynamic range of the device was limited to approximately 10 dB. There are two reasons for this. First, fixed pattern noise suppression was not employed to overcome the high switching noise levels encountered; and second, the array exhibited a significant output pulse shift as a function of the incident light intensity. Since the amplitude of each bit fluctuates over a wide range, the 10 dB dynamic range was not sufficient to recover data at an acceptable BER. As an attempted solution, the readout beam intensity was increased and the array output was allowed to saturate so that the active dynamic range included the decision threshold region for bit decisions. This resulted in improved BER, but at the expense of degraded decision threshold

estimation and degraded synchronization to the hologram illumination rate. Saturation of those photodetector outputs allocated to decision threshold estimation resulted in a threshold which was insensitive to the array output. This required that unacceptably tight tolerances be placed on recording levels and film processing to minimize array output fluctuation. A further effect was that synchronization of the readout system to the hologram rate was degraded, because the peak amplitude of the photodetector outputs, which indicates real-time registration of the readout beam with the hologram, was allowed to saturate; hence the peaks were no longer identifiable.

A second major limitation was excessive crosstalk between adjacent photodiodes, which was produced by the poor diode-to-diode electrical isolation (only 10 to 13 dB). This required that adjacent diodes not be used when the array output was heavily saturated so that crosstalk would not produce erroneous bit decisions. An experiment in which only alternate diodes were used resulted in crosstalk isolation of 16 - 19 dB; this proved acceptable, since crosstalk no longer appeared to be the limiting BER degradation source.

As a result of the photodetector experience acquired on the research prototype, the following critical array characteristics are necessary if only a slight degradation of BER performance is to be attributed to the readout array:

Dynamic range	20 dB
Diode-to-diode isolation	20 dB
Uniformity of response	$\pm 0.5$ dB

An additional important requirement is that the photodetectors should appear as point sensors. This minimizes the data reconstruction inter-symbol interference which results from the recorded truncated Fourier transform (only two transform cycles are recorded) and readout beam

apodization. Analysis indicates that intersymbol interference can be held to a value outside the minimum required dynamic range if the bit detector spacing exceeds the detector width (along the array) by a factor of four.

#### 3.2.2.8.2 Evaluation of Candidate HRMR-II Arrays

To select a detector array unit for use in the HRMR-II system, tests were carried out on four devices, including the Fairchild FPA-602 128-element device used by the HRMR-I system. The tested arrays were;

- Fairchild FPA 602; silicon-gate MOS
- Reticon 256A; silicon-gate MOS
- Reticon 512B; silicon-gate MOS
- Fairchild CCD101; charge-coupled device

These arrays were subjected to a small-spot response test to determine their dynamic range and diode-to-diode isolation. The first three of the arrays were silicon-gate MOS devices and the fourth was a charge-coupled device. The silicon-gate MOS self-scanned linear arrays consist of a row of photodiodes which are gated to a video line(s) for discharge at specific clock intervals. The amount of current required to discharge each element is proportional to the incident light intensity and to the interval between discharge (scan) cycles. During a scan cycle, each diode element is sequentially discharged and the video line common to each element exhibits a serial train of discharge current pulses. These pulses are coincident with clock pulse transitions. A common and flexible video line implementation employs two video lines per array segment; each video line is common to alternate diodes. To gate each diode to the video line, alternate diodes may be interrogated simultaneously or in an interleaved fashion as a function of the clock input phasing.

A more recent linear array device implementation is provided by charge-coupled device (CCD) techniques which serially transport the photodetector charges to an output. This technique holds the greater promise to provide wide dynamic range, since the array is not actively switched or gated and fixed pattern noise is minimized. However, CCD device technology has not yet reached the point where these devices provide appreciably greater dynamic range and SNR or meet the readout rates of silicon-gate MOS devices.

The results obtained from the silicon-gate MOS self-scanned arrays were felt to be representative of presently available devices. The new RL-512B units exhibited sufficient dynamic range and adequate diode isolation if fixed pattern noise suppression is employed and if only alternate diodes are used in readout. Video line neighbor isolation proved to be quite high (every fourth diode is a video line neighbor). Uniformity of response at 1 dB below saturation and 10 dB below saturation for a sample of 10 detector diodes on the same video line was found to be within  $\pm 0.3$  dB.

The RL-256A was found to be worse than the Fairchild FPA 602 in video line neighbor diode isolation (every second diode is a video line neighbor), although neither of these two arrays is considered acceptable for an improved BER reader design.

The CCD unit was difficult to adjust and the recorded results are not believed to reflect optimized performance. Greater than 24 dB dynamic range had previously been observed; however, charge transfer smearing produced an effect similar to poor diode-to-diode isolation.

Based on diode array characteristics and the HRMR prototype equipment performance, a set of desired self-scanned diode array characteristics were defined and are listed in Table 3.2.2.8.2-1. As a

result of the array tests described above, it was also felt that with minor modification to detector sizing and spacing parameters, a version of the Reticon 512B array could meet the characteristics of Table 3.2.2.8.2-1.

TABLE 3.2.2.8.2-1

DESIRED READOUT ARRAY CHARACTERISTICS

● Dynamic Range . . . . .	20 dB
● Diode-to-diode isolation . . . . .	at least 20 dB
● Uniformity of response . . . . .	±10% maximum
● Number of sensors . . . . .	96 - 128
● Sensors per segment* . . . . .	32
● Segment cycle period . . . . .	100 μsec maximum
	10 μsec typical
	2 μsec minimum
● Center-to-center detector spacing . . . . .	1-4 mil
● Detector length . . . . .	16-24 mil
● Ratio of detector spacing to detector length . . . . .	4:1

\*If the throughput readout rate of a reader exceeds 250Kb/s, it is desirable to segment the array and monitor simultaneously each segment output. This achieves the readout rate with array clocks which are less than 10 MHz. Two separate video lines should be provided to simultaneously read out alternate sensors in each segment.

3.2.2.8.3 Testing of the HRMR-II Reticon Array

Based on the conclusions described in the previous sections, a new device was designed and produced for Harris by Reticon, Inc. This device, designated the RL256EBH, was a modification of the RL512B array tested previously. Starting with the basic 512-element device,

which has 1 x 25 mil photodiodes on 1 mil centers, modifications were made to produce a HRMR-II compatible unit. These modifications included:

- 1) deleting alternate diodes by grounding the video lines (video lines 2 and 4) and extending the mask to cover these diodes;
- 2) extending the mask to reduce the center aperture of the 256 active diodes, resulting in a diode size of 0.5 x 24 mils on 2 mil centers; and
- 3) applying CRL AR-7 coating to both sides of the array's quartz window to minimize reflections at the He-Ne laser wavelength (633 nm).

The first tests conducted on the array were bench tests. The photodiode array was mounted on the breadboard array driver assembly and small spot response tests were conducted which included dynamic range, adjacent diode isolation, alternate diode isolation, and uncompensated noise sources. Both test units exhibited 24 dB dynamic range to the fixed pattern noise level. However, the dynamic range should really be limited by the achieved diode isolation, since high level adjacent or alternate diode illumination would produce a diode output response indistinguishable from noise during normal reader operation. Alternate diode isolation suppression of adjacent response (on a common video line) and adjacent diode isolation were 20 and 22 dB, respectively. Each unit with CRL AR-7 coating on the quartz windows exhibited a 1 to 1.5 dB increase in sensitivity when compared to uncoated quartz window arrays. Photodiode saturation of AR-7 coated units occurs at  $1.7 \times 10^{-12}$  joules corresponding to  $1.0 \mu\text{w}$  small spot illumination during a  $16.6 \mu\text{sec}$  readout scan period. Uniformity of response was checked and found to be

within  $\pm 5\%$  at a high illumination level (1 dB below saturation) and within  $\pm 12\%$  at a low light level (10 dB below saturation).

Final testing of the new array was done after it was installed in the HRMR system, with appropriate electronic and optical system modifications to provide temporal and spatial compatibility of the reproduced data with the array. The improvements expected from the Reticon array included: 1) increased scan (readout) clock rate to meet the 500 KHz user data requirements; 2) increased diode-to-diode optical isolation by reduction of the diode aperture to 1/4 of the 2 mil diode spacing; 3) increased optical isolation by two sided, anti-reflection coating of the array's quartz windows; 4) increased electrical isolation between diodes by using every other diode; and 5) improved dynamic range provided by the array, as well as signal enhancement provided by the sample and hold circuitry. Improvements were realized in all the above listed areas; thus, the Reticon array readout is now very representative of the data reconstruction illumination imaged onto the array, i. e., minimal data degradation is contributed by the array. Specifically, the following performance improvements were realized with the Reticon array:

- 1) The increased scan readout clock was implemented at 2.5 MHz with no difficulty.
- 2) Diode-to-diode data bit reconstruction isolation was increased significantly. A minimum of 12 dB isolation between adjacent diodes exists, and isolation of alternate diodes exceeds 12 dB. The performance improvement of the Reticon array over diode arrays with 100% aperture (such as the Fairchild FPA 602) is significant, since operation of those arrays only yields 4-6 dB isolation, thus making bit decisions impossible when all diodes are active.

AD-A068 892

HARRIS CORP MELBOURNE FLA ELECTRONIC SYSTEMS DIV  
HUMAN READ - MACHINE READ MICROFILM MASS MEMORY SYSTEM.(U)  
MAR 79 T H OTTEN, R H NELSON

F/G 14/5

UNCLASSIFIED

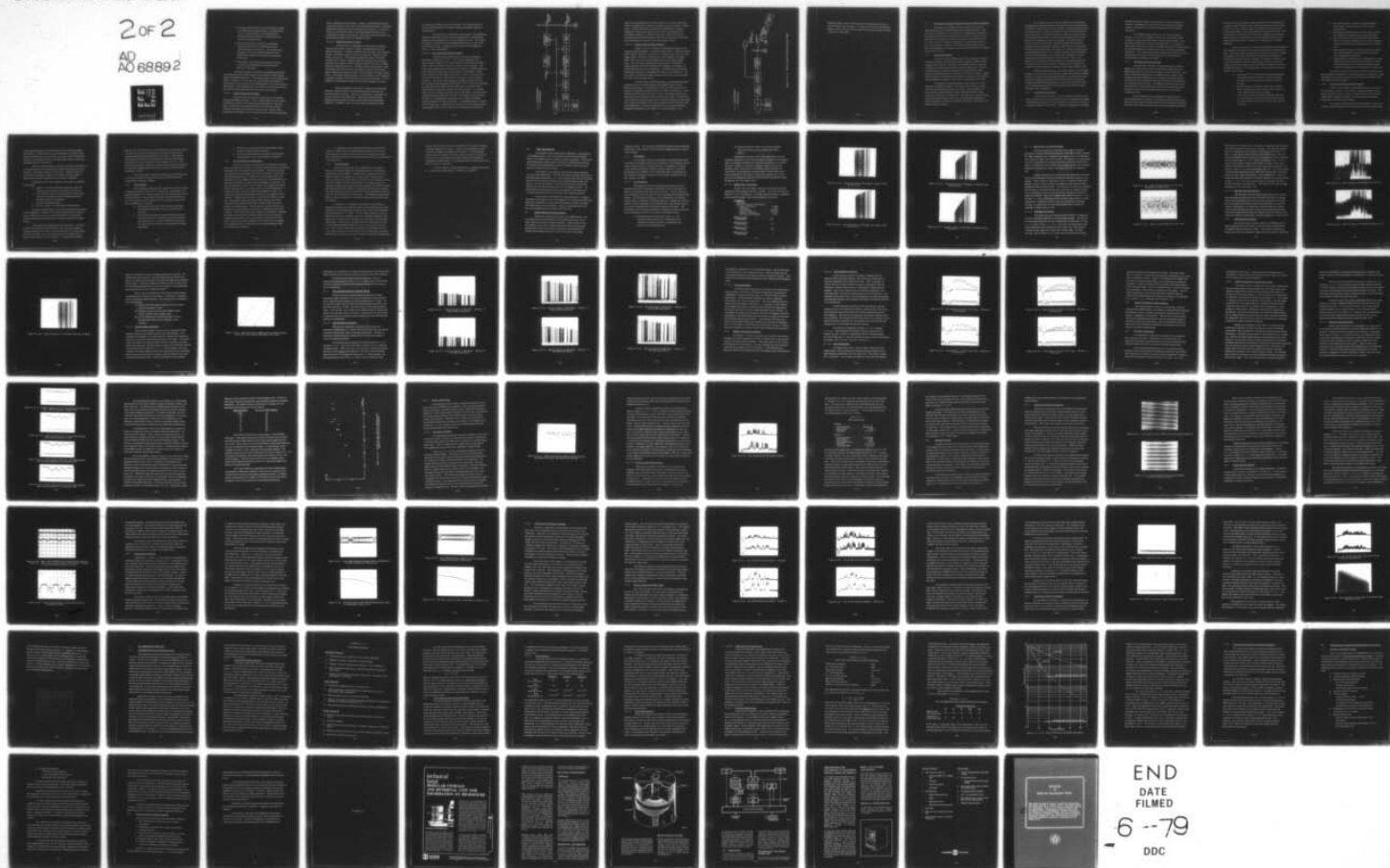
RADC-TR-79-30

F30602-74-C-0152

NL

2 of 2

AD  
A068892



END  
DATE  
FILMED  
6-79  
DDC

- 3) Increased optical isolation with antireflection coating was difficult to appraise; however, an improvement of 1 to 1.5 dB increased array sensitivity was obtained with the antireflection coated array compared to an uncoated array.
- 4) Electrical isolation of 20 dB was a substantial improvement over the 11 dB isolation between adjacent diodes in the FPA 602. This improvement in isolation means that data reconstruction is not significantly degraded by the electrical properties of the array.
- 5) The dynamic range improvement obtained with the Reticon array means that the array need not be operated in saturation.

The improvements in the Reticon RL256EBH (with respect to the previous device) indicated that it was capable of supporting the goals of the HRMR-II system. Even though not quite all the requirements listed in Table 3.2.2.8.2-1 were met, performance was adequate to ensure that the array would not be a limiting factor in the overall system BER results. This conclusion has been borne out by the performance of the array in the system during the remainder of the program.

#### 3.2.2.9 Optical Design and Packaging

There are several important requirements on the optical design of the HRMR-II system. First, a stable platform for the optical components is required to maintain optical alignment on a long term basis, to minimize environmental effects, and to provide a unique reference for design and adjustment measurements. Second, static and dynamic adjustability must be provided to allow initial and continuing

system optimization and alignment. Finally, a highly desirable quality of the optical system is the use of interchangeable assemblies to minimize alignment downtime and guarantee long term performance. In this subsection we will describe some of the tradeoff decisions taken toward achieving these design requirements, and provide a brief summary of the optical design implemented in the HRMR-II system.

#### 3.2.2.9.1 Design/Packaging Tradeoffs

The first area of investigation concentrated on materials which could be used to provide a suitable mounting platform for the optical components. Candidate materials were masonite, cast aluminum jig plate, aluminum castings, aluminum honeycomb, composite honeycombs, and granite. The philosophy guiding the ultimate materials selection was to achieve maximum long term stability in the mounting platform; this permits a greater tolerance latitude in the more complex mounts for individual elements. Extremely heavy materials were ruled out because of the need to elevate the optics in the S & R Unit and the need to minimize the ultimate impact on floor loading at computer installations. Of the light weight materials, the most stable are the honeycomb composites; however, this material type is the most expensive. A combination of cast aluminum jig plate and aluminum castings were used.

Static adjustability will be used to mediate the dimensional difference tradeoffs between economical fabrication tolerances and required optical tolerances. This type of adjustment is intended to be used as a one time only adjustment. Those adjustments requiring frequent attention should be powered adjustments with instrumented feedbacks. In addition, there are some dynamic adjustments which

are functional during an active read/record. The overall intent is to provide minimum operator hardware interface and greatly enhanced maintainability.

The last area of consideration is prealigned, interchangeable optical subassemblies. Such a unit can be fabricated, assembled and aligned to meet a specification for focal distance and size. This means, for example, that bolt-on-interchangeable reconstruction lenses could be stocked as spares. Installation would entail no optical alignment, focus, or other compensation.

#### 3.2.2.9.2 Recorder Optical Design Approach

The basic design approach to the recorder subsystem is described in Figure 3.2.2.9.2-1. The recorder light source is a Spectra-Physics Model 162-02 Argon-Ion laser operating in the TEM<sub>00</sub> mode at 488.0 nm with an output power level of 10 mW nominal. The noise characteristics of the Argon laser are better (<1% RMS) than those of the He-Cd laser previously considered for use (2% RMS). A light level controller is still required to control the light to the record level (which will be equal to or less than the end of life 10 mW provided by the laser). The acousto-optic amplitude modulator controls the intra-pixel intensity level during both MR and HR. The mode selector functions as a light switch into either the HR or MR mode as required, and is implemented by means of a mechanically driven mirror. For the MR mode, the mirror will not interfere with the light beam, but will proceed undeviated along the MR path to the MR record station; in the HR mode, the mirror is inserted into the light path and the beam is deflected through an angle of 90° into the HR path. A mechanical shutter is used to block the light when a lengthy break is sensed in the record data stream; this guarantees that no stray laser light will reach the film and fog it.

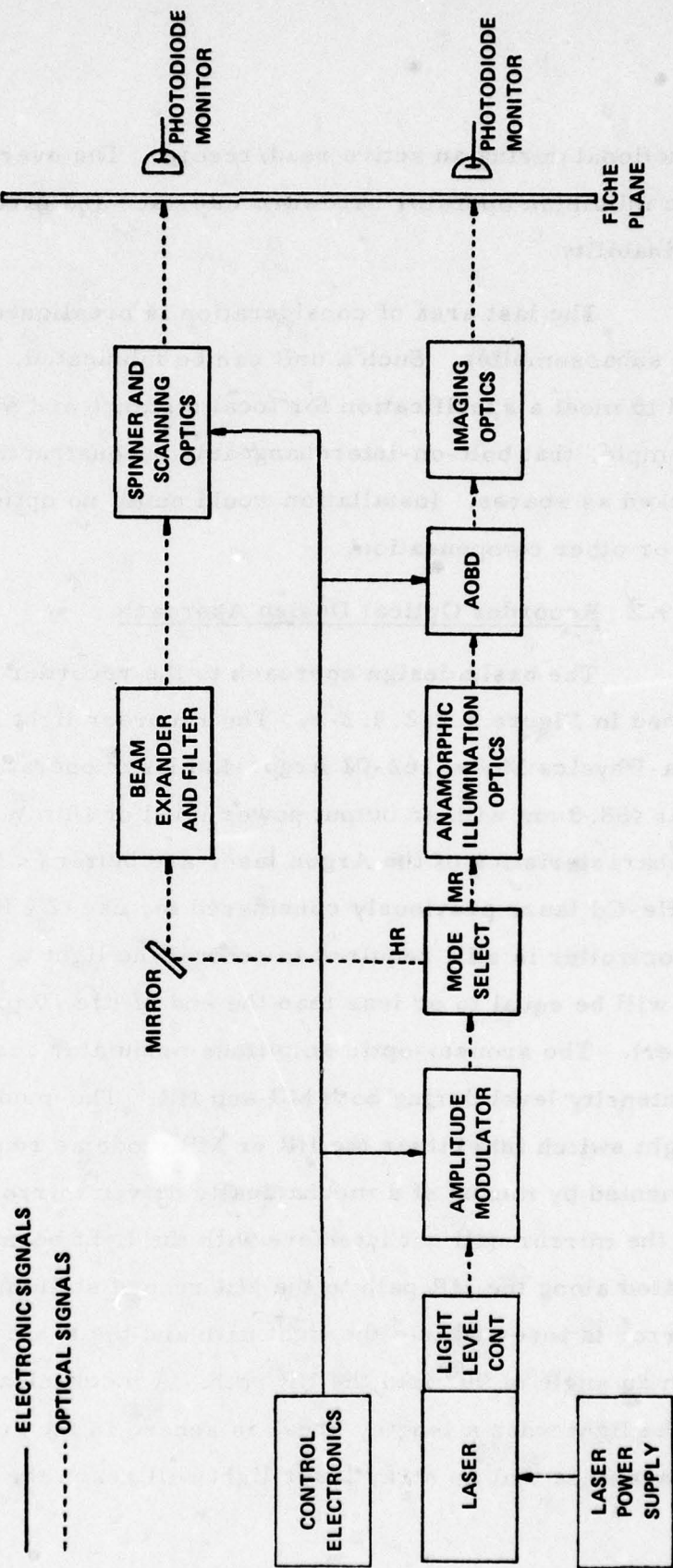


FIGURE 3.2.2.9.2-1. RECORDING SYSTEM BLOCK DIAGRAM

The record scanning devices for MR and HR are an acousto-optic beam deflector (AOBD) and a multifaceted spinning mirror or spinner, respectively. The MR and HR record stations are separated by 2 inches. Photodiode monitors back up each record station for diagnostic and maintenance purposes. A master electronics control unit provides timing and synchronization signals to the various subsystem components, while interfacing the recorder to the main system control.

### 3.2.2.9.3 Verifier Optical Design Approach

Figure 3.2.2.9.3-1 shows the block/optical diagram of the reader/verifier subsystem. The coherent light source, a Spectra-Physics Model 124A He-Ne laser, is operated at a nominal power of 10 mW in the TEM<sub>00</sub> mode. The laser is followed by a beam expander and spatial filter, which serve to provide a uniform beam with minimal spatial noise. The anamorphic illumination optics function to illuminate a single hologram on the fiche such that both hologram-to-hologram and intersymbol interference are minimized. The SNR filter also aids this minimization function by controlling the readout beam apodization. The anamorphic reconstruction optics image the bits at the correct spacing for input to the photodiode array.

The film wedge correction system, not previously mentioned resulted from an observed property of the HRMR storage medium. Microinterferograms of 649F film have shown that film thickness variations are substantial enough to cause loss of SNR in bit detection. Film thickness variations cause the film to act as a thin prism which in turn causes the bits to translate off their respective detectors. This problem is corrected by forcing the light to pass through the platen at a given angle with a position correcting servo loop operating on one of the fold mirrors in the optics path. The error signal for this servo loop is obtained by imaging the nondiffracted (DC) light onto a split photodiode. The

— ELECTRONIC SIGNALS

- - - OPTICAL SIGNALS

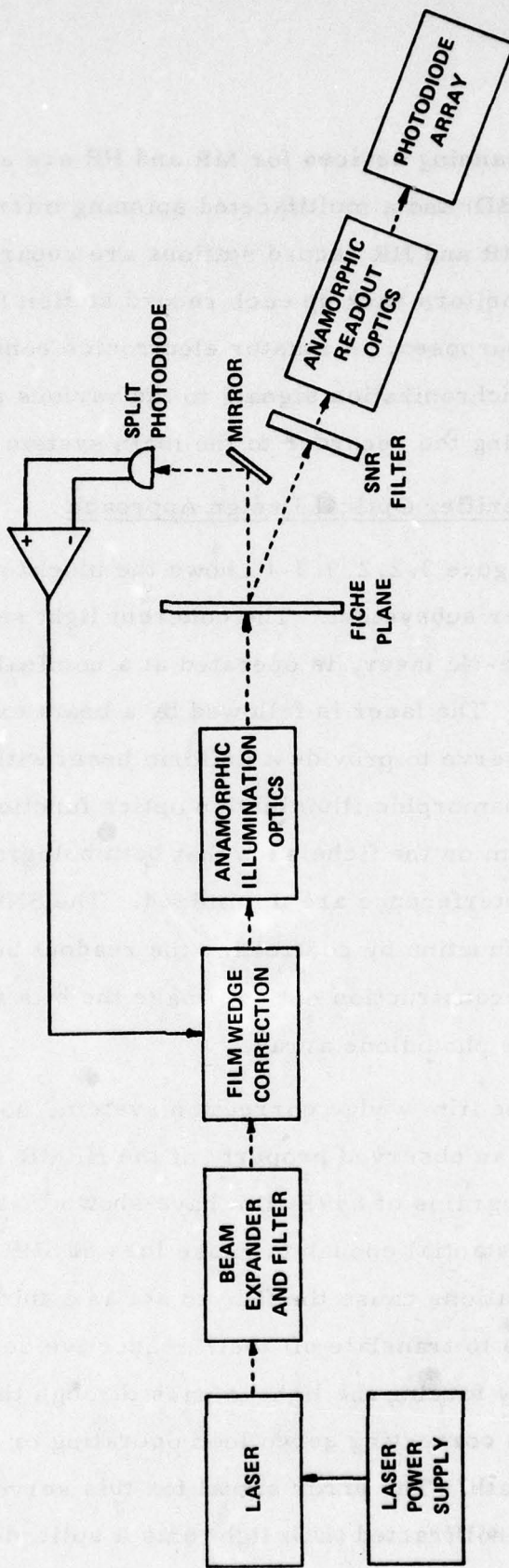


FIGURE 3.2.2.9.3-1. VERIFIER SYSTEM ELECTRO-OPTICAL BLOCK DIAGRAM

difference signal, after processing, drives the piezoelectric mirror which illuminates the hologram. Closing this loop forces the difference signal to zero, thereby forcing the light which passes through the platen to travel at a fixed angle.

### 3.3 Assessment of Selected Approaches and Problems Encountered

The design of the HRMR system required the selection of specific approaches for implementing certain system functions. With the benefit of hindsight at this point in time, assessments of certain of the approaches selected are provided in this section, along with a brief discussion of two specific problems encountered. The topics selected for review here are: synthetic holography, microfiche unit records, carousel storage and retrieval, the computer controller and I/O interface, film handling, X-Y position servo motors and electronic controllers, and the bit error rate.

#### 3.3.1 Synthetic Holography

On both the earlier HRMR program (the exploratory development model) and this one (the engineering development model), blocks of digital data (user plus overhead) were recorded on film in the form of synthetic one-dimensional Fourier transform holograms. The data packing density was limited primarily by the minimum size of the scanned and modulated beam at the film in the direction of scan, coupled with the number of resolvable spots required to represent the computed Fourier transform hologram of each block of digital data on the film.

The synthetic holography approach was selected over interferometric holography because, at the time of the selection, a linear multi-element light modulating array (a linear "page composer") to convert a block of digital data to a line of spatially modulated light beams did not exist in a reliable form. Since that time, proven acousto-optic linear page composers with up to 136 individually modulatable positions along a line have been developed and used on other RADC and NASA programs at Harris.

The rejection of direct spot recording in favor of synthetic holography was primarily because precisely locating and synchronizing to individual recorded spots on film called for mechanical precision and/or closed-loop servo-control techniques that had not been developed or proven at the time. The spatial invariance property of Fourier transform holograms allowed the mechanical precision parallel to the holograms to be relaxed by an order of magnitude. The property that a scratch as wide as several bits through a hologram did not destroy specific bits but decreased the signal-to-noise ratio for all bits in the hologram was also appealing. Since that time, several techniques have been developed and proven for recording, tracking, and synchronizing to spots recorded on film at very high packing densities; the optical video disk activities provided part of the incentive. Also, error detection and correction coding techniques have progressed such that corrected error rates in direct spot recording can be comparable to those with Fourier transform holograms with properly designed codes.

Synthetic holography was successfully exploited in both HRMR systems and was proven as a digital data storage and retrieval technique. However, because increased packing densities are achieved with interferometric holography and especially with direct spot recording and because technological developments now permit their selection, these are the preferred approaches in mass storage and retrieval systems presently under development.

### 3.3.2 Microfiche Unit Records

The selection of 105mm by 148mm standard microfiche as the unit record format was made primarily because of widespread acceptance of this standard format and of the availability of a storage and retrieval mechanism suitable for microfiche. Additional advantages of microfiche

included reasonable random access prospects, ease of purging unit records, compatibility of the HR format with standard microfiche readers, and availability of film and compatible film processing equipment.

The viability of microfiche as a unit record persists at present, not only for the HRMR system but for certain other mass storage and retrieval systems under development for HR data, interferometric holography, and direct spot digital data. In response to these needs, Harris has developed a storage and retrieval module concept for microfiche based on a slotted carousel for unclipped, unmodified microfiche. This storage and retrieval module for microfiche is a key building block for several mass storage and retrieval systems in various phases of design and fabrication.

### 3.3.3 Carousel Storage and Retrieval

As noted above, the basic carousel storage and retrieval approach for microfiche continues as a preferred approach for the HRMR system and for other mass storage and retrieval systems. The specific approach implemented in the HRMR system requires that a notched metal clip be affixed to each microfiche and allows adjacent microfiche to make some physical contact as they are extracted from and reinserted into a carousel. The affixing of the metal clip must be done precisely to transfer positional reference from the edges of the microfiche to the clip; this operation adds cost to the microfiche infiling procedure.

The nine-stack carousel configuration required that the readout subsystem be carried on an elevating structure parallel to the axis of the stack while maintaining fairly precise mechanical alignment between the elevating microfiche extractor and the fixed carousel stack.

In the course of this program certain changes to the intended sequence of elevator control functions were made to permit more precise control of elevator motion. These changes provided the required positional control while adding to the average and worst case retrieval time. The retrieval time can be reduced, but the more complex control sequence should remain as implemented to assure the required positional precision of the elevator and to stabilize the relatively heavy elevating subsystem.

Partly as a result of the experience gained by Harris engineers who designed and worked with the stacked carousels with clipped microfiche, a new type of carousel storage and retrieval module was designed; a feasibility model has been fabricated and tested successfully on a Harris IR & D project that is continuing. The brochure included in this report as Appendix A provides a description of this new microfiche storage and retrieval approach that incorporates a slotted carousel for unclipped microfiche. Key improvements over the previous carousel concept are as follows:

- Dedicated slots in top and bottom plates hold individual microfiche such that no contact is made by adjacent microfiche and the location of a microfiche is keyed to a slot;
- Microfiche are not modified (no slips and no requirement to transfer positional reference information) and can be infiled directly after recording;
- A two-stack carousel holds 1000 microfiche with only a modest extension of the range of travel on one of the X-Y axes required to move the extractor from one level to another;

- The readout optics, air platen, and photodetection unit are fixed relative to the two-stack carousel (not elevated);
- Each group of 1000 microfiche in a two-stack carousel have independent retrieval and readout subsystems;
- The two-stack carousel structure loaded with microfiche can be removed readily and remounted on another module if the retrieval or readout portions of a module fail;
- With multiple storage and retrieval modules, retrieval and readout operations can be performed in parallel with an appropriate controller;
- Large numbers of modules can be configured for on-line, parallel operation with even larger numbers of off-line carousels available to load onto any available module when off-line information is demanded by a system user.

The slotted carousel storage and retrieval module for unmodified, unclipped microfiche is a key building block for systems now under consideration for massive amounts of both HR data (microimages) and MR (digital) data on microfiche.

#### 3.3.4 Computer Controller And I/O Interface

A PDP 11/45 computer and peripheral options was selected as the system controller. The computer, mag tape transport, disc drive, and CRT provide not only a cost effective data I/O function but provide data management capability, in-progress status and fault monitoring, and a data readout display.

By utilizing the standard PDP unibus interface, the Recorder, Verifier, and S & R Unit data I/O and command/status transfers could

be easily implemented to a proven interface with a minimum design uncertainty. Once this interface is accommodated, the computer and options provides data I/O for mag tape, disc pack, CRT and keyboard, teletype, and a unibus port for a communications channel, without any additional hardware development.

Indeed, by standardizing on the DR11-B (data I/O) and DR11-C (command and status), and defining the interface functions early in the program, the hardware design of the Recorder, Verifier, and S & R Unit and data management software development then proceeded in parallel and were then integrated with a minimum of difficulty.

Modifications to the DEC equipment were kept to a minimum and included:

- Addition of acoustic absorbing material to reduce the ambient noise generated by the blowers in each rack.
- Logic added to a general purpose DEC wire-wrap card to provide run length encoding and DMA interface to the DEST Graphic Arts Digitizer.
- AC power distribution panel
- DR11-B and DR11-C connectorized interface panel

In general the DEC PDP 11/45 computer and option performed very satisfactorily. However, the system performance with regard to the time required to record and read microfiche was substantially greater than planned because an entire microfiche could not be staged on disc.

The system was configured with two disc drives. One drive reserved for operational software and the other used for temporary storage of data to be recorded by the Recorder Unit or to being read in from the S & R Unit. As one disc pack could only be staged with, at most, one-half the data for a microfiche, it was planned to transfer

data onto (or from) disc from (or to) mag tape during microfiche record (or read) retrace and thereby support one continuous recording (or readout) before the disc data demand was exceeded. Unfortunately, interleaving these functions from Mag tape to disc was not possible and presently, only one microfiche track is staged at a time. This results in interrupted recording or readout with pauses at the beginning of each track and adds approximately two minutes to full microfiche recording or readout.

A low risk solution requires the addition of a third disc drive to allow full microfiche staging on the second and third drives for uninterrupted recording or readout.

#### 3.3.5 Film Handling

Film handling encompasses film removal from a film cassette, transporting the film to/from the X-Y Transports, accurate film chip positioning against X-Y Transport guide pins, film transporting to/from the film processor, and microfiche selection/removal/reinsertion to the S & R carousel. These functions were very capably incorporated into the HRMR system utilizing:

- Center-drive pinch roller film transport assemblies, each assembly individually driven by a synchronous AC motor.
- Air cylinder and pistons to provide transverse motion with status provided by adjustable position switches to sense piston travel. Each air cylinder actuated by an AC solenoid driven 4-way air valve activated by a Solid State Relay.

- Microfiche presence detected by interrupted air-flow switch or edge-guide roller switches.
- S & R microfiche handling by incorporating Rem/card Image Systems selector and spreader mechanisms.

### 3.3.6 X-Y Microfiche Positioning Servo

The X-Y servos for providing precise movement of the microfiche in the Recorder, Verifier, and Reader subsystems were troublesome throughout much of the system checkout phase. The major problems were with the motor bearings and the drive electronics. The motors and bearings selected by the vendor were an improper match to the specified X-Y servo loading conditions; each time a bearing failed, the precision shaft position encoder would be damaged or destroyed. The drive electronics for the X-Y servo motors were unstable and tended to drift throughout the day, causing record or read misalignments. A decision was made not to take legal action against the vendor or to repro cure because of the anticipated impacts to the program cost and schedule. A Harris team was sent to work with the vendors to select more appropriate motors and higher quality bearings; this action required several iterations and visits to vendors before the motor problem was under control. In the meantime, system checkout was hampered by motor failures and the lack of replacement motors and encoders. A Harris team was also assigned to troubleshoot, redesign, and repair the motor drive electronic units; this action resulted in enough improvements to servo-loop stability to permit use of these units, but long-term drift continued to be a problem that was handed by reinitializing the X-Y position reference when appropriate faults were detected and reported.

In retrospect it is considered possible that the decision to repair the vendors' servo-motors and drive electronics and to seek work-arounds for residual problems was more costly than rejecting them early and seeking a more competent design using more sophisticated servo approaches.

### 3.3.7 Bit Error Rates

Raw (uncorrected) bit error rates (BER's) were initially higher than anticipated based on extrapolations from the exploratory development model of HRMR. Improvements (reductions) in the raw BER by an order of magnitude were made, and the variations from read-to-read and from microfiche-to-microfiche were reduced to a level such that consistent results were observed. The engineering effort required to adjust system parameters and procedures to achieve tolerable and consistent BER performance was significantly greater than planned. The chief remaining source of raw errors was less than ideal processing of the film in the automatic film processor. With additional engineering effort to improve this process, it is believed that further improvements are possible.

In Section 5.1 an analysis of achievable corrected BER is presented, leading to the conclusion that a more sophisticated but easily realizable error detection and correction code can provide performance closely approaching a  $10^{-7}$  BER. The key change required to improve BER performance is to interleave data from hundreds of adjacent holograms and to construct error detection and correction codes after data interleaving. In such a case, the obliteration of a large portion of one or a few adjacent holograms affects only one or a few bits in the code word. The erroneous assumption made early in the program that led to the implementation of non-interleaved error detection and correction code hardware was that the raw errors would be statistically independent.

In fact, the occurrence of raw errors tended to be in bursts, showing statistical dependence of errors. (That is, the probability of many errors per hologram was higher than expected.) The interleaving process tends to scramble the burst errors such that the occurrence of errors in the interleaved data streams tends toward statistical independence (randomness). Error detection and correction codes work best on such error statistics.

With the addition of data interleaving, as suggested in Section 5.1, performance approaching  $10^{-7}$  BER can be achieved.

#### IV. TEST AND RESULTS

In the course of the construction, initialization, and operation of the HRMR system, a body of technical data has been accumulated which is an essential part of a complete system description. This section will document that technical data, detailing the experiments performed, the results of those experiments, and the conclusions and recommendations to be drawn from each result.

The results to be presented in this section will be organized into three main subsections. The first will detail the system optimization and initialization procedures, i. e. , those tests through which the operating points of the key system components were selected during system integration. The second subsection will present some of the results that characterize the achieved performance of the completed system. The third subsection will describe some of the diagnostic techniques used to track and minimize data error sources in the completed system.

For each area of investigation in each subsection, a complete description will be given of the test conditions, the variable and observable quantities or qualities, the experimental procedure, the data recorded, the implications of the observations, and any recommendations which may have emerged from the results in that test area.

##### 4.1 System Optimization and Integration

During the assembly and checkout of the HRMR system, the key activities were the performance verification studies done on the major optical and electro-optical subsystems. These studies served two purposes: first, they provided confirmation that the subsystems would perform according to design; and second, they delineated the tradeoff relationships necessary to select the system's operating

parameter values. This subsection will describe some of these important experiments, their results, and the system operating parameter choices which resulted.

#### 4.1.1 TGA Studies

The Transform Generator Assembly (TGA) performs the basic translation of the digital data from the bit domain to the frequency domain, using a discrete Fourier Transform process. In addition, the TGA (a more complete description of which is given in Section 2.4) performs a filtering or pre-emphasis on the transformed data to compensate for the nonuniform frequency responses of such system components as the film, lenses, and AOBD.

##### 4.1.1.1 Test Procedure

The purpose of the first test performed on the TGA was to determine the effects of parameter variations on the output signal, as well as to verify the proper functioning of the unit. The two main parameter settings which were varied were the TGA gain and the Digital Filter setting. The TGA gain controls the overall amplitude of the resultant discrete Fourier transform coefficients (subject to clipping when the 8-bit dynamic range is exceeded), and the Digital Filter (DF) setting controls the amount of enhancement received by the higher frequencies. The functioning of the TGA and its response to variations in these parameters were documented by means of two types of oscilloscope photos:

- (1) Photos showing the output of the TGA, i. e., the repetitively generated 512 DFT coefficients which represent the spatial variation of amplitude to be recorded in the holograms; and

- (2) Photos showing the output of a spectrum analyzer which received as input the signal described in item (1).

The features of interest in the TGA output photos are: the amplitude uniformity (or lack thereof), which is indicative of the performance of the phase-randomization algorithm (see Section 2.4) and the presence or absence of coefficient clipping, which, because of its nonlinear nature, can cause intermodulation noise to degrade the system SNR. In the spectrum analyzer photos, the bit height fluctuations caused by the intermods (or other noise sources) can be seen, as well as the frequency-dependent profile which is intentionally added through the use of the Digital Filter.

#### 4.1.1.2 Digital Filter Test Results

The first test was simply to document the effect that the DF setting has on the frequency profile of the data. The series of photos in Figures 4.1.1.2-1 through 4.1.1.2-4 show spectrum analyzer outputs for the various DF settings. Data for these photos is as follows:

##### All Figures

TGA Gain	5
<u>Spectrum Analyzer Parameters</u>	
Center Frequency	1 MHz
Bandwidth	3 KHz
Freq/division	200 KHz
Scan time/division	50 msec
Vertical scale/division	2 dB

##### Fig. 4.1.1.2-1

DF Setting	1/4
------------	-----

##### Fig. 4.1.1.2-2

DF Setting	1/2
------------	-----

##### Fig. 4.1.1.2-3

DF Setting	3/4
------------	-----

##### Fig. 4.1.1.2-4

DF Setting	1
------------	---

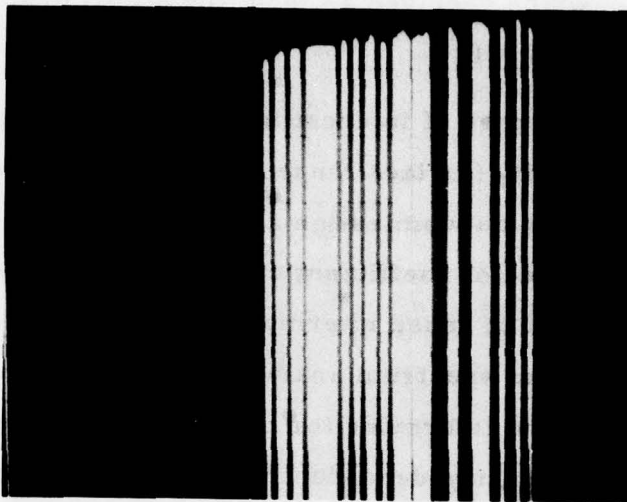


Figure 4.1.1.2-1. Spectral Analysis of TGA Output for Digital Filter Setting of  $1/4$

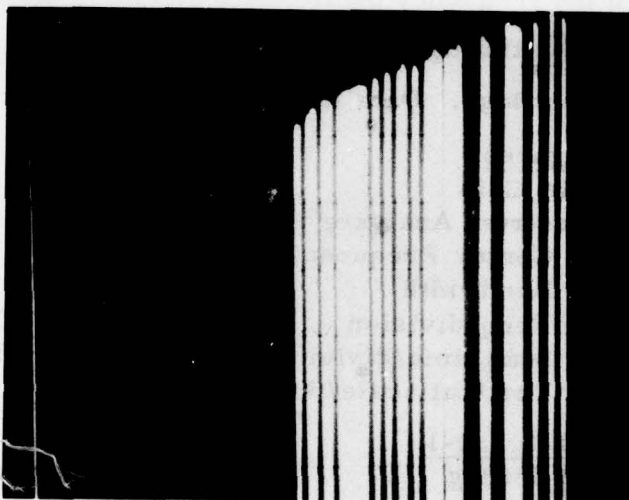


Figure 4.1.1.2-2. Spectral Analysis of TGA Output for Digital Filter Setting of  $1/2$

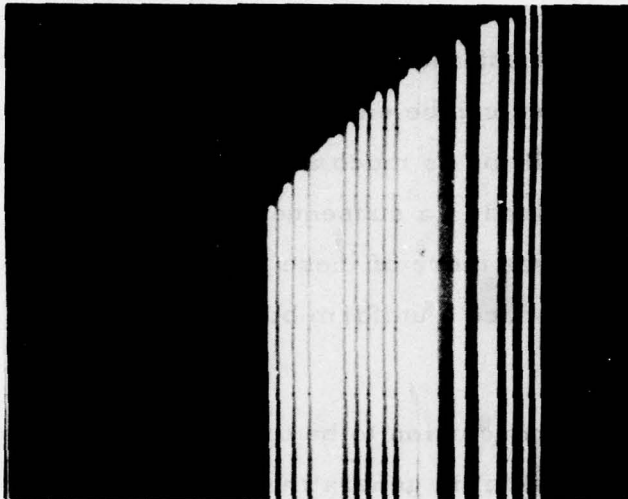


Figure 4.1.1.2-3. Spectral Analysis of TGA Output for Digital Filter Setting of  $3/4$

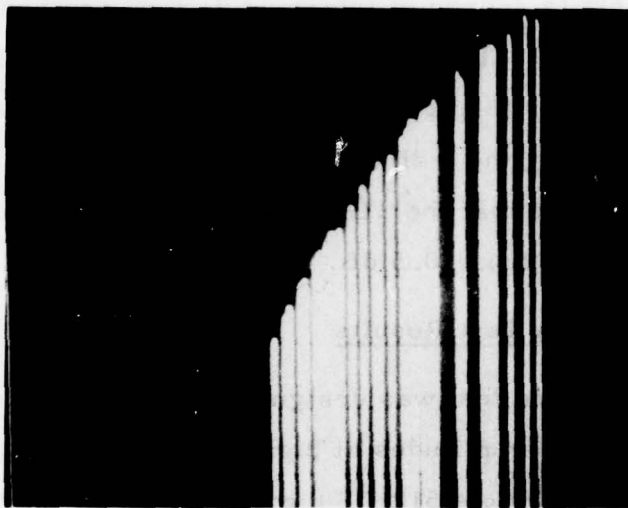


Figure 4.1.1.2-4. Spectral Analysis of TGA Output for Digital Filter Setting of 1

#### 4.1.1.3 Digital Filter Test Interpretations

This test shows that a reasonably wide range of frequency preemphasis can be obtained through the use of the Digital Filter technique. The high frequencies can be enhanced with respect to the low frequencies by as little as 1.5 dB or as much as 10 dB. The selection of an operational value will be described in a subsequent section, and will be based on the extent to which one or more of these filter settings applied to the recorded frequencies can produce a uniform bit height profile in the reproduced data.

Another conclusion to be drawn from this experiment is that the TGA is quite successful in generating uniform amplitude frequency components. These frequency components, which correspond to data bits in playback, must be kept as uniform as possible to permit optimal thresholding and hence minimized BER. The TGA gain of 5 which was used here will be shown in the following subsection to produce no clipping of transform coefficients (a source of intermodulation, and hence spurious bit height fluctuations). Thus the bit height profile shown in photos 4.1.1.2-1 through 4.1.1.2-4 is (neglecting the DF envelope) representative of TGA performance. Using the 2 dB/cm value from the Spectrum Analyzer settings, we can see that the TGA output frequencies are uniform in amplitude to better than  $\pm 0.5$  dB.

#### 4.1.1.4 TGA Gain Test Results

The second test was designed to show the effect of clipping of the DFT coefficient amplitudes at high TGA gain settings. The first set of scope photos shows the 512 DFT coefficients for TGA gains of 5 (Fig. 4.1.1.4-1) and 10 (Fig. 4.1.1.4-2). Note that in the latter photo many of the coefficients have exceeded the 8-bit range of the TGA, and are therefore being clipped at the upper limit of that range. For both pictures, the DF setting is 1/4, and the scan time/division is 20  $\mu$ sec.

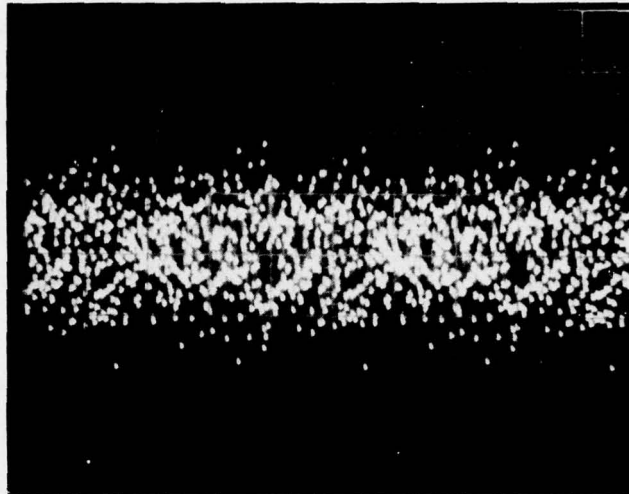


Figure 4.1.1.4-1. Output of TGA for Gain of 5, DF of 1/4,  
Showing 512 DFT Coefficients

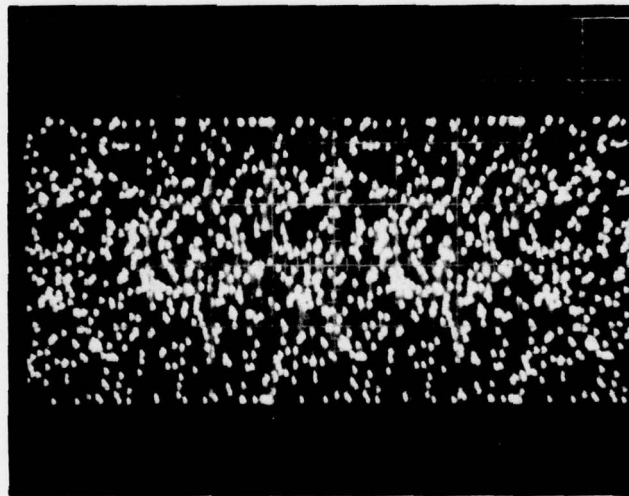


Figure 4.1.1.4-2. Output of TGA for Gain of 10, DF of 1/4

The second set of pictures shows the result of sending the TGA outputs in the previous photos through spectrum analysis. The spectrum analyzer data for these pictures are the same as those given in Section 4.1.1.2 above, except that the vertical scale is now 10 dB/division. Note the dramatic difference which is made by the clipping of the TGA coefficients. The first photo (Fig. 4.1.1.4-3, which corresponds to Fig. 4.1.1.4-1) shows a fairly uniform sideband suppression of at least 30 dB, and a coefficient uniformity of better than 1 dB (see previous subsection). By contrast, Fig. 4.1.1.4-4 (corresponding to Fig. 4.1.1.4-2) shows barely 20 dB sideband suppression in the region near the data band, and the bit heights are now visibly non-uniform. This nonuniformity, a result of intermodulation noise caused by coefficient clipping, is illustrated further by Fig. 4.1.1.4-5, where the previous figure is repeated, but with a vertical sensitivity of 2 dB/division. This makes it clear that bit height fluctuation is now worse than  $\pm 1$  dB.

#### 4.1.1.5 TGA Gain Test Interpretation

This test shows that the dynamic range provided by the TGA Gain adjustment is sufficient to drive the TGA to the point of clipping, beyond which significant deterioration of the system SNR is inevitable. Some quantitative information has also been generated to indicate the amount of degradation to be expected for specific TGA gain settings. The tradeoffs affecting the actual selection of the operating parameter values (DF setting and TGA gain) will depend on the relationships of the illustrated effects to readout BER, and will be detailed in a later section.

#### 4.1.2 AOM Equalization Studies

The acousto-optic modulator (AOM) in the HRMR system is used to modulate the light intensity as the laser beam is deflected (by the AOBD) along the hologram's length. The intensity modulation is thus used to write the holographic fringes which represent the coefficient

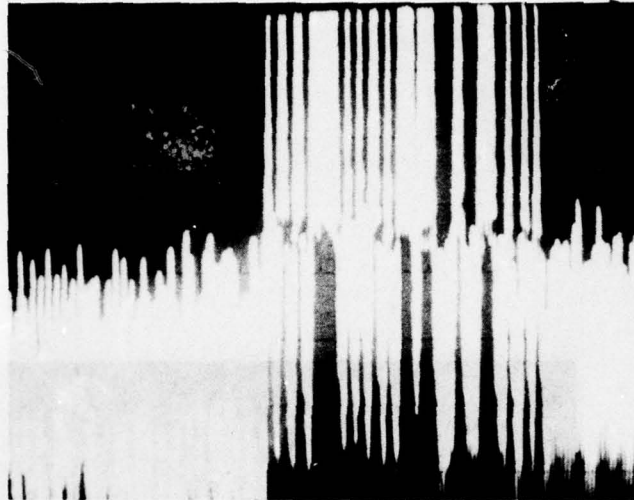


Figure 4.1.1.4-3. Spectral Analysis of TGA Output with Gain of 5

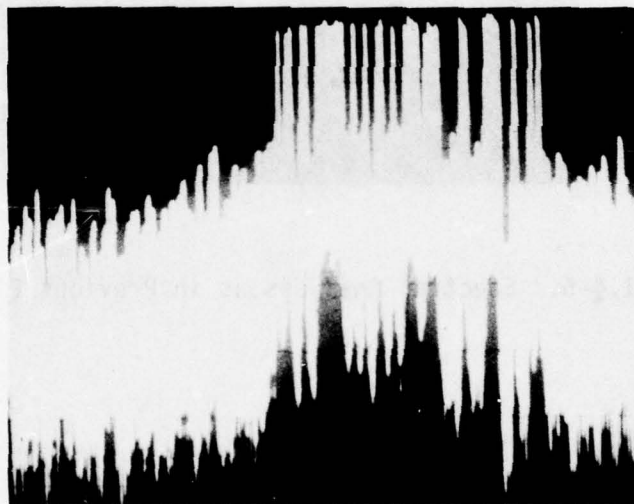


Figure 4.1.1.4-4. Spectral Analysis of TGA Output with Gain of 10

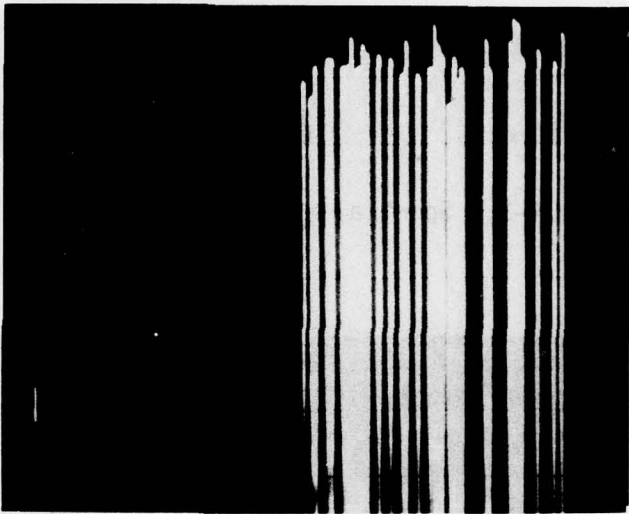


Figure 4.1.1.4-5. Spectral Analysis as in Previous Figure but at 2dB/div.

values of the discrete Fourier transform generated by the TGA. For optimal information transfer, the relationship between the RF power input to the AOM and the intensity of the diffracted light output should be strictly linear. Nonlinear transfer functions can result (as above with the TGA clipping experiment) in bit-to-bit crosstalk or intermodulation which degrades the system's BER performance.

Since a real-world AOM has a drive power/output intensity relationship which is somewhat non-linear, a technique to compensate for this nonlinearity had to be found. The selected method consisted of the following steps:

- (1) Measure the AOM output response to a linear series of input drive power levels;
- (2) Program a memory device with an appropriately scaled version of the response curve;
- (3) Let the AOM drive circuit look up in the memory the appropriate drive level to produce a linear response.

#### 4.1.2.1 Test Procedure and Result

This procedure simply verifies that the programmed AOM equalizer memory successfully linearizes the AOM response. The procedure is to display on an oscilloscope the contents of the equalizer memory as well as the actual linearized output of the AOM. The desired result is produced by setting the TGA to produce a linearly increasing ramp as the data input, and displaying the output of the AOM data receiver. The result is shown in Figure 4.1.2.1-1. The thin bright curve is the contents of the AOM equalizer memory (the horizontal axis is increasing input drive power; two cycles are shown), while the thicker, fuzzy line is the linearized AOM output. Note the nonlinearity of the equalizer

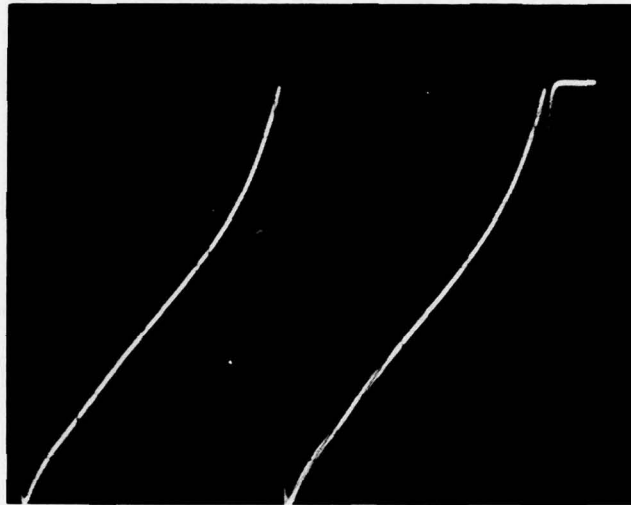


Figure 4.1.2.1-1. AOM Linearization, Showing Equalizer Memory Contents (Thin Line), and Linearized AOM Output (Fuzzy Line)

coefficients (corresponding to an equivalent nonlinearity in the uncorrected AOM response) and the relative linearity of the corrected AOM response.

The effect of this linearization procedure as a means of suppressing data dependent noise (i. e., in a system context with the TGA in normal operation and some intermodulation present) will be shown in the next subsection.

#### 4. 1. 3 TGA and AOM Equalizer Combined Effects

We have seen in a previous subsection that the bit height fluctuations which result from bit-to-bit crosstalk via system nonlinearities at high TGA gain settings can be an important source of noise. We can therefore expect that the AOM linearization process described in the previous subsection will have a beneficial effect on this intermodulation noise. To verify this, and to obtain some additional data on the practical values of the available system parameters, experiments were performed to determine the intermodulation noise performance of the TGA and AOM equalizer in combination.

##### 4. 1. 3. 1 Test Procedure and Results

This test was essentially a repetition of the experiment described in subsection 4. 1. 1, except that here the TGA output is actually modulated onto the laser beam by the (linearized) AOM. The light so modulated is then detected by a photodiode and the resulting signal is sent to the spectrum analyzer.

The results of this procedure are shown in Figures 4. 1. 3. 1-1 through 4. 1. 3. 1-6. There are three pairs of photos, each at a different TGA gain setting. Within each pair, the first picture shows the spectrum analyzer's output without AOM equalizer correction, while the second picture gives the result with AOM equalization. In these pictures, the spectrum analyzer has been set in a linear vertical sensitivity mode



Figure 4.1.3.1-1. Spectral Analysis of AOM Output. TGA Gain = 5  
Without AOM Linearization



Figure 4.1.3.1-2. Spectral Analysis of AOM Output. TGA Gain = 5  
With AOM Linearization

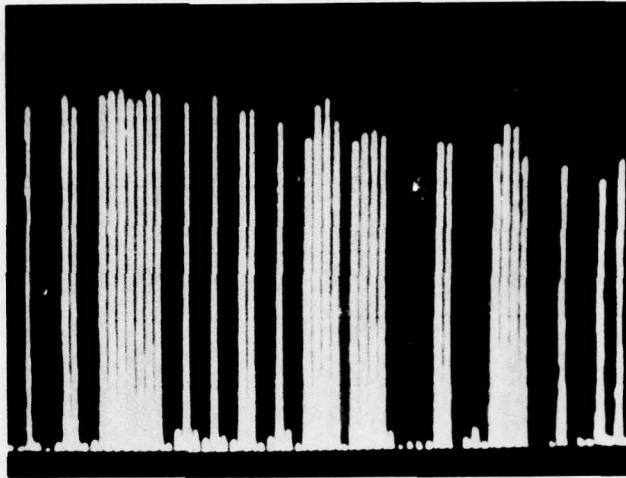


Figure 4.1.3.1-3. Spectral Analysis of AOM Output. TGA Gain = 8  
Without AOM Linearization



Figure 4.1.3.1-4. Spectral Analysis of AOM Output. TGA Gain = 8  
With AOM Linearization

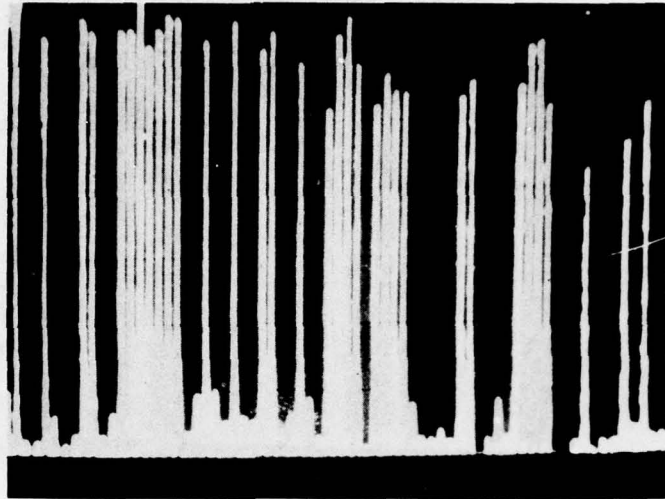


Figure 4.1.3.1-5. Spectral Analysis of AOM Output. TGA Gain = 11  
Without AOM Linearization



Figure 4.1.3.1-6. Spectral Analysis of AOM Output. TGA Gain = 11  
With AOM Linearization

(as opposed to logarithmic as in the previous cases). The vertical scale is 10 mv/division, with a sensitivity of 0.4. Note the smaller amount of bit height fluctuation in the pictures with the equalizer activated. This indicates that the AOM linearization does help to suppress intermodulation noise.

#### 4.1.3.2 Test Interpretation

At the lower gain (TGA gain of 5) the effect of the AOM linearization is minor, because the small gain setting limits the transform coefficients to a narrow dynamic range over which the AOM is already fairly linear. The intermediate TGA gain of 8 shows a noticeable improvement as a result of equalization. The most significant improvement is seen at the higher TGA gain of 11. Note that a  $\pm 10\%$  variation in bit heights was reduced to less than  $\pm 5\%$ , and that the intermods at the zero bit sites were reduced by approximately a factor of three. At even higher TGA gains (not illustrated), the effect of clipping at the TGA predominates, and AOM linearization has little or no effect on the extent of the intermodulation noise present. The conclusion reached on the basis of these experiments is that operation of the system at TGA gains of 5 to 11 is feasible, provided that film nonlinearity can also be compensated in the equalizer to prevent further intermodulation noise increases.

#### 4.1.4 Digital Filter Effect at Readout

In section 4.1.1 above it was seen that, viewed at the recorder, the digital filter (DF) response correction mechanism had a wide dynamic range of correction options available. The actual choice of a DF setting for operation of the full system, of course, depends on the performances of the various settings as seen at the reader. In this subsection we detail the results of the experiment which investigated those performances.

#### 4.1.4.1 Test Procedure and Result

In the previous sections, the data bit heights had to be observed with a spectrum analyzer, since they were present only as spectral components of the output of the TGA. After recording, of course, they are present as spatial frequency components within the holograms, and the readout process is essentially a spatial spectral analysis. Thus at the readout array, the spectral components, now called data bits, are present simultaneously and may be detected. The procedure followed here was to record holograms at various DF settings (and TGA gain settings) and to playback and display the detected data bits on an oscilloscope.

In these holograms the data pattern was constant, and was chosen to be an "every-fourth-bit" pattern to minimize bit-to-bit cross-talk and permit easy observation of the envelope produced by the DF pre-emphasis. The data bits are detected by the Reticon detector array in two channels, the even and odd bits being separated, so that the "every-fourth-bit" pattern resulted in an "every-other-bit" pattern on the odd channel and a "no-bit" pattern on the even channel.

The results are displayed in Figures 4.1.4.1-1 through 4.1.4.1-4. The horizontal and vertical scales for all pictures are  $2 \mu\text{sec/cm}$  and  $0.2 \text{ volt/cm}$ , respectively, and the TGA gain setting for all the fiche was 11. The four pictures present a series of increasing DF values:  $DF = 1/4$ ,  $DF = 1/2$ ,  $DF = 3/4$ ,  $DF = 1$ .

#### 4.1.4.2 Test Interpretation

The Digital Filter has a clear-cut effect on the overall bit height profile, with increasing DF putting increasing emphasis on the high frequency (right hand) end of the data array. The extreme values,  $DF = 1/4$  and  $DF = 1$  are clearly not optimum, since they each enhance

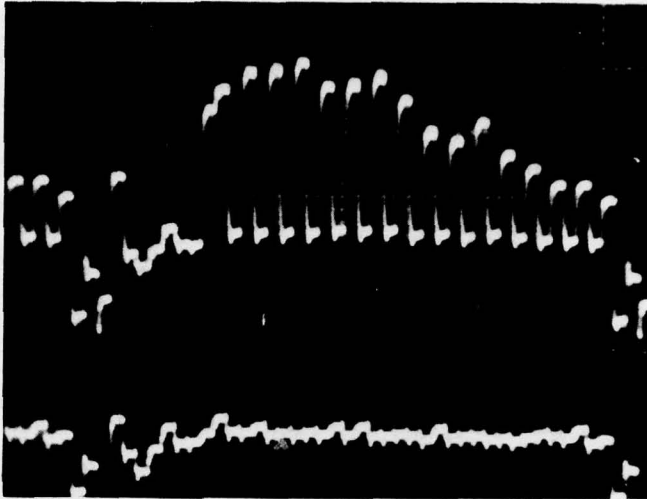


Figure 4.1.4.1-1. Detected Data in Digital Filter Study. TGA Gain 11,  
DF Setting 1/4

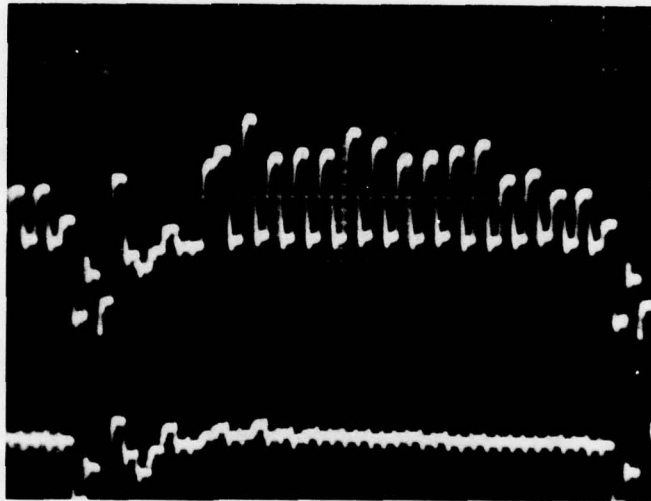


Figure 4.1.4.1-2. Detected Data in Digital Filter Study. TGA Gain 11,  
DF Setting 1/2

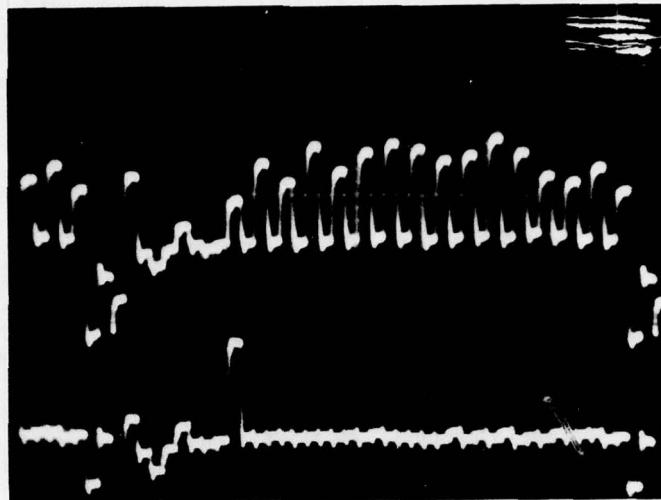


Figure 4.1.4.1-3. Detected Data in Digital Filter Study. TGA Gain 11,  
DF Setting  $\frac{3}{4}$

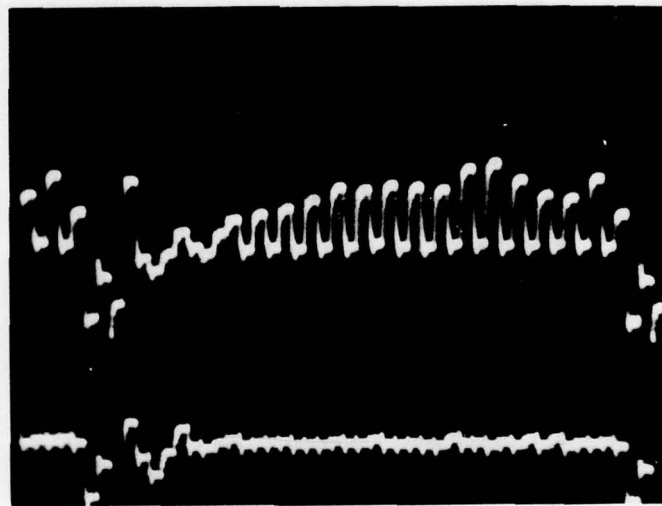


Figure 4.1.4.1-4. Detected Data in Digital Filter Study. TGA Gain 11,  
DF Setting 1

one end of the array at the expense of the other. The other values (DF = 1/2 and DF = 3/4) are more successful in producing an even, more easily thresholded, profile. The DF = 3/4 setting may be slightly more attractive in the illustrations shown, but in general both settings are acceptable. Another conclusion is that the proper DF setting depends on the TGA gain setting. This is an expected result, since the TGA gain also contributes to the amount of nonlinearity in the system. The conclusion reached as a result of this and similar studies is that the preferred operational parameter settings for normal use are TGA gain of 11 with DF = 1/2, or TGA gain of 13 with DF = 3/4.

#### 4.2 System Performance Characterization

After the integration, checkout, and parameter selection process for the HRMR system was complete, continued system operation and testing was done to provide a thorough file of information on the system's capabilities and limitations. This section will present some of the more significant experimental results concerning the system's capabilities and performance values, while the following section will detail some of the procedures undertaken in attempting to correct the system's problems and limitations.

##### 4.2.1 Recorder Performance

It is convenient to separate the material to be presented in this section into two parts. Subsection 4.2.2 will describe some important performance characteristics of the verifier subsystem; this subsection details two of the key areas of recorder performance.

In the system development process, successful recorder operation clearly must predate the testing and operation of the verifier. The complete set of criteria for proper recorder operation is complex, and is well summarized in the operations manual, as well

as elsewhere in this report. The purpose of this subsection is to document two of the more interesting experiments which were carried out to verify correct recorder operation.

#### 4.2.1.1 AOBD Frequency/Linearization Interaction

To provide a correct, minimum-noise transfer of information from electronic signals to photographic film, the acousto-optic beam deflector (AOBD) must provide a uniform intensity laser beam as a function of the RF input frequency. This is similar to the requirement for linearity of the AOM discussed above in section 4.1.2. The method of achieving a linear device response is also similar: the input signal is modified in a pre-programmed way to produce the desired output. Unlike the AOM, however, the AOBD has a third parameter, center frequency, which must be controlled to ensure proper performance. Specifically, if the band of frequencies over which the AOBD operates is even slightly different from the band for which it has been linearized, the equalization will not succeed, and will in fact produce a worsening of the device's output intensity fluctuations.

Because of the existence of this effect, an experiment was performed to document the effect of frequency errors on the AOBD linearization, and to quantify the relationship for future system design tolerancing. The basic test procedure for this experiment was a simple one: perform the AOBD equalization (pre-programming) at one center frequency, then record the beam intensity fluctuations (as a function of frequency) produced when the device is operated at other center frequencies. The two sources of these intensity fluctuations are: variations in the output of the VCO which drives the AOBD; and the power coupling (impedance) resonances of the AOBD transducer itself. The combined effect of these two sources can produce significant intensity variations in the device output. Thus a pre-programmed correction intended to

enhance the intensity at one particular frequency can, if applied at the wrong frequency, add to an intensity level already at or above the desired value.

The results of this experiment are shown in Figures 4.2.1.1-1 through 4.2.1.1-4. The first picture shows the light intensity detected at the film plane as a function of scan position; it was taken with the AOBD operating over its nominal frequency band of 145 MHz to 260 MHz. The remaining pictures present a series of similar pictures with the frequency band shifted by a fixed increment each time.

The pictures show that a fairly small (4%) change in the center frequency can make a significant difference to the effectiveness of the equalization process. The importance of this is that it shows that the optical alignment of the recorder system, which interacts with the frequency band used in the AOBD (i. e. , both can cause positional shifts of the laser beam), must always be done in such a way that the pre-programming of the AOBD equalization circuit remains valid.

#### 4.2.1.2 Diffraction Efficiency Studies

Another important feature of a holographic recording system is the ability to produce holograms of adequate diffraction efficiency. In general, to obtain high diffraction efficiency holograms, a large modulation depth is required. In the HRMR system, the modulation depth is controlled by the TGA gain setting; and, as shown in a previous section, that setting is also interactive with the amount of undesirable intermodulation noise experienced by the system. Thus the proper gain setting becomes a tradeoff between intermodulation noise and diffraction efficiency. When the previously described experiments had set the maximum acceptable level for the TGA gain, readout tests showed that the achieved diffraction efficiency levels were adequate.

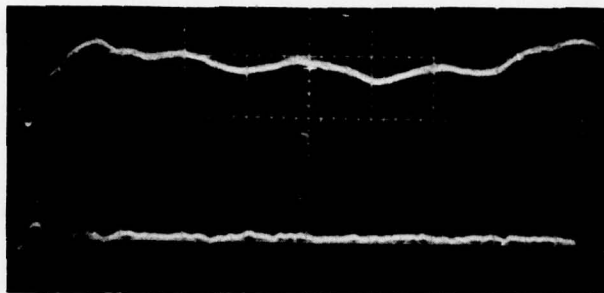


Figure 4.2.1.1-1. Detected Intensity of Film Plane During One Hologram Scan Time - AOBBD Using Nominal Frequency Band

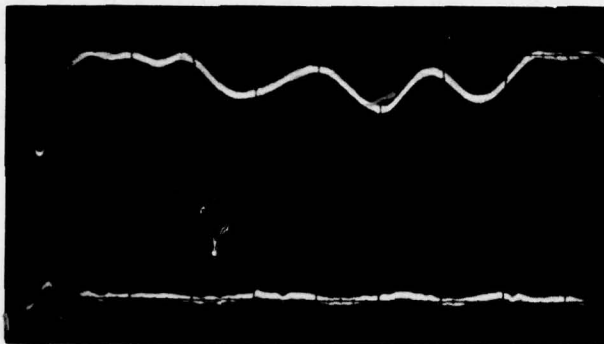


Figure 4.2.1.1-2. Same as Previous Photo, But With AOBBD Frequency Band Displaced Downward by 6 MHz

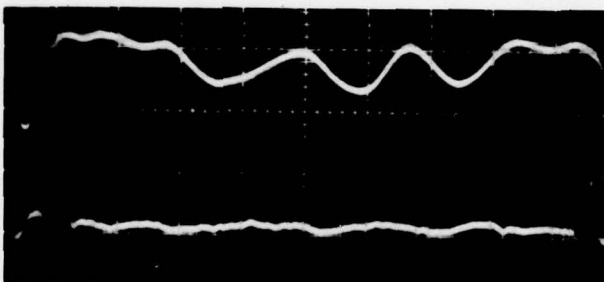


Figure 4.2.1.1-3. Same as Previous Photo, But With AOBBD Frequency Band Displaced Downward by an Additional 6 MHz

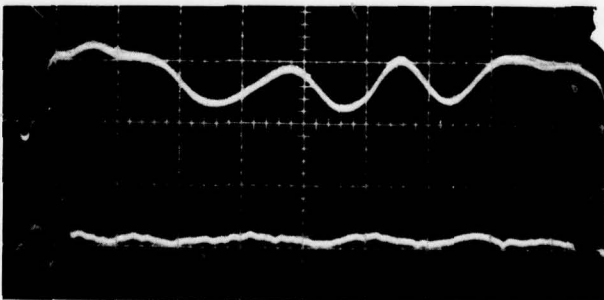


Figure 4.2.1.1-4. Same as Previous Photo, But With AOBBD Frequency Band Displaced Downward by an Additional 6 MHz

The experimental procedure was a simple one: a laser beam was passed in an unfocused condition through the hologram tracks of the fiche under test. The diffracted and undiffracted (DC) portions of the beam were then separately collected and detected to provide a measure of the fiche's diffraction efficiency. It should be noted that, since the relatively large beam illuminated several dozen holograms at any given time, the resulting efficiency values are not true efficiencies, but efficiency-proportional numbers (which are nevertheless highly useful in characterizing and later repeating a given diffraction performance).

A notable feature of this test was the attempt to measure the effect of varying data content on hologram diffraction efficiency. In a completely linear system, theory predicts strict proportionality: the more data bits a hologram contains, the more light it should diffract, with the diffraction efficiency per bit being essentially constant. The next more complicated model predicts some saturation at high bit content, due to nonlinear effects in the film emulsion. To document these effects in the HRMR system, the diffraction efficiency tests were made on a fiche with controlled variable data content.

Due to the addition of parity bits by the error correction coding electronics (and the sync and threshold bits added to each hologram), the minimum number of "one" bits in a hologram is approximately 14. Similarly, because data patterns which would result in a more-than-50% populated hologram are inverted before recording (to avoid the nonlinear effects mentioned above), the maximum number of "one" bits in a hologram is 34. Within this range the holograms can vary in bit population according to the nature of the data to be recorded, with a corresponding variation in the light which will be diffracted from each hologram. To document and quantify this effect, a fiche was recorded in which the bit population varied in a controlled way from 14 to 34. Specifically, ASCII

characters were recorded in blocks of 256 holograms each, so that the laser beam could pass through each type (population density) of hologram individually. The ASCII characters used and the resulting "one" bit populations of the holograms were as follows:

<u>ASCII Character</u>	<u>No. of "1" bits/hologram</u>
NULL	14
@	18
B	22
A	24
D	24
C	26
o	27
E	28
G	32
F	34

The data for this fiche were taken using a 2.0 mW Helium-Neon laser. The typical transmitted portion of the beam was 0.59 mW, while the amount of light diffracted into the data band ranged from 5.0 to 12.9  $\mu$ W. Thus, using a conventional definition of diffraction efficiency (the ratio of diffracted to transmitted light), our result shows a value ranging from 0.84 to 2.2%, depending on bit population density. The complete results for the various populations are shown in Figure 4.2.1.2-1, which plots the diffraction percentage against the number of "one" bits in the hologram. The error bars result from the averaging of data taken at four different locations on the fiche to negate any spatial variations of recording intensity.

The result confirms an approximately linear relationship of bit population to diffraction intensity; it also shows a tendency toward deviation from linearity at the higher population densities, providing a partial confirmation of the validity of the decision to invert the data of holograms which would otherwise be more than 50% populated.

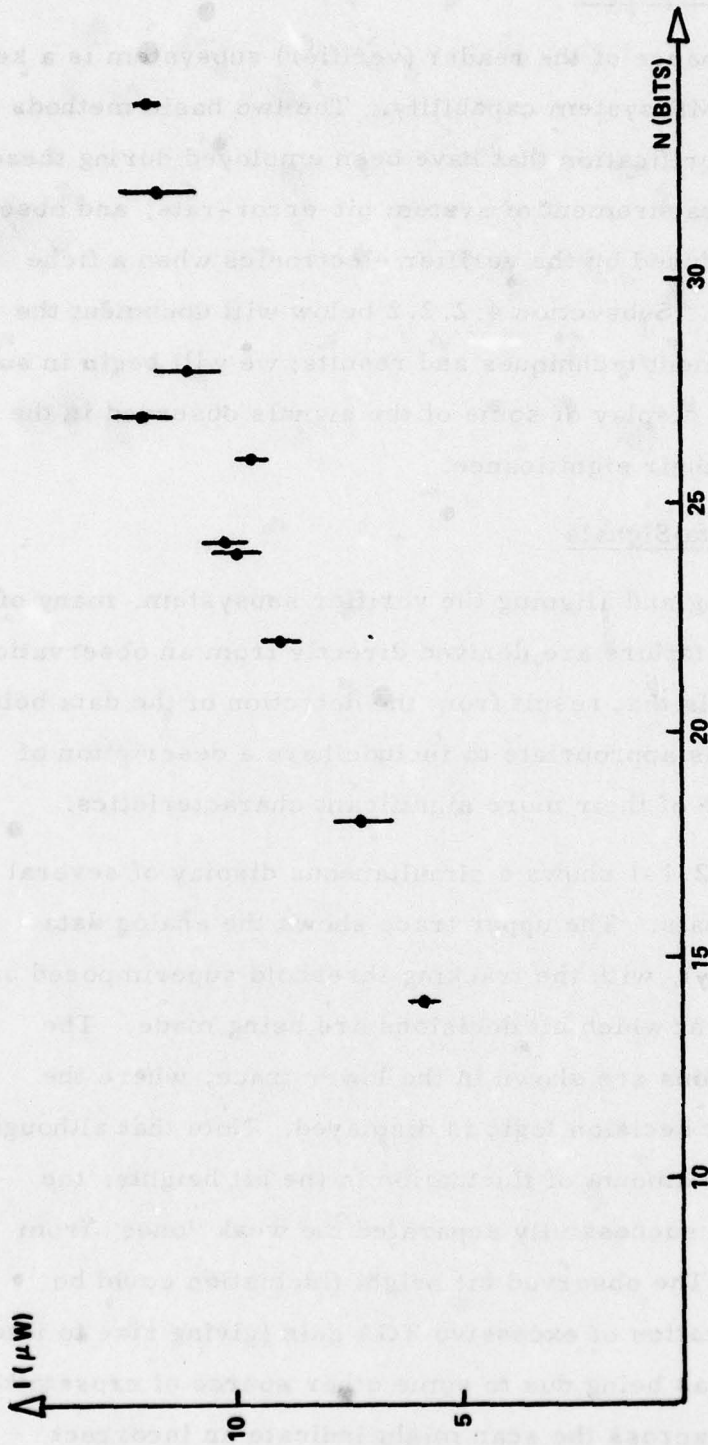


Figure 4.2.1.2-1. Diffracted Light Intensity Received Versus Number of "One" Bits Set in Holograms

#### 4.2.2 Reader Performance

The performance of the reader (verifier) subsystem is a key part of the overall HRMR system capability. The two basic methods of reader performance verification that have been employed during these studies are: direct measurement of system bit-error-rate, and observation of the signals produced by the verifier electronics when a fiche readout is in progress. Subsection 4.2.2.2 below will document the system BER measurement techniques and results; we will begin in subsection 4.2.2.1 with a display of some of the signals observed in the verifier and describe their significance.

##### 4.2.2.1 Detected Data Signals

In integrating and aligning the verifier subsystem, many of the criteria of success or failure are derived directly from an observation of the electronic signals that result from the detection of the data being played back. Thus it is appropriate to include here a description of these signals and some of their more significant characteristics.

Figure 4.2.2.1-1 shows a simultaneous display of several important readout signals. The upper trace shows the analog data detected (even bits only), with the tracking threshold superimposed on it to indicate the level at which bit decisions are being made. The results of those decisions are shown in the lower trace, where the digital output of the bit decision logic is displayed. Note that although there is a rather large amount of fluctuation in the bit heights, the tracking threshold has successfully separated the weak "ones" from the strong "zeroes". The observed bit height fluctuation could be interpreted as an indication of excessive TGA gain (giving rise to intermodulation noise), or as being due to some other source of crosstalk. The sloping threshold across the scan might indicate an incorrect setting of the Digital Filter. How the various interpretations of certain

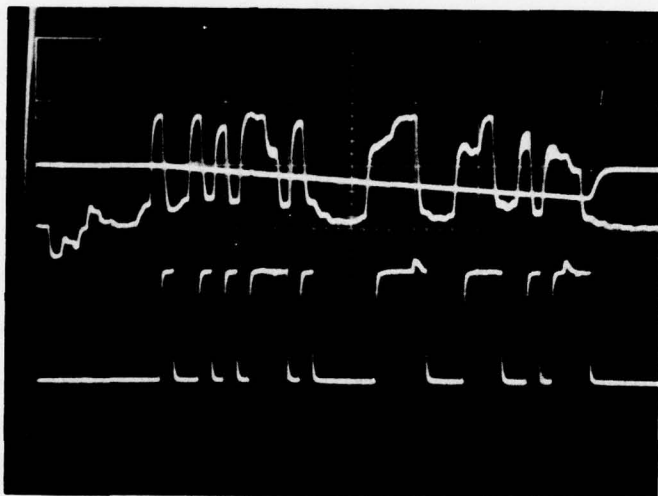


Figure 4.2.2.1-1. Output Signals During Readout: Analog Data With Superimposed Threshold, and Resulting Digital Data

readout indications can be used to track down and possibly correct some of the system's problem areas will be discussed below in the section on Diagnostics (Section 4.3).

Another verifier signal display which is of frequent use is shown in Figure 4.2.2.1-2. This is a display of both channels (even and odd bits) of the hologram readout electronics, taken while the film was in motion. The motion of the film guarantees that any bit profile or fluctuations are due to some fixed-pattern noise recorded into all holograms, such as intermodulation noise. The fuzzy top of the "one" bits is due to the fact that there are 6 Reticon scans per hologram; thus the scans made roughly between holograms are responsible for the lower part of each trace, while the peaks, where the bit decisions are made, come from the scans that are well aligned with the holograms. Some of the characteristics of this display which may be of use in the alignment or operation of the system are: uniformity and symmetry of the overall envelope, indicative of proper digital filter operation and optical system alignment; bit height uniformity or fluctuation, which can be indicative of the absence or presence of certain types of noise; and synchronization of the display with various system timing signals, which can verify proper reader alignment in the bit-to-bit direction as well as proper scaling of the recorded data.

#### 4.2.2.2 Bit-Error Rate Measurements

BER analysis software is provided by the system's host computer; this makes BER measurement a straightforward process. Available error printouts include the number of errors per track, the number of errors per block, and complete block data and error printouts to the bit level. To determine the raw and corrected BER values for the HRMR system, the block and track level programs were employed. A representative fiche was selected for analysis. The data was

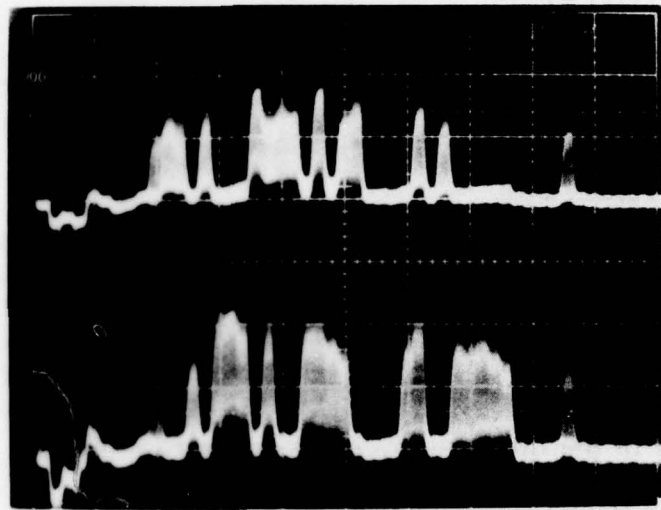


Figure 4.2.2.1-2. Even and Odd Analog Data Readout Channels

reproduced by the verifier and sent to the computer, which performed an "exclusive or" of the originally recorded data with the recovered data. The result was a difference file representing only those bits reproduced incorrectly; counting algorithms were then performed and the results output to a hard copy device. The data taken in this way are summarized in Table 4.2.2.2 below.

Table 4.2.2.2  
BER Analysis Data

Trial #1

Bits Examined	40,040,448
Raw Errors	8,485
Raw BER	$2.12 \times 10^{-4}$

Trial #2

Bits Examined	15,052,800
Raw Errors	4,152
Corrected Errors	1,280
Raw BER	$2.76 \times 10^{-4}$
Corrected BER	$8.5 \times 10^{-5}$

As the data in the table show, an average raw BER of about  $2.4 \times 10^{-4}$  was observed, with the corrected average about  $8.5 \times 10^{-5}$ . It should be noted, however, that some systematic errors remained in the system at the time of these measurements, and have been counted in the above data. There are two types of such systematic errors: one, which affects only the raw data, is apparently responsible for 50% of the raw errors currently observed in the system, and is also discussed in Section 5.1 of this report; the other, which affects only the corrected data, appears to be arising in the data transfer or decoding electronics, and accounts for approximately 50% of the observed corrected errors. Thus, although the current error rates are somewhat high, correction of the two systematic errors could reduce raw BER by a factor of 2, and corrected BER by as much as a factor of 16 (2X directly, and up to 8X indirectly

as a result of the raw BER reduction). As a specific example, if in Trial #2 above the systematic errors are not included in the total, the observed error total falls from 1280 to about 580, and the corrected BER is then about  $3.7 \times 10^{-5}$ .

A final note about BER performance concerns the use of interleaving techniques. The system as currently implemented does not interleave the recorded codewords; as a result, any burst errors that occur are sure to produce a decoder failure, because many of the errors fall into the same codeword. Interleaving (or interlacing) of codewords can prevent this, effectively sharing the burst errors among a number of codewords. This technique and its potential results will be discussed in detail below in Section 5.1, where it will be shown that for a sufficiently great interleave depth, the system as currently configured is capable of reaching the  $1 \times 10^{-7}$  BER region.

#### 4.3 Diagnostic Studies

An important phase in the development of any complex system is the diagnosis and correction of the various expected and unexpected problems that are encountered during system operation. In some cases, the diagnosed problem may be simply corrected, either by a change in the operational routine or by a minor modification of some part or subsystem. In other cases, either the design complexity of the affected area or the cost and schedule commitments of the program may prevent total resolution of the problem. In all cases, the information gathering process is crucial, in that it provides a solid base of experience on which future programs can build.

In this section we present some of the main technical problems that have arisen in the path of the HRMR system development activity; included are descriptions of each problem and the diagnostic techniques applied to it, solutions that have been implemented or could be

implemented, and recommendations for elimination of the problems in future systems.

#### 4.3.1 Along-Track Recorder Signatures

The nominal operational mode of the HRMR recording system calls for holograms to be recorded at equal spacings along the tracks. This provides the opportunity during readout to use the holograms to derive a clock signal, which may be used to predict hologram locations and thus synchronize the bit decision logic with the maximum received bit intensities. This is done with a phase-locked loop circuit (PLL).

Several problems can be caused by deviations of the holograms from equal spacings (as might result for example from nonlinear motion of the X-Y transport): if the rate of change of spacing is great enough, the PLL will fail to keep up, resulting in incorrect phasing between the holograms and the hologram clock; this in turn will produce bit decisions made at less than peak signal intensities (or even between holograms), which will raise the bit-error rate substantially. Additional effects include loss of resolution and hologram crossread in the along track direction due to partial fringe overlap of adjacent holograms.

The early experiments performed on the HRMR system showed this to be a noticeable problem, and some effort was devoted to reducing it. For example, Figure 4.3.1-1 shows a close-up of the hologram tracks of an early fiche. A variation of hologram spacing with a period of approximately 22 holograms is clearly visible; a peak to peak variation in spacing of nearly 20% can be measured. Also visible in this Figure is a rather large amount of "x-axis wobble" or variation in the spacing between tracks as a function of position down the track. The potential impact of this kind of wobble is that it may introduce crossread from holograms in adjacent tracks during readout, causing interference with the true data bits and hence increased BER.

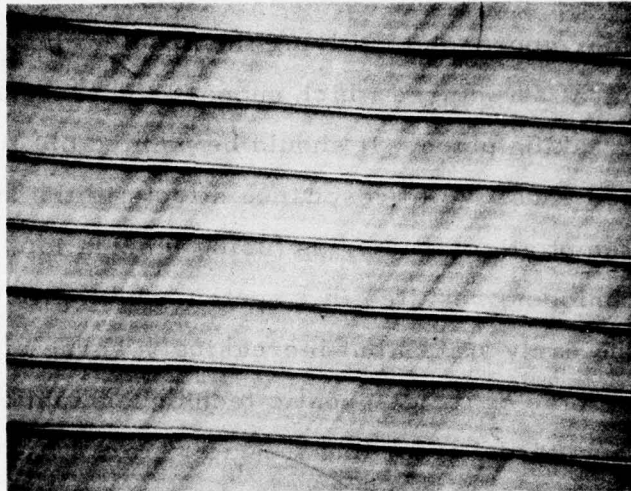


Figure 4.3.1-1. Early Recorded Fiche, Showing Inter-Track Spacing Variation.

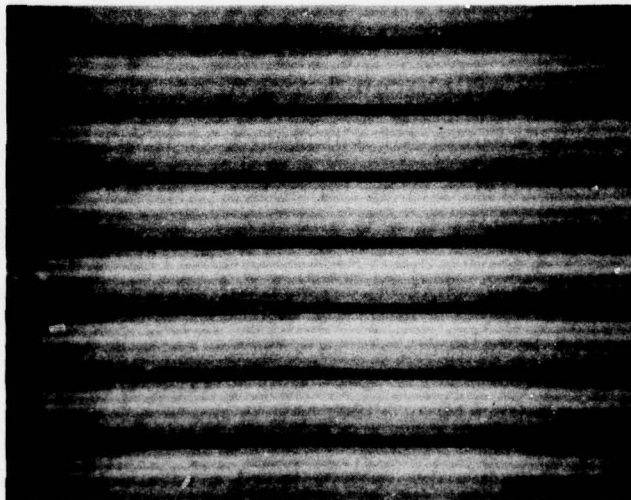


Figure 4.3.1-2. Recently Recorded Fiche, Showing Reduced Inter-Track Spacing Variation

Both of these problems (hologram rate FM signature and x-axis wobble) result from mechanical vibrations in the recorder system, hence the proper approach to solving the problem involves modification of the mechanical structures which support and translate the fiche when a recording is taking place. It should be pointed out that these vibration effects are also sensitive to resonance effects in the support structures. Thus, one attempt at restructuring (using lubrication, preloading, and alignment techniques) resulted in a system which produced very little vibration in the early tracks but increasingly worse signature in the later tracks. Some of the diagnostic techniques applied to investigate this problem included: recording the later tracks first to eliminate any AOB drive drift effects (see Section 4.3.3); recording at slower than normal speeds to see if the resonance would be affected (it was); shock mounting of the fiche transport structure; and varying the alignment of the transport lead screw.

Finally the application of a particular combination of techniques resulted in a system which could record at full rate and produce an acceptably reduced amount of along-track microsignature. Figure 4.3.1-2 presents a view of the hologram tracks which may be compared with that of Figure 4.3.1-1. Some signature is still visible, but readout experiments confirmed that the mechanical adjustments had reduced this effect to tolerable levels.

#### 4.3.2 Reader Vibration Effects

The verifier subsystem is of course also subject to vibration arising from the various mechanisms of the RPV unit. For this reason several experiments were carried out to determine the magnitude and consequences of these vibration effects and, if necessary, to determine appropriate remedial procedures.

The experimental procedure was a relatively simple one. First, a recorded fiche was loaded into the reader unit and aligned such that the readout beam was illuminating a hologram. Next, the sample and hold output (monitoring the intensity of a sync bit) was fed to an oscilloscope. Finally, since the reader x-y transport was not moving, variations in the detected intensity of the sync bit could only be interpreted as resulting from a vibration-induced periodic misalignment of the film and the readout beam. Also, the amplitude of the intensity fluctuation could be interpreted as an indication of the extent of the vibration (e. g. , the amplitude should fall to zero when the beam is completely off of the hologram).

The result of the first experiment of this type is shown in Figure 4.3.2-1. The upper trace is the detected signal when the processor and fan are off; no amplitude variation is observed. The lower trace shows the result when the processor and fan are on; now some amplitude variation is present. Estimates derived from this picture indicate that the amount of vibration was approximately 1/5 of a hologram spacing, with a period of 34 msec. This corresponds (at the nominal system readout rate) to 354 hologram periods. Thus the vibration of 20% of a hologram period in every 354 corresponds to a perceived frequency error in readout of 0.06% peak-to-peak. The conclusion is that this is well within the tracking capabilities of the phase locked loop used to generate the readout clock signal.

The second experiment was essentially a repetition of the first, but with the MR Recording mechanisms as the source of the vibrations. The result, shown in Figure 4.3.2-2, is a considerably stronger variation in received amplitude. Note that the secondary peaks are indicative of a misalignment greater than one hologram, that is, the beam produces a secondary peak when it is displaced far enough to begin reading out

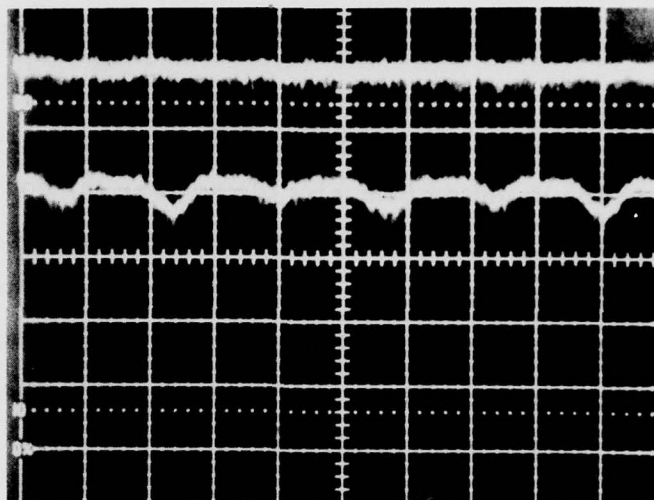


Figure 4.3.2-1. Upper Trace: Detected Sync Bit Amplitude With Vibration Sources Off. Lower Trace: Same With Processor and Fan On. 10 ms/cm, 0.5 V/cm, Both Curves Riding on 1.5 V Bias

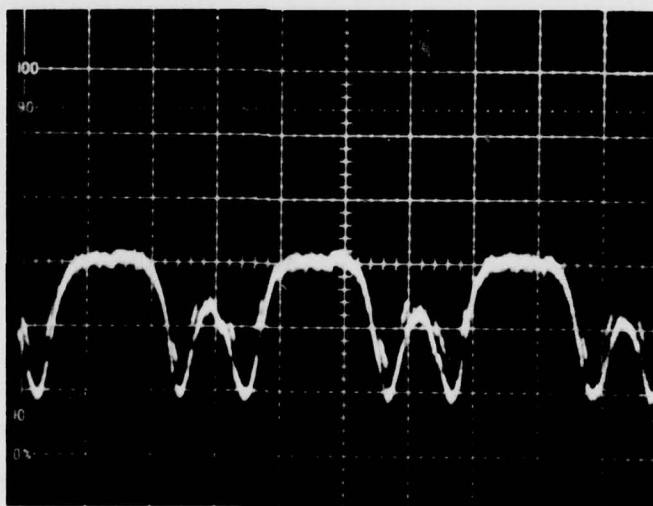


Figure 4.3.2-2. Same as Previous Figure, Showing Vibration Due to MR Recording Process

an adjacent hologram. The estimates derived from this figure show that approximately a 1.5 hologram displacement is being observed with a period of 32 msec. Thus at normal readout rates this would be perceived as a peak-to-peak frequency deviation of approximately 0.4%. This is again well within the design tolerance levels of the readout phase-locked loop circuit, and is therefore not a cause for concern.

The results of these experiments have shown that, unlike the situation in the recorder unit, vibration effects in the verifier are sufficiently minor that they require no additional design constraints or structural modifications to be added to the verifier unit.

#### 4.3.3 AOBD Linearity Stability

In Sections 4.1.2 and 4.1.3 the techniques of linearizing the modulation AOM were discussed, and Section 4.2.1.1 discussed the fact that a similar linearization process is performed on the AOBD (acousto-optic beam deflector). This process (discussed in more detail in the operations manual) consists of controlling the level of the VCO drive to the AOBD such that the beam's sweep rate remains constant. Control is achieved during linearization by a two-step process: 1) a time-of-flight measurement forces the ends of scan to coincide with physical reference points in the optical system; and 2) the chirp rate at many points across the scan is forced to be constant by comparing the differential frequency to a reference frequency. The result of this comparison is then stored in a RAM memory, which eventually drives the VCO via a DAC.

Circuitry to perform this task was implemented in the HRMR system and has performed well. Considerations of thermal drift in the VCO circuits were known from the outset to require that the linearization process be frequently repeated (i. e., prior to every recording). However, the original design called for programming of the RAM using

an algorithm which did not perform as anticipated. Specifically, the assignment of values to each cell in the RAM independently without reference to or resetting of the other cells, resulted in an unstable process. Success was obtained only upon resorting to an algorithm which included all previous cells as well as the next cell in each new sweep. This process was more time consuming than the earlier attempt, and hence resulted in some restructuring of the sequence of operations during fiche recording.

Some of the signals used to diagnose this problem, and to verify proper linearization when it was achieved, are shown in the following photos. Figure 4.3.3-1 shows the sum of the reference frequency and the chirp differential frequency across the hologram scan. Note that these signals do not stay in phase, but have a beat about 25% of the way through the scan. This indicates that the chirp frequency is not constant and hence that linearization of the AOBD is not correct. The result of this fault is shown in Figure 4.3.3-2, where the upper trace is the VCO signal, while the lower trace is a PMT detection of the light from the AOBD after it sweeps a grating positioned in the film plane. Note that at a point corresponding to the beat in the previous figure, the focus of the beam sweeping the grating is lost.

Compare to the previous photos the results shown in Figures 4.3.3-3 and 4.3.3-4, where the same signals are displayed for a situation in which linearization is correct. Note that Figure 4.3.3-3 shows that the reference and difference frequencies remain well phased throughout the scan (except for the retrace and scan start periods, about 10  $\mu$ s total, where linearization is not employed). Similarly the wide modulation depth of the second trace in Figure 4.3.3-4 is maintained throughout the scan, indicating proper focal performance and hence correct linearization.

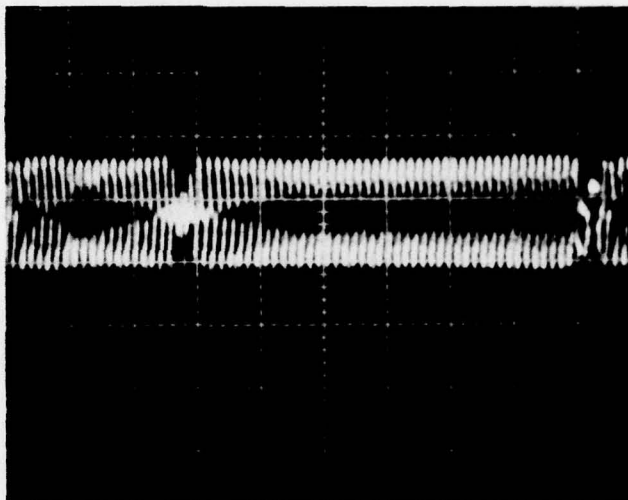


Figure 4.3.3-1. Sum of AOB Reference Frequency and Chirp Differential Frequency Showing Poor Linearization

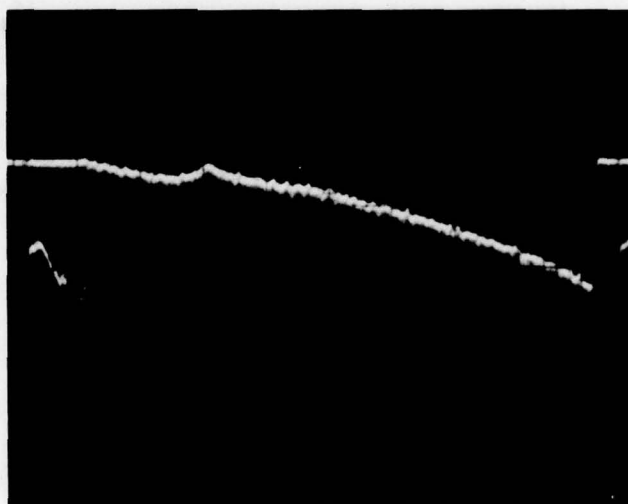


Figure 4.3.3-2. VCO Signal (Upper Trace) and PMT Detected Focus Signal Corresponding to Figure 4.3.3-1

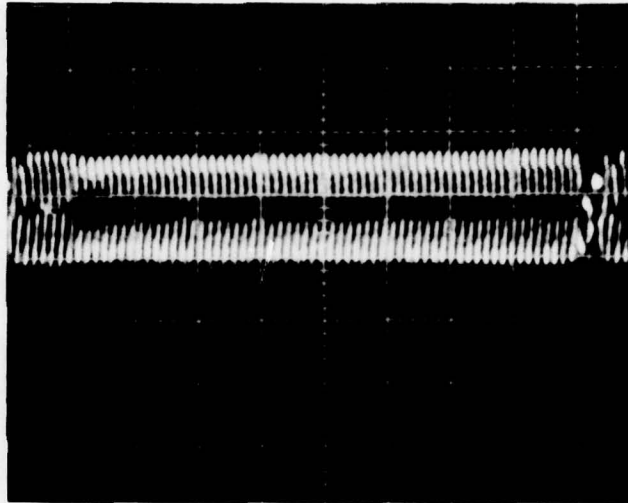


Figure 4.3.3-3. Sum of AOB Reference Frequency and Chirp Differential Frequency Showing Good Linearization

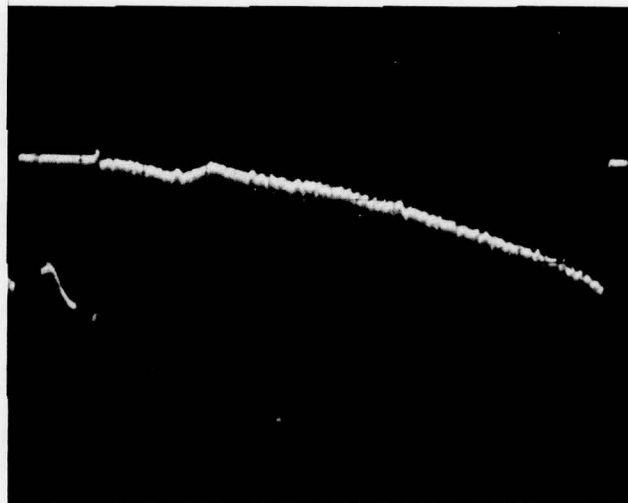


Figure 4.3.3-4. VCO Signal and Focus Signal Corresponding to Figure 4.3.3-3

#### 4.3.4 TGA Gain Vs Bit Height Fluctuation

Section 4.1 presented some discussion of the role that TGA gain plays in the recording process and the effect it can have on the stored data. Basically, two nonlinear effects can interact with the TGA gain (which controls the dynamic range of the recorded holographic fringes) to produce crosstalk effects: coefficient clipping in the TGA itself, and film response nonlinearity. In Section 4.1 the effects of coefficient clipping were shown to be avoidable by limiting the TGA gain to values of 13 or less. The effects of film nonlinearity are not as easily eliminated; the AOM equalizing filter functions attempt to correct for the problem, but some nonlinearity remains. This provides a potential mechanism for TGA/intermodulation coupling.

One of the effects which appears to be limiting the currently attainable BER performance of the system is the fluctuation in the heights of the "one" bits which occurs from hologram to hologram and from bit site to bit site. This fluctuation, which appears to be a fixed-pattern, data content dependent type of noise, restricts the range of threshold voltages over which a given hologram can be successfully read out, making it much more susceptible to errors caused by the expected random noise fluctuations (film grain noise, film surface defects, dust, etc.). The most likely candidate for the cause of this effect is intermodulation noise resulting from attempted overusage of the film's dynamic range (resulting from an excessive TGA gain setting). During the system optimization and testing phase of the program, several experiments were carried out in an attempt to confirm or deny the relationship of TGA gain to the observed bit height fluctuation effects.

The experimental procedure followed in all cases was to vary the TGA gain in recording, then attempt to observe a corresponding increase or decrease in the magnitude of the amplitude fluctuations

during readout. The results of one of these experiments are presented in the series of photos in Figures 4.3.4-1 through 4.3.4-4. The Figures present the even and odd video data channels recorded during a readout run. Each Figure represents a different value of TGA gain used during recording, with all other parameters being held constant. The series shows that, although the overall amplitude of the readout signal may vary (simply due to varying laser power settings), the relative bit-to-bit intensity profile is clearly fixed. This is an indication that the bit height fluctuations cannot be attributed to a simple intermodulation effect, and therefore cannot be corrected by a simple reduction in TGA gain. This negative result has at least one positive aspect: it indicates that film response is not currently a limiting factor in system performance; thus it may be possible in future systems to achieve even greater film dynamic range usage.

The inability to implicate intermodulation noise as the main cause of the bit height variations was confirmed by several other experimental trials essentially similar to the one just described. This fact, coupled with the apparent importance of these variations as a limiting factor in system BER performance, makes further investigation of this problem highly desirable.

#### 4.3.5 Effect of Film Processing on BER

One of the most important system performance parameters is the raw bit-error rate (BER). For this reason, all potential error sources must be investigated and their effects minimized. Of additional importance is the nature of the errors produced, that is, their temporal and spatial statistical distributions. This is because the application of proper spatial and temporal information distribution and coding techniques can greatly minimize the final error rate perceived by the user of the system. In Section 5.1 we have discussed the statistical nature

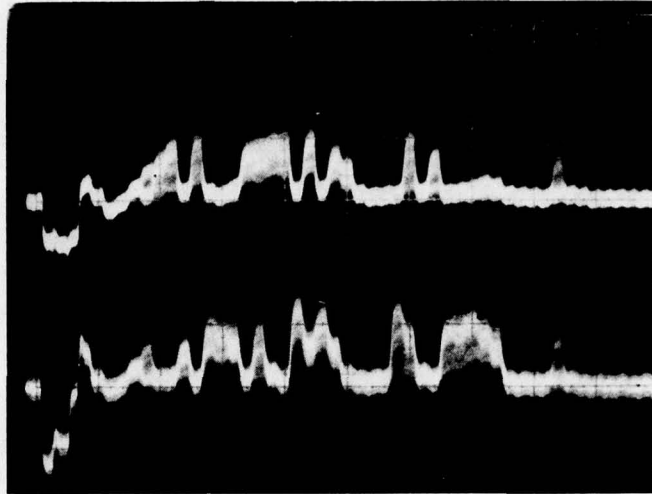


Figure 4.3.4-1. Even and Odd Video Data Channels. TGA Gain 5

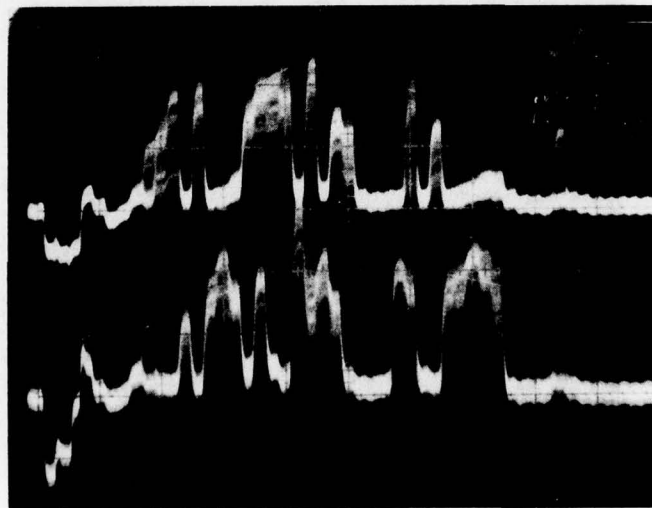


Figure 4.3.4-2. Even and Odd Video Data Channels. TGA Gain 7

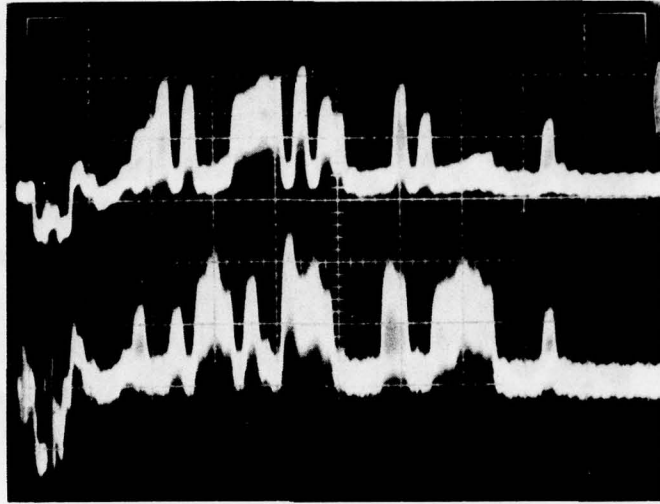


Figure 4.3.4-3. Even and Odd Video Data Channels. TGA Gain 9

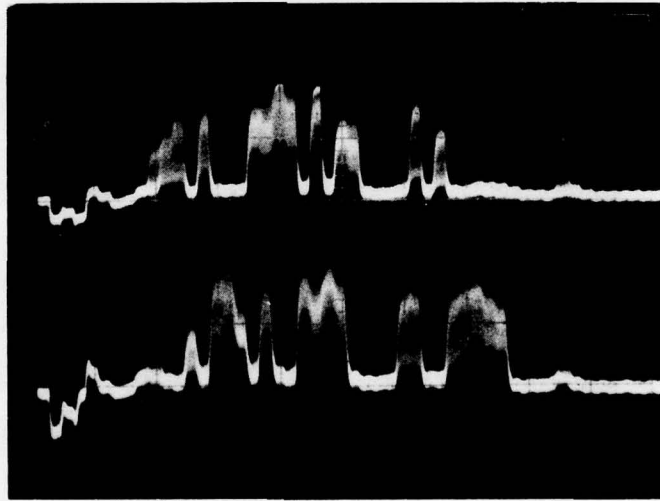


Figure 4.3.4-4. Even and Odd Video Data Channels. TGA Gain 10

of the errors in some of the recorded and reproduced data observed during system testing procedures; we have also shown that, because of the presence of burst errors in significant numbers in the reproduced data, the full power of the error correction code implemented in the system is not achieved, and the BER is unnecessarily (and remedially) high. Section 5.1 also discusses the proper remedial measures, specifically the addition of interleaving to the error correction code to minimize the effect of burst errors.

One of the major error sources in the system, particularly notable for its tendency to generate burst errors, is the passage of the film through a moderate quality mechanical film processor (a system requirement). Thus it is appropriate to attempt to quantify the nature and extent of the errors introduced in this manner. Toward this end, an experiment was run on the system to compare the error rates and patterns produced by a standard machine processed fiche with those of one that had been processed by hand. Hand processing is, of course, not an option for an HRMR-II type system, but such an experiment is still of value as an indication of the range of improvement in BER performance that could be attained with higher quality processing of any form.

Two methods of characterizing the BER performance of the fiche under study were used. The first was simply recording an average BER value as displayed by the system front panel. To minimize the effects of statistical fluctuations or spatial variations, several data runs were averaged together, and data was taken from the same location on each fiche. The second method, called the "Z-mod" technique, involved recording with an oscilloscope what is essentially an error map of an entire track; in these displays, each of the 64 bit locations in the holograms appears as a vertical column, with errors

at the beginning or end of the track being indicated by bright spots at the bottom or top of the column, respectively. The resolution of the Z-mod display is not great enough to resolve individual errors, but error patterns and concentrations may be interpreted based on the total brightness of a given area.

The result of the first comparison may be simply stated: the BER of the hand processed fiche was approximately 4 times better than that of the machine developed fiche. Specifically, the former produced an average track error count of 150, while the latter averaged 652. The result of the Z-mod test confirmed this result. Figures 4.3.5-1 and 4.3.5-2 show the two Z-mod pictures. The error concentration is clearly greater in the machine processed case. An intriguing facet of this latter result is the apparent constancy of the error pattern from one picture to the other, with only its intensity being enhanced in the machine processed case. This could mean that we are seeing a kind of synergism between error sources, with some other source (perhaps vibration resonances, see Section 4.3.1) making the signal to noise ratio marginal, and the processing technique being the deciding factor between good and poor performance.

Regardless of the interpretation of the error pattern question, the conclusion to be drawn from this test appears clear: the quality of the processing performed by the system can have a major impact on the system's BER performance, and future systems designs should devote significant effort to obtaining improved quality automatic film processing.

#### 4.3.6 Fixed Pattern Noise Investigation

The discussion of Section 4.1.4 centered on the production of uniform envelopes or bit pattern profiles extending across the entire data band; Section 4.3.4, by contrast, detailed some investigations into the rapid, bit-to-bit amplitude fluctuations encountered in many readout

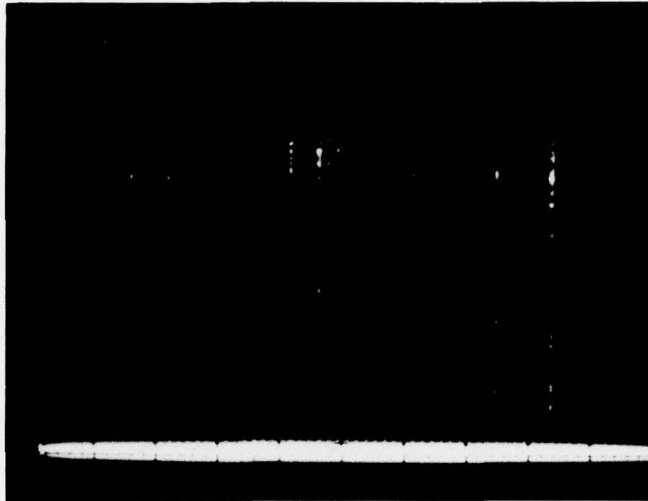


Figure 4.3.5-1. Z-Mod Error Display - Hand Processed Fiche

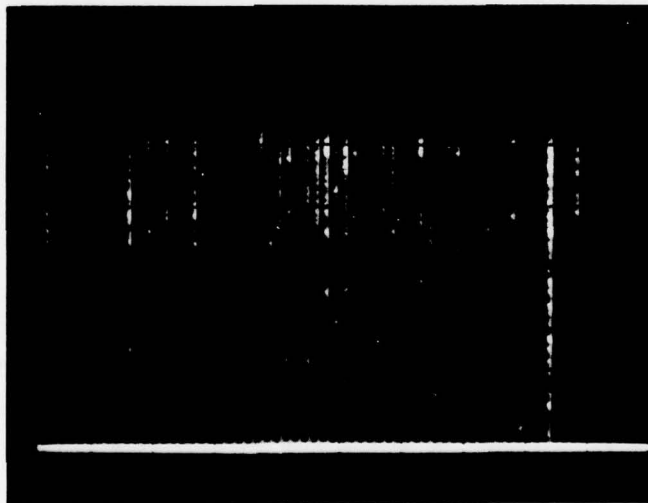


Figure 4.3.5-2. Z-Mod Error Display - Machine Processed Fiche

operations. We now turn to an intermediate frequency effect: the fluctuation of bit intensities through several apparent cycles through the data band. This effect, which can have much the same deleterious effects on the readout process as those discussed in Section 4.3.4, has been present only intermittently during the system testing activities, making it very hard to diagnose and treat. In this section we present the results of an attempt to verify that this effect happens during recording, and if so, to identify it with an intermodulation effect.

The effect in question is clearly seen in Figure 4.3.6-1, where the two video output channels are again displayed. Note the almost periodic fluctuation in bit intensities, making around six cycles along the length of the data band. This recording was made with a relatively low TGA gain of 5, so intermodulation should not have been a factor; nevertheless, an investigation was made using a spectrum analyzer, of some of the signals which are input to the film during recording.

Figure 4.3.6-2 shows a spectrum analysis of the signal detected by the AOM monitor photodiode in the recorder. The picture was recorded in "free run" mode, i. e., the hologram signals are gated normally, but phase continuity is maintained, as opposed to the reset procedure normally followed; this is done to minimize the artifacts the phase reset process produces when seen by the spectrum analyzer. With this exception, the figure depicts conditions identical to those under which the test fiche was recorded (TGA gain of 5, DF setting 1/4, etc.). The uniform bit heights in this picture indicate that the effect searched for has not been introduced at this point.

This experiment was carried out numerous times under a variety of conditions and in all cases the result was negative. Increasing the TGA gain to 13 did produce some intermodulation effect as indicated

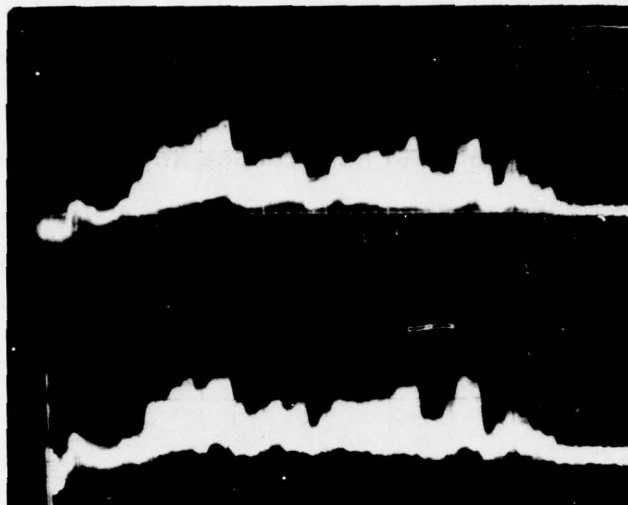


Figure 4.3.6-1. Even and Odd Video Data, Every Other Bit Set.  
TGA Gain 5, DF Setting 1/4

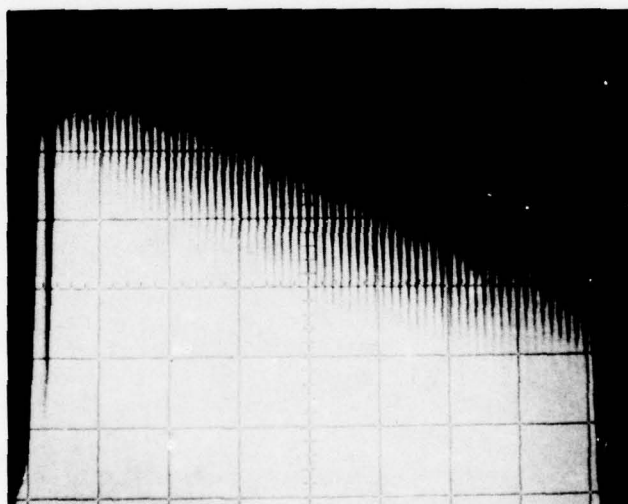


Figure 4.3.6-2. Spectrum Analysis of Data Input to Recording System.  
TGA Gain 5, DF 1/4

by bit height fluctuations in the spectrum analyzer output; this corroborates the data described in Section 4.1.1. However, the fluctuations did not appear to be correlated with the variations observed in, e.g., Figure 4.3.6-1. This negative result exonerated the TGA gain and intermods in general, but did not produce any alternative candidates for sources of the fixed pattern noise. Since this noise has not always been present, and does not appear to be a major limiting factor to the system's performance, this is not a serious setback. However, this topic does merit additional investigation.

## V. BIT ERROR RATE ANALYSIS

### 5.1 Achievable Bit Error Rate Improvements

The integrity with which stored data can be recovered is one of the most important parameters of any data storage and retrieval system. The bit error rate (BER) of the current HRMR system, as documented elsewhere in this report, is adequate to support some important system operation scenarios; however, it is considerably worse than its predicted levels as given in the initial system design studies. The technique used in those studies to predict a system BER level was threefold: (1) through a light budget calculation and analysis of system noise sources, calculate a SNR and hence a raw BER; (2) assume statistical independence of the raw errors; and (3) calculate the achievable system BER based on the well known theoretical performance of an easily implemented error-correcting code. It is the false assumption in the second of these three steps which produced the discrepancy between the early design predictions and the current HRMR system performance.

Experience obtained at Harris since the completion of the initial performance predictions, both on the HRMR system and on the several phases of the Wideband Recorder program, has shown that: (1) the dominate noise source in current optical data storage and retrieval systems is film surface noise (generated by handling, processing, etc.); (2) the errors that result are highly correlated rather than statistically independent; and (3) these errors can be made to appear independent by means of relatively low-risk interleaving techniques. Specifically, experiments performed during Phase III of the Wideband Recorder program showed that the full theoretical power of a given error correcting code could be realized, provided that the codewords are interleaved to a spatial extent of approximately 130 to 200  $\mu\text{m}$ . To verify the applicability of this result to the HRMR system, experiments were performed to document the actual

error statistics of the system. In this section we will provide a brief summary of the original BER analysis, describe the results of the new system characterization experiments, and summarize the resulting recommendations for system modifications and the lowered system BER that they should produce.

#### 5.1.1 Initial System BER Predictions

The initial system BER values were predicted based on an analysis of the various noise sources to which a system of this kind is subject. The list of noise sources used, reproduced below in Table 5.1.1-1, is a fairly comprehensive one. Based on this list, it was calculated that a nominal system SNR of 17.9 dB would be achieved (with a worst case of 14.9 dB). Then, using published relationships between the optical SNR and the theoretically achievable BER (W. H. Lee, JOSA, 62, 797), this was shown to correspond to a raw BER of approximately  $10^{-7}$  (worst case  $10^{-4}$ ). Predictions for corrected error rates were then made, based on the use of a (63, 51) BCH code and the assumption that the raw errors could be treated as statistically independent.

The demonstrated system raw BER of about  $2 \times 10^{-4}$ , documented in subsection 4.2.2.2 above, indicates that the worst case SNR prediction of 14.9 dB was within approximately 0.5 dB of being correct; however, the nominal prediction of 17.9 dB was 2.5 dB too high, and the relative importance of the various error sources was apparently misjudged. The error diagnostic activities documented in section 4.3 include at least three effects not explicitly included in the early calculations: recorder vibration signatures, machine processing effects, and crosstalk-like bit height fluctuations of uncertain origin. These problems, together with those originally anticipated, resulted in an effective system SNR of about 14.5 dB. More work will have to be done, however, before a complete assignment of relative responsibilities for this noise figure can be made to the various noise sources.

TABLE 5.1.1-1

BIT ERROR SOURCES

Recorder Generated

1. Noise Inputs (laser, modulator, air bearing, arithmetic).
2. Exposure Variations (light power, ambient light).
3. Transfer Function Nonlinearities (equalizer, D/A, modulator).
4. MTF Fluctuations (spot shape, bandwidth, sampling, mechanical tolerances).
5. Mechanical Positioning Tolerances (registration, transients, drive nonlinearities, vibration).

Film Generated

6. Wiener Noise (matte particles, base material).
7. Light Transmission Nonlinearities and Instabilities ( $T_A$  curve, processing, static discharges).
8. MTF Response (spot size, emulsion thickness).
9. Physical Properties Variations (dimensional humidity and temperature dependence, thickness variations, etc.).
10. Obscurations Induced by Handling (scratches, surface contaminants).

Reader Generated

11. Reconstruction Optics Defects (wave field distortion, scale factor, focus).
12. Interbit Crosstalk.
13. Detection Errors (intermodulation, crosstalk, timing jitter, electrical noise).
14. Detection Circuit Fluctuations (timing and threshold estimation errors).
15. Mechanical Positioning Tolerances.

The SNR predictions made during the early system analysis activities, while not totally correct, were within a few dB of the achieved values as derived from the observed raw error rates. The same cannot be said for the corrected error rate predictions. These predictions, because they were based on the assumption of statistical independence of the raw errors (an assumption shown experimentally in the next subsection to be false), were far from correct. The implemented error-correcting code, BCH (63, 51), theoretically can translate a raw BER,  $P_r$ , into a corrected rate,  $P_c$ , according to the approximate formula

$$P_c \approx 3152 P_r^3 .$$

Thus the predicted worst case raw rate of  $10^{-4}$  would correct to a rate of about  $3.1 \times 10^{-9}$ , provided that burst errors are statistically negligible. The fact that no such low corrected rates were achieved (even though raw rates of around  $10^{-4}$  were achieved) is strong evidence of significant burst error source activity. Experimental verification of these burst errors, as well as recommended techniques for eliminating their effects, are given in the following sections.

#### 5.1.2 Error Statistics Evaluation Experiments

The first step in the evaluation of the error statistics of the HRMR system was the collection of data. A typical HRMR fiche was selected for analysis; this fiche contained as data an ASC II coded text file, which was repeated in each of the 70 tracks; thus a good range of variation in the data patterns stored in each hologram was assured. Each track contained 105 blocks of 4096 bits each. The first evaluation was simply to use the standard system software to print out the number of raw errors contained in each block; this was done for the first 7 tracks and also for slightly more than 2 tracks near the film's center. Thus block error data were obtained for a total of 1010 blocks. These blocks were then examined and those with unusually high error rates were selected for further analysis. A total of 24 such burst-prone blocks were identified, and for each of them

a complete bit-by-bit error printout was obtained. For track analysis, a complete error printout was also obtained for tracks 0, 1, and 34 (105 blocks each).

#### 5.1.2.1 Track Analysis

The tracks selected for full analysis (tracks 0, 1, and 34) did not exhibit significant burst error activity, so they were primarily analyzed for raw error rate and for the identification of systematic error patterns. One important systematic error was immediately identified: the 34th user bit in each hologram was responsible for a strongly disproportionate share of the observed errors. This is made clear by the following table.

	<u>TRACK 0</u>	<u>TRACK 1</u>	<u>TRACK 34</u>
Total Errors Detected	136	200	156
Total Errors Bit 34	69	92	94
BER Including Bit 34	$3.19 \times 10^{-4}$	$4.70 \times 10^{-4}$	$3.66 \times 10^{-4}$
BER Excluding Bit 34	$1.57 \times 10^{-4}$	$2.54 \times 10^{-4}$	$1.46 \times 10^{-4}$

At a hypothetical BER of  $4 \times 10^{-4}$ , each bit should be in error an average of 3 times per track. Thus the observed values of 69, 92, and 94 are nearly certain proof that a systematic error is involved. The cause of this systematic error was not determined during this investigation, but several possibilities were identified, including: a weak or intermittent photosite in the detector array, an intermittent fault in the transform generator unit, or a software or interface problem. Since this systematic error is observed to occur consistently (in other tracks as well as those just mentioned), it is readily attackable and should be easily eliminated; furthermore, even if this prediction is overly optimistic, since only one bit is affected an acceptable brute force solution would be simply to record an additional user bit and use it in place of the error prone bit. Thus it seems reasonable to assert that the raw error rates observed in the system

(during ATP and as described in previous sections of this report) should be reduced by approximately a factor of 2 to make them truly representative of system performance.

A secondary analysis performed on the track error data was run length evaluation. For this test, the error locations in the track to be evaluated were stored in a computer, and operated on by the analysis program. The analysis program calculated run lengths between errors, converted each of these lengths in bits to a number of holograms, and tabulated the probabilities of the various run lengths. Since there was no important burst activity in the selected tracks, the result was relatively uninformative: only the less than one hologram and more than 48 hologram distances accumulated more than their share of run lengths. Thus interleaving of up to 1 hologram (68 bits) would have been slightly beneficial, but the exact depth required was not determinable, and in any case the result would not have been applicable to tracks affected by burst errors. However, we can say as a result of this analysis that any interleaving scheme which can improve the performance of burst laden tracks should also suffice for the non-burst laden tracks. A final benefit of this secondary analysis was the development of a computer program to handle HRMR error data and compute run lengths and error positions; this program in various modified forms was used extensively in the more fruitful analyses described below.

#### 5.1.2.2 Burst Block Analyses

Twenty-four blocks from tracks 0-7 and 34 were selected for analysis because of their high error rate and/or burst characteristics. The number of errors in these 4096 bit blocks ranged from 3 to 133 with an average of about 30. In most cases the errors in each block were fairly well localized in well defined bursts, but a few blocks were analyzed which exhibited general high BER behaviour with few identifiable burst areas. To investigate these 24 blocks, two computer simulations of error correcting code performance were made.

#### 5.1.2.2.1 Single-Error Correcting Code

In the first simulation, the performance of single-error correcting codes was examined. These codes, which can correct one error per codeword, are typified by the BCH (63, 57) code, where 6 parity bits are added to each 57 user bits to form 63-bit codewords. The procedure used was quite simple: within each block, each error was assigned to an appropriate codeword depending on (1) its modulus with respect to the interleave depth being investigated, and (2) its distance from the other errors in the block. When this assignment was complete, those interleave depths with zero or one error in each codeword (i. e., those which would have successfully corrected the entire block) were printed out. The result, though strongly dependent on the distribution of errors within each burst, was an indication of the interleave depth necessary to make a single-error correcting code viable in the HRMR system. Of the 24 bursts investigated, 12 were typically correctable with interleave depths of 100 bits or less, while 7 were not fully correctable by an interleave depth of 256 bits (the maximum investigated). This indicated that, for data typified by the blocks under study, a single-error correcting code would not be adequate to reach the BER goals of the HRMR program. This qualitative conclusion was to be quantitatively confirmed by the results of the second simulation.

#### 5.1.2.2.2 Interleave Depth Studies

In the second simulation a closer modeling of the performance of an interleaved error correcting code was done, and more quantitative results were obtained. For a number of interleave depths between 1 (i. e., no interleaving) and 256, each burst-prone block was analyzed to determine the number of codewords which would be uncorrectable at each interleave depth. Then the simple relationship between word error rate (WER) and bit error rate (BER) allowed a BER value to be calculated and averaged over all investigated blocks. A number of assumptions were made in arriving at the results presented below, and these assumptions

should be stated clearly at the beginning. To do so, we must first outline the characteristics of the data set upon which these experiments took place; these are presented in Table 5.1.2.2.2-1.

TABLE 5.1.2.2.2-1  
DATA SET FOR INTERLEAVE DEPTH STUDIES

Total Blocks Examined	1010
No. of Bits per Block	4096
Total Bits Examined	$4.13 \times 10^6$
No. of Burst Blocks	24
No. of Non-Burst Blocks	986
BER of Burst Blocks	$7.2 \times 10^{-3}$
BER of Non-Burst Blocks	$1.85 \times 10^{-4}$
Total No. of 63-Bit Words in Data Set	86187

The approximate theoretical relationship between the raw bit-error rate,  $P_r$ , and the corrected bit error rate,  $P_c$ , is

$$P_c \approx \frac{D}{N} \binom{N}{M+1} P_r^{M+1},$$

where  $N$  is the codeword length,  $M$  is the correcting power (1 or 2), and  $D$  is the distance of the code (usually equal to  $2M + 1$ ). This value of  $P_c$ , of course, is the rate to be expected in the absence of burst errors. The first assumption made was that the only codewords in error were those resulting from the burst blocks. This is justified by observing that the predicted word error rate (given by the above formula with the factor of  $D/N$  removed) for a raw BER of  $1.85 \times 10^{-4}$  is  $2.5 \times 10^{-7}$ ; thus within the 86187 words investigated, the expected number of words in error due to random errors is about 0.02 (i. e., it is unlikely that any words would be in error on a given trial). A second assumption is that the blocks following the burst blocks being analyzed were substantially error free. This

is necessary because, at the higher interleave depths, the codewords extend past the burst prone blocks' boundaries; thus the simulation program, having no access to error data from the adjoining blocks, must assign them a "zero error" pattern. This can be partially justified by noting that, at the raw BER of  $1.85 \times 10^{-4}$ , the expected number of errors in the adjacent block is about 0.75, i. e., one error in most blocks; combined with the requirement that to cause trouble for our analysis, one error must fall in a codeword with exactly two errors from the previous block, this seems to be an event of sufficiently low probability that our results will not be materially affected (but no rigorous calculation has been done on this to date). A final assumption involves the size of the data set. With only  $4 \times 10^6$  bits to be evaluated, firm conclusions about BER values below about  $1 \times 10^{-6}$  cannot be reached. However, it is felt that by generating curves which are valid for lower BER's (e. g., versus interleave depth), moderate (and cautious) extrapolation of these curves can carry us to the regions of interest.

The results of the simulation are presented below in Table 5.1.2.2.2-2 and Figure 5.1.2.2.2-2.

TABLE 5.1.2.2.2-2  
NO. OF WORDS IN ERROR VERSUS INTERLEAVE DEPTH

	<u>Interleave Depth (bits)</u>				
	<u>31</u>	<u>51</u>	<u>61</u>	<u>128</u>	<u>256</u>
Single-Error Correcting Code	136	127	123	88	42
Double-Error Correcting Code	65	45	29	9	2

In the Table, 6 words (the number to be expected due to the raw error rate) have been added to the single-error correcting code entries; as already explained, no such correction is necessary for the more powerful

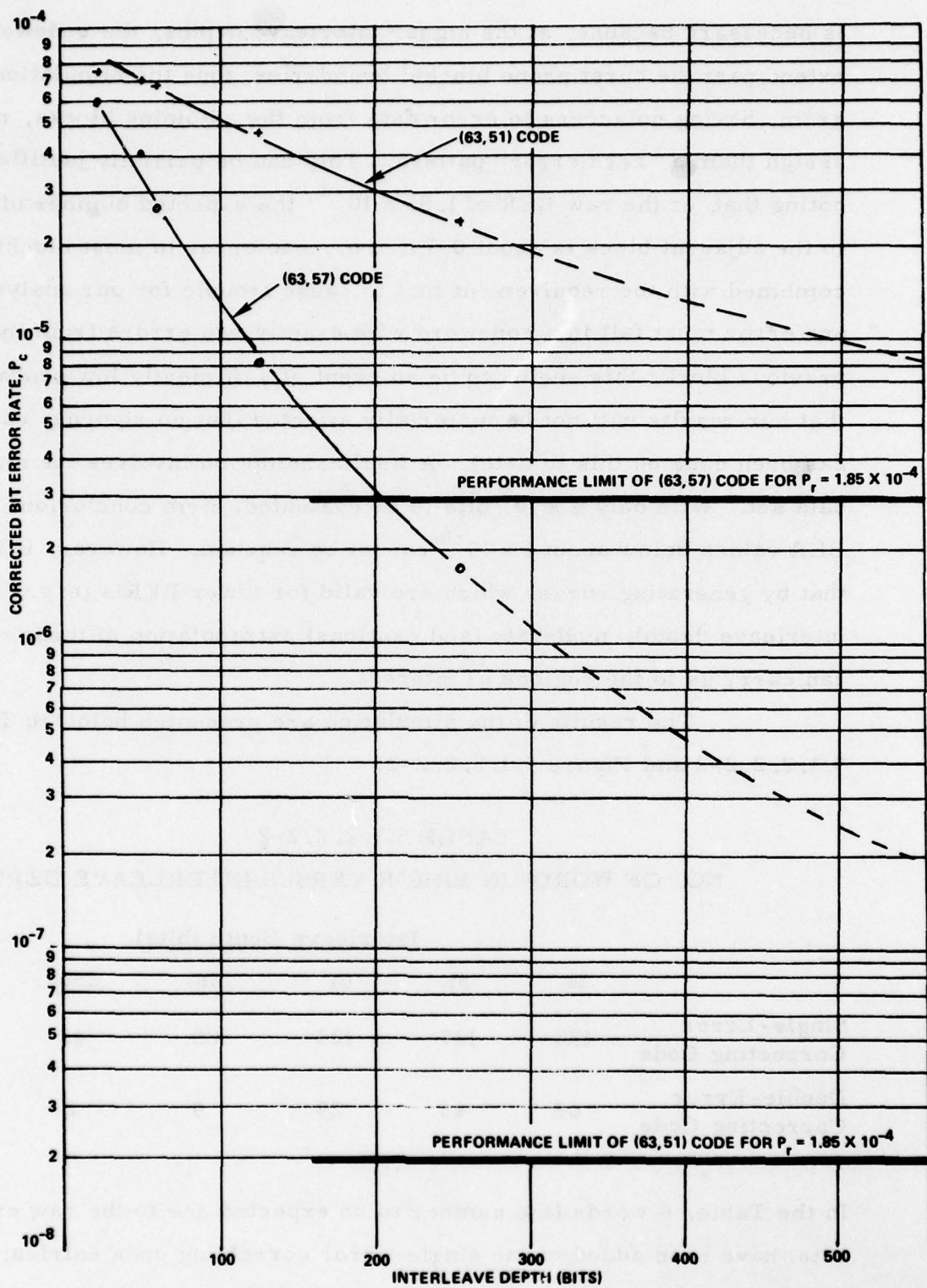


Figure 5.1.2.2.2-2. Result of Interleave Simulation Experiment

double-error correcting code. By combining the results in the Table with the formula given above, a set of corrected BER values can be obtained and plotted versus interleave depth; the result is Fig. 5.1.2.2.2. The Figure shows the calculated BER values resulting from the word errors detected by the simulation program. Note that the lower bounds have been included; these are the values given by the formula when the raw BER is used, and therefore correspond to the performance achievable when the raw errors are statistically independent (either naturally, or by means of a sufficiently great interleave depth). Note also that the curves have been extrapolated to show projected performance at interleave depths higher than those actually investigated. The proper extrapolation technique is subject to some question, since the curve is a system characteristic dependent upon error statistics; however, experience with another film-based data storage system of similar packing density (the Wideband Recorder System) indicates that a smooth continuation of the curve as drawn is the most likely situation.

The curves in Figure 5.1.2.2.2 show that, if the data analyzed here is typical of the HRMR system's performance, then at an interleave depth of 256 bits, the (57, 63) single-error correcting code could achieve a corrected BER of about  $2.3 \times 10^{-5}$ , while the (51, 63) double-error correcting code (as implemented in the HRMR system) could achieve  $1.8 \times 10^{-6}$ . Since the asymptote for the weaker code (assuming a raw BER of  $1.85 \times 10^{-4}$ ) is above the required level of  $10^{-7}$ , no amount of interleaving can enable that code to support such a low BER. The (63, 51) code, however, can reach the  $10^{-7}$  level, since its asymptotic level is around  $2 \times 10^{-8}$ . A rough extrapolation of the curve in the figure indicates that an interleave depth of about 640 bits would be required to produce a system BER of  $1 \times 10^{-7}$ . This amount of interleaving would require a very large buffer, but is not inconceivable with current memory technology.

### 5.1.3 Achievable Improvements and Recommendations

The experiments detailed in the previous subsection show that a significant amount of burst error activity is present in the recovered data; this confirms the earlier conclusion reached as a result of the inability of the implemented error correcting code to achieve its full theoretical correcting power. Thus a significant improvement to system BER performance can be made by implementing a deep interleaving scheme to complement the error correction coding. Such interleaving will always improve system performance, with the cost of the improvement coming in terms of the size of the buffer memory required to interleave the codewords.

As a specific example, consider a depth 256 interleaving scheme. Since there are 63 bits per codeword, the last bit of any word is  $63 \times 256$  or about 16K bits away from the first bit of the word. Thus, both in recording and readout, a 16K bit buffer is required to permit parallel shifting out of the interleaved words. The buffer size (and cost) increases linearly as the interleave depth is increased above 256.

The experimental results summarized in Figure 5.1.2.2.2-2 indicate that the larger the interleave depth, the lower the achievable BER (and this is, of course, true independent of the validity of the particular data set on which the experiments were performed). This means that the cost and complexity of the buffer memory becomes the key tradeoff in achieving improved BER performance. The curve in Figure 5.1.2.2.2-2 indicates that a BER of  $1 \times 10^{-7}$  (the system goal) can be achieved at an interleave depth of approximately 640 bits. At a minimum, an interleave depth of 512 (at which a corrected BER of about  $2 \times 10^{-7}$  should be achieved) is the recommended value for future system developments.

## VI. PERFORMANCE DEMONSTRATIONS AND CONCLUSIONS

### 6.1 Results of Acceptance Testing

Each of the requirements of the HRMR System were formally tested as documents in the Test Plan/Procedures with Data, an appendix to this report available under separate cover. These tests verified the achievement of many significant performance parameters and indicated those areas where performance improvements may be addressed. The following lists some of the key parameters achieved as verified by these tests:

- Utilizes 105mm by 148mm sheet film
- Automated Machine-Read Recording
- Machine-Read Data Recording
  - 30 x 10<sup>6</sup> Bits/Microfiche
  - 500 Kb/s Record Rate
  - 48 MR information bits per hologram
- Automatic Film Processing
- Verifier Readout
  - Readout Bit Error Rate 1 x 10<sup>-4</sup>
  - 250 Kb/s Readout Rate
  - 5.5 minutes to read 30Mb from microfiche including film transport and handling time.
- Throughput time to record, process and read out fill fiche is 12.5 minutes
- Input/Output Devices
  - Accepts inputs in either binary data or hard copy format
  - Automatic data reduction/compression of 5 to 1 for scanned hard copy

- Storage and Retrieval

- 6750 Fiche Storage Capacity

- 31 Seconds Random Fiche Access

- Automated Purge and Refile

The above performance parameters represent a significant advance in mass memory technology. With further engineering effort the full potential of the HRMR System can be realized.

Experiments previously documented in this report promise that significant improvement in bit-error-rate performance is achievable with additional error detection and correction electronics.

The time required to record a full fiche was dictated by available computer memory and not the electro-optical implementation of the recorder. Because a significant portion of the computer disk was used to store control programs, sufficient disk was not available to also store a complete microfiche. Therefore, with additional computer memory, the fiche record time could be reduced to approximately two minutes.

The readout rate was limited to 250 Mb/s by the efficiency of the readout electro-optics including the hologram diffraction efficiency. This rate could be doubled to 500 Kb/s with the addition of a higher power laser and/or more efficient optical implementation. However, then the readout rate will be computer memory limited (as during recording) unless additional computer memory is added.

It is noteworthy that the testing of Human Read capabilities of the HRMR System were, for the most part, deferred during the ATP. Because of the limitation in program funding, integration of the Human Read electro-optics was not completed. Although the system contains

the electronic and optical components designed to meet all the Human Read specifications, further effort will be required to bring these to full operational status.

Access to seven of the nine carousels in the storage and retrieval unit was implemented. Because of funds limitations, efforts to improve access speeds and provide access to all carousels were incomplete. However, all system functions were demonstrable. The readout electro-optics for the storage and retrieval unit are essentially identical to those in the Verifier. However, because of funds limitations, integration of these electro-optics was not completed and testing was not included in the ATP.

As tested, the HRMR System was fully demonstrable for MR functions. With some further recommended engineering effort, the system performance capabilities could be improved significantly.

## 6.2 Recommendations of System Upgrade

Five areas of the system are recommended for upgrade:

- 1) Data interleaving to improve error correction performance
- 2) Integration of readout electro-optics into Storage and Retrieval Unit
- 3) Increase access speed and provide access to top and bottom carousels in Storage and Retrieval Units
- 4) Integrate Human Read electro-optics into Recorder
- 5) Further investigate techniques for reducing raw bit error rate of MR data recording and readout.

Section 5.1.3 described the need for data interleaving and the promise that bit error rates approaching  $1 \times 10^{-7}$  are achievable.

Implementation of such interleaving electronics should be the most cost effective approach to realizing significant HRMR improved performance.

The Storage and Retrieval Unit can be brought to full operational status by undertaking the above second and third recommendations. Essentially all the electro-optics necessary to implement the readout capability in the S & R are available. Therefore, adding readout capability to the S & R should be readily achievable. Improving the access to microfiche can be achieved by further effort on the servo loops and control of the elevator drives.

Realization of Human Read should require little added effort. The hardware and software is available. Integration and checkout is required.

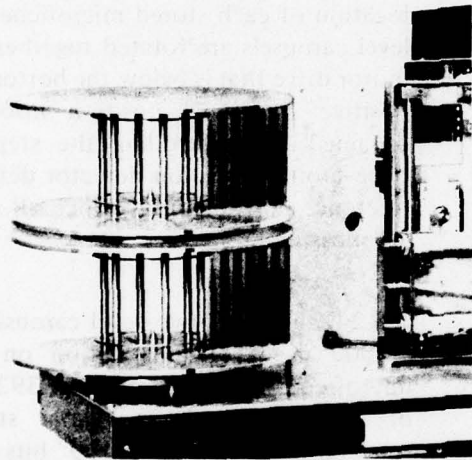
In conclusion, little time was available between system integration and acceptance testing to conduct further investigations of raw bit error sources. Such an investigation is recommended to realize the maximum potential performance of the HRMR System.

APPENDIX A

# technical brief

ISBN 011

## MODULAR STORAGE AND RETRIEVAL UNIT FOR INFORMATION ON MICROFICHE



### GENERAL DESCRIPTION

The Modular Storage and Retrieval (S&R) Unit, developed as part of an IR&D project at Harris Government Systems Group, provides storage for 1000 standard 105mm x 148mm microfiche in a two-level carousel. The unit offers automatic retrieval and X-Y positioning as well as scanning of any selected microfiche. The microfiche need not be modified in any manner (e.g., clips affixed or notches cut) to be stored and retrieved in an S&R module. Existing data bases, consisting of conventional microfiche, can be directly

in-filed to one or more S&R modules. Filed microfiche can be readily removed for use with existing standard viewing or handling equipment, if desired. The two-level carousel is easily mounted and removed from an S&R module in such a way that any S&R module can accept and retrieve microfiche from any two-level carousel mounted in the module. A single S&R module can be configured for stand-alone operation. Operator interface is achieved through a keyboard linked to a microprocessor controller. Many S&R modules can be configured for a much larger data base with independent retrieve and X-Y positioning or scanning functions within each module. All functions are under the control of a centralized processor unit; any module can be used as a backup for any other by exchanging two-level carousels.

The present design incorporates incremental X-Y positioning for a standard (7 x 14 = 98) image, NMA 24X microimage format. Command signals, from a keyboard or a CPU, can call for any image to be positioned in the read aperture. An aerial image of the accessed page is formed at a plane where a linear, self-scanned photosensor array is translated from top to bottom through the image. The photosensor array scans successive lines in the image, as it is translated from the top to the



Modular Storage and  
Retrieval Unit

10140



**HARRIS**  
COMMUNICATIONS AND  
INFORMATION HANDLING

HARRIS CORPORATION Government Systems Group  
Information Systems PO Box 37, Melbourne, FL 32901 (305) 727-4000  
A-1

bottom of the image. The output of this array is a video signal. A normalizing circuit determines the maximum and minimum video sample level during the back sweep (bottom to top) of the array through the image plane. All video samples obtained from the array on the subsequent forward sweep (top to bottom) are clocked into an A/D converter. The digitized video data is then available from the S&R module, including the normalizing levels. This digitized video data may then be routed to appropriate soft-copy or hard-copy display subsystems.

Other operating modes are available for accessing images on microfiche with changes to the imaging optics and/or the image sampling scheme. For example, a conventional TV camera can replace the photosensor array and its associated mechanical scanning mechanism to convert the aerial image to conventional video for a TV monitor. Alternatively, a projection display formed directly from the portion of the microfiche in the read aperture to a back-lighted display screen can be provided. If required, the projection display mode can be combined with certain video conversion modes. In all of these modes the carousel, the microfiche extractor/insertor, the X-Y positioning apparatus, the read aperture platen for holding the microfiche at a predetermined plane, and the related control electronics are the same.

Microfiche which contain digital data, recorded as individual densely packed spots or as holograms, can be stored, retrieved, and read with another version of the S&R module. One axis of the X-Y positioning apparatus is modified to provide precise continuous motion in accordance with the arrangement of files of digital data on the microfiche. The readout (image conversion) design is modified to read digital data as a microfiche is translated through the read aperture. A similar S&R approach has been implemented at Harris for RADC on the Human Read/Machine Read (HRMR) Mass Storage System

for microfiche, which contain digital data in linear files of one-dimensional holograms.

## **DETAILED DESCRIPTIONS**

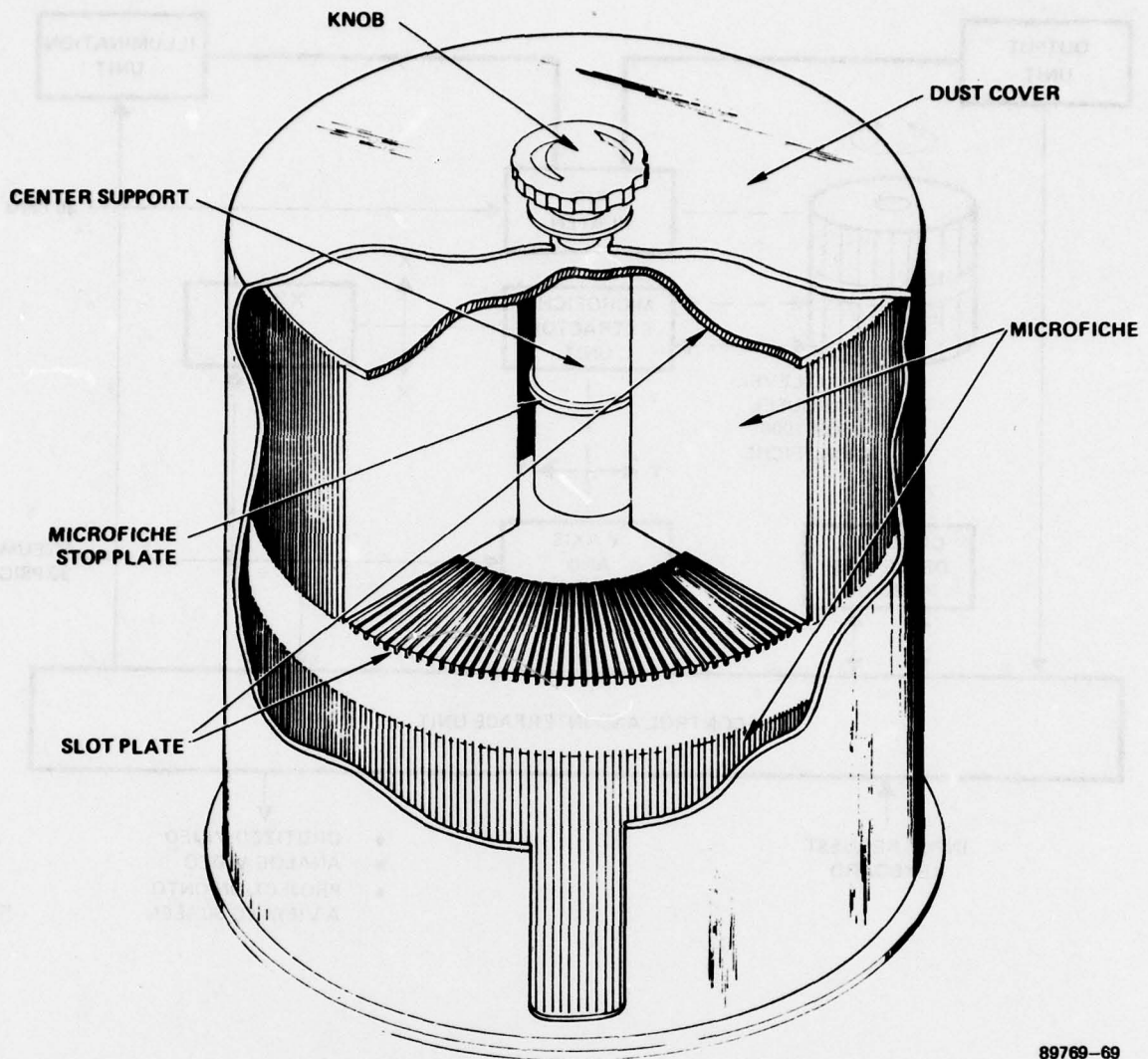
### **CAROUSEL**

The microfiche are stored in easily mounted and removed two-level carousels. Each carousel level can store up to 500 standard 105mm x 148mm microfiche. Each carousel level consists of slotted top and bottom plates and a center support with stops to control the depth of penetration of the microfiche along a radius. Each microfiche is assigned to a particular top and bottom pair of corresponding slots in a carousel. A carousel code and slot code are logged into an index file along with the corresponding microfiche code for location of each stored microfiche. The two-level carousels are rotated together by a step-motor drive that is below the bottom carousel. Positive rotational position information is obtained by controlling the step count; a once-around position detector defines a zero reference position from which all step counts are measured.

AT 24X a single, two-level carousel can store 98,000 pages of information on the 1000 microfiche; at 48X, it can store 392,000 pages of information. In a digital storage and retrieval mode with  $0.5 \times 10^9$  bits per microfiche, a total of  $0.5 \times 10^{12}$  bits can be stored in a single two-level carousel. In either the analog image store or digital store modes, typical random access times to a unit record are 3 to 6 seconds. Random access times to other portions of a microfiche already in the X-Y positioner are typically 0.5 second.

### **RETRIEVING AND REFILING**

To retrieve a microfiche, the carousels are rotated to position the required microfiche at a retrieval station. The X-axis drive centers the Y-axis at either the upper or lower carousel. A spring activated clamp, affixed to a pair of pneumatic cylinders, is extended by pneumatic action so that the clamp fits over

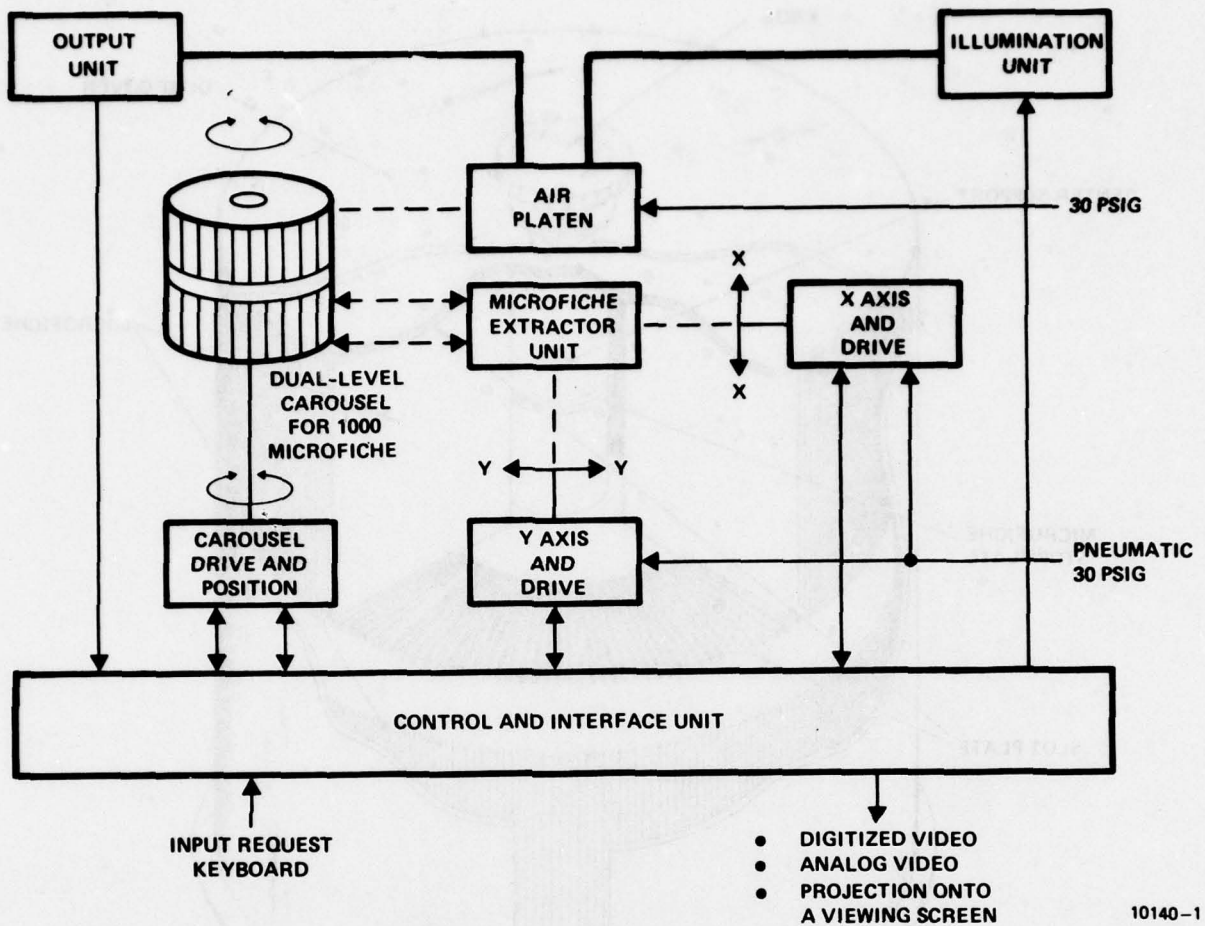


89769-69

## READ STATION PLATEN

optics to produce uniform illumination of the portion of the microfiche in the read aperture. Projection optics to form an aerial image of the information in the read aperture at a photosensor device or at a display screen (or both in special cases) are provided to fit the application. Typically, conventional off-the-shelf illumination and projection optics can be incorporated.

Precision axial position control of the portion of the microfiche in the read aperture is provided by an air-bearing platen. This approach eliminates contact with any portion of a microfiche that contains the user's information. The axial position of the portion of the microfiche in the read aperture can be maintained to  $6\ \mu\text{m}$ , or better, with this air-bearing platen.



the outer edge of the microfiche. The spring is released by a cam to capture the microfiche and the pneumatic cylinders are contracted to extract the captured microfiche and position it at a reference location. The X-Y drive then positions the required page in or translates the required digital file through the read aperture. The retrieve sequence is essentially reversed to refile the extracted microfiche.

### ***X-Y POSITIONING***

The X-axis drive is designed to position the extractor mechanism (which moves along the Y-axis) at the retrieval position for both carousel levels and to provide the required

incremental motion to specific microimage locations or continuous linear motion to read digital files of data. The Y-axis drive provides the required incremental motion to specific microimage locations or to specific digital file centers. Step-motor, closed-loop servo motor, digital pneumatic, and closed-loop servo pneumatic drive options can be provided, as required for the specific application, for the X- and Y-axes.

### ***ILLUMINATION AND IMAGE PROJECTION***

Both incoherent and coherent illumination sources can be provided with the appropriate

## PHOTOSENSOR FOR CONVERSION TO ELECTRONIC SIGNALS (VIDEO OR DIGITAL)

A self-scanned linear photodetector array of up to 2048 elements is affixed to a linear translation mechanism consisting of a pneumatic piston and a precision position sensing device to provide scan-start signals to the self-scanned array. This photodetector array sweeps through the projected aerial image from bottom to top while a normalizing circuit determines the maximum and minimum signal values (two numbers per backward sweep). During the subsequent forward sweep (top to bottom), the self-scanned photodetector array is scanned to collect video samples on a line-by-line basis with the scan and sweep rates adjusted for the required top-to-bottom resolution. As the array sweeps, a linear position encoder provides precision absolute instantaneous position information as electronic signals which are used to initiate an array scan sequence each time the array has been translated one scan line spacing. The video samples are clocked into an A/D converter. The digitized video data is available from the S&R module, with the two maximum and minimum normalizing values, to be provided to appropriate soft-copy or hard-copy display subsystems.

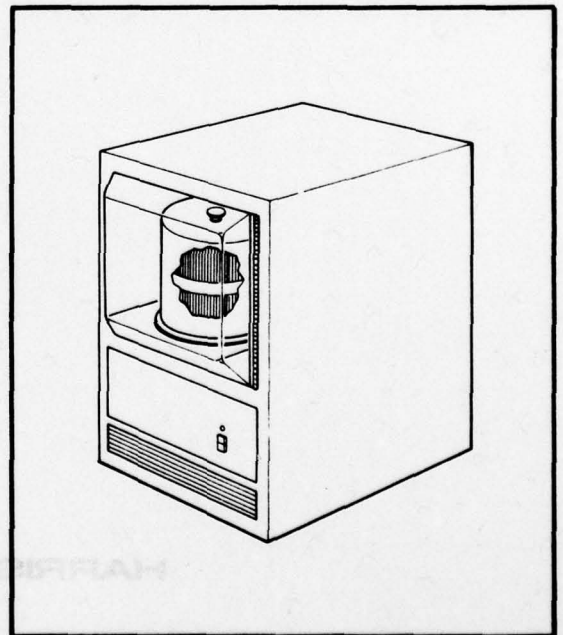
An alternative readout technique which can be implemented is the use of a conventional or solid-state TV camera unit in place of the photodetector array and linear sweeper. Also, a projection display on a back-illuminated screen can be provided, in some cases, in combination with a video conversion capability. Furthermore, for bi-level (black-white only) microimages, normalizing information is not required, and video conversion and data transfer can occur on both the forward and backward sweeps of the photodetector array, with appropriate adjustments to control software for sequencing the retrieved data.

## DRIVE AND CONTROL ELECTRONICS

Each S&R module includes electronics to drive and control the carousel (rotate and stop), the microfiche extractor/insertor, the X-Y positioning, the illumination, the photodetector array sweeping and scanning, and the collection of maximum and minimum video values (on the backward sweep). Also, appropriate interface electronics to accept and interpret access commands for an image or data file on a particular microfiche are included. Access commands can be provided from a microprocessor controller with keyboard command entry (typical for single S&R module operation) or from a central processor unit (typical for many S&R modules on line).

## PHYSICAL CONFIGURATION

An S&R module, with all required drive and control electronics, fits into a standard 19-inch wide electronic half-rack less than 36 inches high.



## APPLICATIONS

- S&R of photo reduced hard copy
  - Documents (98,000 at 24X; 392,000 at 48X)
  - Fingerprints
  - Map and chart repro mats
  - Other graphics
- S&R of digital data
  - Multiple modules for mass stores
  - HRMR
  - High-density direct spot
  - Single module for tactical and local stores
- S&R of COM
- S&R of any data on standard 105 x 148 mm fiche
- Projection display of images from microfiche to viewing screen

## FEATURES

- Storage for 1000 standard 105 x 148 mm NMA microfiche
- No clips required on fiche
  - Existing fiche data can be directly entered for S&R
- Fully automatic fiche extraction, positioning, and translation/scanning
- No image/data scratching or degrading
- From 3 to 6 seconds typical cycle times
- Fully compatible with TV camera or linear photosensor array image/data retrieval
- Standard 19-inch rack mounting



**HARRIS**



COMMUNICATIONS AND  
INFORMATION HANDLING

*MISSION  
of  
Rome Air Development Center*

*RADC plans and conducts research, exploratory and advanced development programs in command, control, and communications (C<sup>3</sup>) activities, and in the C<sup>3</sup> areas of information sciences and intelligence. The principal technical mission areas are communications, electromagnetic guidance and control, surveillance of ground and aerospace objects, intelligence data collection and handling, information system technology, ionospheric propagation, solid state sciences, microwave physics and electronic reliability, maintainability and compatibility.*

